DENDROCHRONOLOGY AND NEAR-INFRARED SPECTROSCOPY (NIR) OF WHITE ASH INFESTED BY EMERALD ASH BORER IN MICHIGAN

By

Kaelyn Anne Finley

A THESIS

Submitted to
Michigan State University
in partial fulfillment of the requirements
for the degree of

Forestry - Master of Science

2015

ABSTRACT

DENDROCHRONOLOGY AND NEAR-INFRARED SPECTROSCOPY (NIR) OF WHITE ASH INFESTED BY EMERALD ASH BORER IN MICHIGAN

Bv

Kaelyn Anne Finley

Emerald ash borer (EAB) (*Agrilus planipennis* Fairmaire), is a non-native beetle responsible for widespread mortality of several North American ash species (*Fraxinus* sp.). Current non-destructive methods for early detection of EAB in specific trees are limited, which restricts the effectiveness of management efforts. This study explored the potential of dendrochronology and near-infrared spectroscopy (NIR) as novel methods for detection of EAB on white ash (*Fraxinus americana*) in Michigan using a handheld increment borer. Increment borers are used to non-destructively and efficiently collect increment cores from trees. While the potential of dendrochronology for early detection of EAB in Michigan was inconclusive based on the results of this study, white ash in Michigan was shown to have a strong negative relationship with precipitation and available moisture in the summer of the previous year. Increased risk of branch failure due to EAB infestation may further increase ash susceptibility to wind damage. Near-infrared spectroscopy was successfully used to discriminate between bark, phloem and xylem tissues from EAB infested and visually healthy trees using linear discriminant analysis. The xylem spectra transformed using a Savitzky-Golay, 1st derivative smoothing filter over the full NIR wavelength range observed in this study (1134-2190 nm) had the highest discriminating power at 97% correct classification accuracy.

Copyright by KAELYN ANNE FINLEY 2015

ACKNOWLEDGMENTS

I would like to express my sincere gratitude to my major advisor, Dr. Sophan Chhin for the guidance, continuous support and opportunity to work with ash in Michigan. You have been a tremendous mentor for me and I have learned so much working with you. I would also like to thank the rest of my thesis committee, Dr. Pascal Nzokou and Dr. Deborah McCullough for insight and advice on focusing my research. Their comments and suggestions were instrumental for the completion of this project and are greatly appreciated.

Data collection was facilitated by many people throughout Michigan. Without the collaboration with Joe O'Brien and Steven Katovich from the USDA Forest Service, this project would not have been possible. Alicia Ihnken, Patricia Thompson, Brian VanPatten, and Michelle Holland provided logistical support in obtaining permission to sample in Michigan. Additional thanks to Eric Thompson, Jason Hartman, Scott Whitcomb, Cody Stevens, Joyce Angel, and Karen Rodock for their advice on sampling MI DNR lands. Thank you to everyone from the MSU Forest Biomass Innovation Center, Gladwin City Park, and the Genesee County Parks. I would like to extend my thanks to the support staff, professors, and colleagues from the Department of Forestry at MSU. Funding for my project and graduate studies was provided by MSU AgBioResearch (Project GREEEN), MSU College of Agriculture and Natural Resources, MSU Department of Forestry, and the USDA Forest Service Health and Protection (FHP).

I am incredibly grateful for the help I received in the collection and preparation of samples used in completing this project. Undergraduate research assistants, Justin Brabon, Devin Berry, Brie-Anne Breton, and Patrick Shults provided essential support in field work and sample processing. I would also like to thank my fellow graduate students Reinardus Liborius, Katie Minnix, Christal Johnson and Isaac Hayford for their assistance and support with this project.

Finally, I would like to thank my family: my parents, Allan and Kim, and my sister Bri for their love and encouragement.

TABLE OF CONTENTS

LIST OF TABLES				
LIST O	F FIGU	URES	ix	
INTRO			1	
		g Knowledge	1	
		Objectives 1 Approach	1	
		er Implications	2 3	
REFER			4	
KLI LIV	CLIVEL	,		
CHAP	ΓER 1		6	
INTRODUCTION AND LITERATURE REVIEW				
1.1.	Introdu	action	6	
1.2.	Detect	ion Techniques for Invasive Insects	6	
1.3.	Emera	ld Ash Borer	8	
	1.3.1.	Life Cycle	8	
	1.3.2.	Host Species and Spread	9	
	1.3.3.	Past and Present Detection Methods and Treatment Options	10	
1.4.	Dendre	ochronology	12	
1.5.	Near-I	nfrared Spectroscopy (NIR)	13	
1.6.	Study .	Area and Ash Species of Michigan	16	
1.7.	Thesis	Objectives and Structure	19	
REFER	RENCES	\mathbf{S}	20	
CHAPT	red 2		27	
		CLIMATE ON DADIAL CDOWTH OF WHITE ACHINECTED DV EMED		
EFFECTS OF CLIMATE ON RADIAL GROWTH OF WHITE ASH INFESTED BY EMERALI BORER ALONG A LATITUDINAL GRADIENT IN MICHGIAN				
2.1.	Introdu		27 27	
2.2.	Metho		30	
2.2.	2.2.1.		30	
		Field Sampling	31	
	2.2.3.	1 0	35	
	2.2.4.	<i>E</i> , <i>E</i> ,	35	
	2.2.4.	2.2.4.1. Infestation Symptoms	35	
		2.2.4.2. Tree Level Data	36	
		2.2.4.3. Competition Level Data	37	
	2251	Dendrochronological Data Analysis	38	
	2.2.3.	2.2.5.1. Standardization	38	
		2.2.5.2. Climate	39	
2.3.	Result		41	
2.3.	2.3.1.	Infestation Symptoms	41	
	2.3.2.	Focal Tree Level Data	42	
	2.3.3.	Nearby Tree Competition and Light Availability	42	
	2.3.4.	Tree Ring Chronologies	43	
	2.3.5.	Growth Climate Relationships	44	
2.4.	Discussion			
•	2.4.1.	Infestation Symptoms	46 46	

	2.4.2.	White Ash Form and Productivity	48	
	2.4.3.	Effects of Competition and Light Availability	48	
	2.4.4.		49	
	2.4.5.	5 •	49	
2.5.	Conclu	*	55	
APPE	NDIX		56	
REFEI	RENCES		69	
CHAP	TER 3		75	
USE C	F NEAF	R-INFRARED SPECTROSCOPY (NIR) AS AN INDICATOR OF EMERALD ASH		
BORE	R INFES	STATION IN WHITE ASH IN MICHIGAN	75	
3.1.	Introdu	action	75	
3.2.	Method	ds	78	
	3.2.1.	Study Site and Field Sampling	78	
	3.2.2.	Sample Preparation	79	
	3.2.3.	Acquisition of NIR Diffuse Reflectance Spectra	79	
	3.2.4.	Spectral Pretreatment	81	
	3.2.5.	Data Analysis	82	
		3.2.5.1. Infestation Symptoms, Competition, and White Ash Form and Productivity	82	
		3.2.5.2. Discriminant Analysis and Classification	84	
3.3.	Results			
	3.3.1.	Infestation Symptoms, Competition, and White Ash Form and Productivity	86	
	3.3.2.	Discriminant Analysis and Classification of Tissue	86	
	3.3.3.	Discriminant Analysis and Classification of EAB Infestation	87	
3.4.	Discussion			
	3.4.1.		89	
	3.4.2.	Classification of EAB Infested White Ash	89	
		3.4.2.1. Previously Assigned Wavelength Bands of Wood Defense Components	93	
3.5.	Conclu	sions	96	
APPE	NDIX		97	
REFEI	RENCES		111	
CHAP	TER 4		116	
CONC	CONCLUSIONS			

LIST OF TABLES

- **Table 2.1.** Average infestation symptoms and tree measurements by infestation groups (standard error in parentheses). Number of trees sampled per infestation group (n). Parametric variables include, percent fine twig mortality, surface area (area of stem inspected for D-shaped exit holes), and adult exit holes per surface area. Non-parametric variables include s-shaped larval galleries (presence/absence), bark splits, woodpecker damage, and epicormic sprouts. All statistical analysis was compared between groups, a one-way ANOVA performed for parametric data and Kruskal-Wallis for non-parametric data (two Kruskal-Wallis tests: one to compare between all groups, and one to compare between only the EAB infested groups). Groups with different letters are significantly different (p < 0.05). P-values < 0.05 indicate significant differences in infestation symptoms between dieback classes (Kruskal-Wallis). For all I2 groups, epicormic sprouting had p = 2.
- **Table 2.2.** Mean (standard error of the mean) for the surface area (m^2) and larval density (#galleries/ m^2) of branches (>1.5 cm base diameter) sampled in Michigan separated by crown dieback class. Number of trees with branches sampled (n (trees)). Number of trees with EAB detected on sampled branches (n (EAB)). Crown dieback classes with different letters are significantly different (p < 0.05).
- **Table 2.3.** Tree level productivity for white ash sampled in Michigan based on 15 infestation groups. Number of trees sampled per infestation group (n). Average (SEM) tree level productivity variables: DBH, tree height, crown ratio, slenderness, basal area, total aboveground biomass, and total stem biomass. Significant difference between infestation groupings is designated by different letters (p < 0.05). For all I2 groups, crown ratio has n = 2.
- **Table 2.4.** Nearby live competition productivity and light availability for white ash focal trees sampled in Michigan. Number of focal trees sampled per infestation group (n). Mean (standard error of the mean in parentheses) for live competition productivity (basal area (m^2/ha), total aboveground biomass (ton/ha), and light availability (percent openness)) of focal white ash trees in fifteen infestation groups. Groupings with different letters are significantly different (p < 0.05).
- **Table 2.5.** General statistics of the standard chronologies of white ash sampled in Michigan for each of the 15 Infestation groups.
- **Table 3.1.** Average infestation symptoms and tree measurements by group. The lower and upper limits of a 95% confidence interval of the mean are shown in parentheses. Number of trees sampled per group (n). For the branch segments: Control n = 16 and EAB n = 14. The adult exit holes per surface area on the stem (#/m2), branch larval galleries (#/m2), and the live competition basal area (m2/ha) were the only comparisons made based on log transformed data. Groups with different letters are significantly different (p < 0.05).
- **Table: 3.2.** Average tree growth and form characteristics (standard error in parentheses). Number of trees sampled per group (n). Significance difference between group is designated by different letters (p < 0.05).
- **Table 3.3.** Summary of discriminant analysis on reflectance spectra for living white ash comparing the three tissue types using the Savitzky-Golay first derivative, and second derivative. Results of the discriminant analysis are reported for the full wavelength range (Full NIR: 1134-2190 nm.
- **Table 3.4.** Summary of discriminant analysis on reflectance spectra for living white ash for the three tissue types using the Savitzky-Golay smoothing filter, first derivative, and second derivative. Results of

the discriminant analysis are reported for the full wavelength range (Full NIR: 1134-2190 nm), and the reduced wavelength ranges (Lower NIR: 1134-1696 nm and Upper NIR: 1703-2190 nm) for each tissue and pretreatment type. Xylem: Control n = 43, EAB n = 36. Outer bark: Control n = 43, EAB n = 33.

Inner bark: Control n = 43, EAB n = 33.

Table 3.5. Summary of significant wavelengths identified by Stepwise Discriminant Analysis (Full NIR: 1134 - 2190 nm) that best separated between EAB infested and control spectra using the first derivative pre-treatment method. Wavelengths are separated tissue type (xylem, bark and phloem). Wavelengths from the literature that have been assigned to wood components within ± 10 nm of the measured significant wavelengths are included.

Table 3.6. Summary of significant wavelengths identified by Stepwise Discriminant Analysis (Full NIR: 1134 - 2190 nm) that best separated between EAB infested and control spectra using the second derivative pre-treatment method. Wavelengths are separated tissue type (xylem, bark and phloem). Wavelengths from the literature that have been assigned to wood components within ± 10 nm of the measured significant wavelengths are included.

LIST OF FIGURES

- **Figure 2.1.** Site map representing general locations of white ash sample sites in Michigan. UP = Upper Peninsula Control, LP = Lower Peninsula Control, Control = non-symptomatic sites, EAB = emerald ash borer infested regions (R1, R2 and R4). Solid shapes represent "natural" sites while open shapes represent recreation "use" sites.
- **Figure 2.2.** A) Mean monthly temperature and mean total monthly precipitation were averaged from 1992 2012 for the six plot locations in the UP (western UP). Line represents temperature and bars represent precipitation. B) Mean monthly climatic moisture index averaged from 1992 2012 for the six plot locations in the UP. C) Mean monthly temperature and mean total monthly precipitation average from 1992-2012 for all plot locations in the Lower Peninsula. Line represents temperature and bars represent precipitation. D) Mean monthly climatic moisture index averaged from 1992-2012 for all plot locations in the Lower Peninsula.
- **Figure 2.3.** Sampling design of the regions sampled in Michigan's (3 control regions, 3 EAB regions). Each EAB infested region sampled had 16 trees for a total of 48 infested trees sampled. The LP control region had four plots with only non-symptomatic white ash sampled in natural stands. Each of the three EAB infested regions was separated between two land-use classes (recreational use and natural). There were two plots sampled in each land-use class with four trees per plot. In the EAB region plots, trees were selected so that there was one tree representing one of four crown dieback classes. Later in the dendrochronology analysis, these four dieback classes were further consolidated into two infestation levels (I1 represents both the low and moderate dieback classes and I2 represents the combined severe and dead dieback classes).
- **Figure 2.4.** Detrended residual ring width chronologies of white ash grown in Michigan from 1992 to 2012. The thin solid line represents Infestation group "I1" (lower severity crown dieback) and the thick solid line represents Infestation group "I2" (higher severity crown dieback).
- **Figure 2.5.** Regression models representing monthly and/or seasonal mean monthly temperature influences on growth and the associated adjusted r^2 value for white ash in Michigan's Lower Peninsula and Upper Peninsula. Regression models presented are all statistically significant (p < 0.05). For each model, the climate variables that have a positive influence on growth are represented by light gray boxes, and climate variables with a negative influence on growth are represented by the darker boxes. Infestation groups with R^2 denoted by N/A have no significant growth response to mean monthly temperature. Groups with multiple significant variables are ranked in order of importance using Beta regression coefficients (i.e., a rank of 1 is the most influential predictor variable in the regression model).
- **Figure 2.6.** Regression models representing monthly and/or seasonal total precipitation influences on growth and the associated adjusted r^2 value for white ash in Michigan's Lower Peninsula and Upper Peninsula. Regression models presented are all statistically significant (p < 0.05). For each model, the climate variables that have a positive influence on growth are represented by light gray boxes, and climate variables with a negative influence on growth are represented by the darker boxes. Groups with R^2 denoted by N/A have no significant growth response to total monthly precipitation. Groups with multiple significant variables are ranked in order of importance using Beta regression coefficients (i.e., a rank of 1 is the most influential predictor variable in the regression model).
- **Figure 2.7.** Regression models representing monthly and/or seasonal total climatic moisture index (CMI) influences on growth and the associated adjusted r^2 value for white ash in Michigan's Lower Peninsula and Upper Peninsula. Regression models presented are all statistically significant (p < 0.05). For each

model, the climate variables that have a positive influence on growth are represented by light gray boxes, and climate variables with a negative influence on growth are represented by the darker boxes. Groups with R² denoted by N/A have no significant growth response to total monthly CMI. Groups with multiple significant variables are ranked in order of importance using Beta regression coefficients (i.e., a rank of 1 is the most influential predictor variable in the regression model).

- **Figure 3.1.** Site map representing general locations of white ash sample sites in Michigan. UP = Upper Peninsula Control, LP = Lower Peninsula Control, Control = non-symptomatic sites, EAB = emerald ash borer infested regions (R1, R2 and R4). Solid shapes represent "natural" sites while open shapes represent high impact "recreation" sites.
- **Figure 3.2.** A) Diagram of increment core samples and B) reflectance probe positioning for NIR measurement collection for bark, phloem and outermost 20 mm of the xylem.
- **Figure 3.3.** Canonical Scores Plots combined live white ash sampled in Michigan using discriminant analysis for 1134 2190 nm wavelengths to classify between tissue types (bark, phloem, xylem): A) 1st Derivative, B) 2nd Derivative. Xylem: n = 79, bark: n = 76, phloem: n = 76.
- **Figure 3.4.** NIR reflectance mean spectra by tissue type (bark, phloem, xylem) from 1134 to 2190 nm wavelengths. A) presents spectra of living trees transformed using the SG-1st derivative, B) presents spectra of living trees transformed using the SG-2nd derivative. Xylem: n = 79, Bark: n = 76, Phloem: n = 76. Solid squares denote wavelength bands that allowed for significant separation between the spectra of the three tissue types during stepwise discriminant analysis.
- **Figure 3.5.** Percentage correct classifications of non-symptomatic (control) and EAB infested reflectance spectra: A) xylem first derivative, B) xylem second derivative, C) bark first derivative, D) bark second derivative, E) phloem first derivative, F) phloem, second derivative. Black bars represents control, light grey bars represents EAB. Xylem: Control n = 43, EAB n = 36. Bark: Control n = 43, EAB n = 33.

 101
- **Figure 3.6.** Means of xylem spectra derivatives for control (thin line) and EAB (bold line) samples from 1134 to 2190 nm wavelengths: A) first derivative, B) second derivative. Control n = 43, EAB n = 36. Solid squares denote wavelength bands that allowed for significant separation between the Control and EAB spectra during Stepwise Discriminant Analysis.
- **Figure 3.7.** Means of bark spectra derivatives for control (thin line) and EAB (bold line) samples from 1134 to 2190 nm wavelengths: A) first derivative, B) second derivative. Control n = 43, EAB n = 33. Solid squares denote wavelength bands that allowed for significant separation between the Control and EAB spectra during Stepwise Discriminant Analysis.
- **Figure 3.8.** Means of phloem spectra derivatives for control (thin line) and EAB (bold line) samples from 1134 to 2190 nm wavelengths: A) first derivative, B) second derivative. Control n = 43, EAB n = 33. Solid squares denote wavelength bands that allowed for significant separation between the Control and EAB spectra during Stepwise Discriminant Analysis.

INTRODUCTION

Existing Knowledge

Since its discovery in 2002, emerald ash borer (EAB), (*Agrilus planipennis* Fairmaire) (Coleoptera: Buprestidae), has killed millions of ash trees (*Fraxinus* spp.) in the eastern U.S. and parts of Canada, and is continuing to spread throughout North America (Herms and McCullough, 2014). Emerald ash borer is considered to be the most destructive invasive insect pest in North America to date (Herms and McCullough, 2014). Decline and mortality of North American *Fraxinus* spp. is caused when a tree is girdled due to larval feeding on the phloem, cambium, and outer xylem (Poland et al., 2015). As larval feeding is internal, and a delay in visible signs and symptoms during initial infestation is common, early detection remains difficult and current methods in detecting emerald ash borer infestation in individual trees at a large landscape scale are limited (Ryall, 2015). This severely restricts the ability to effectively mitigate damage and slow the spread of EAB. Current survey methods include but are not limited to: the use of external signs and symptoms, sticky traps baited with ash volatile lures, baited multi-funnel traps, and using girdled "trap" trees (Ryall, 2015). Research is ongoing for improvements to existing detection methods and developing new methods for effective EAB detection.

Major Objectives

This project explores the potential of dendrochronology and near-infrared spectroscopy (NIR) as non-destructive indicator tools of emerald ash borer infestation in white ash. Dendrochronology is the study of tree ring dating and is used to explain environmental information (climate, disturbance, stand composition, etc.) throughout the lifetime of a tree (Speer, 2010). Valid inferences can be made using dendrochronology to indirectly explain the ecophysiological mechanisms of a tree's response to its environment (Fritts, 1976). Near-infrared spectroscopy measures the vibrational properties of objects in the near-infrared wavelength range of the electromagnetic spectrum (780-2500nm) rapidly and non-destructively (Roberts et al., 2004). NIR provides physical and chemical information by producing a

spectrum along the near-infrared wavelength range unique to the measured sample (Roberts et al., 2004). Commercially available spectrometers paired with multivariate analysis have led to NIR becoming an increasingly popular technique with a wide range of applications in different fields (i.e. agricultural, pharmaceutical, wood-products and forestry) (Roberts et al., 2004; Schwanninger et al., 2011).

Overall Approach

Sites with infested white ash (Fraxinus americana) from different land-use categories (i.e., natural forests vs. high-use recreational areas) were selected along a latitudinal gradient in Michigan. Infested trees were selectively sampled based on predetermined crown condition (vigor) classes. While control sites with visually healthy white ash were not available at the same latitudes as the EAB infested sites, the nearest possible controls were sampled in the northern Lower Peninsula and western Upper Peninsula of Michigan. Control sites were based on trees that were visually healthy (no major crown mortality or visible signs and symptoms of EAB). Increment borers were used to non-destructively collect cores of bark, phloem and xylem for both dendrochronology and near-infrared spectroscopy. For the evaluation of dendrochronology, the long-term (21 year) response of white ash to climatic variables was assessed for trees with known EAB infestation and trees that were visually healthy using multiple regression modelling. Bark, phloem and the outermost 20 mm of xylem were measured using NIR spectroscopy to evaluate the ability to differentiate between visually healthy and trees with known EAB infestation using stepwise, linear discriminant analysis. As systemic physical and chemical changes have been observed in girdled and EAB infested trees, this study attempts to use NIR as an indicator of EAB infestation (McCullough et al., 2009a, 2009b; Crook et al., 2008b). Specific wavelengths in the NIR spectrum have been previously assigned to plant structural and chemical defense compounds (Schwanninger et al., 2011). Determining the specific physical and chemical changes as well as assigning NIR wavelength bands to structural and chemical defense compounds is beyond the scope of this project.

Broader Implications

As this exotic insect spreads across the U.S. the economic damage is estimated to reach billions of dollars (Aukema et al., 2011). The ability to detect and delineate infestations of destructive forest insects is essential for management and mitigation of damage. Treatment options using systemic insecticides have proven to be highly effective in preventing mortality of high value urban and shade trees (Herms et al., 2014). As current detection methods for individual trees are often destructive, this project evaluated the potential of two non-destructive methods as indicators of emerald ash borer infestation. Future research would be required for further development of these techniques as detection tools.

REFERENCES

REFERENCES

- Aukema, J.E., Leung, B., Kovacs, K., Chivers, C., Britton, K.O., Englin, J., Frankel, S.J., Haight, R.G., Holmes, T.P., Liebhold, A.M., McCullough, D.G., Von Holle, B. 2011. Economic impacts of non-native forest insects in the continental United States. Plos One 6 e24587.
- Crook, D.J., Khrimian, A., Francese, J.A., Fraser, I., Poland, T., Sawyer, A.J., Mastro, V.C., 2008b. Development of a host-based semiochemical lure for trapping emerald ash borer *Agrilus planipennis* (Coleoptera: Buprestidae). Environmental Entomology 37, 356-365.
- Fritts, H.C., 1976. Tree Rings and Climate. The Blackburn Press, Caldwell, New Jersey, U.S.A.
- Herms, D.A., McCullough, D.G., 2014. Emerald ash borer invasion of North America: history, biology, ecology, impacts, and management. Annual Reviews of Entomology 59, 13-30.
- Herms, D.A., McCullough, D.G., Smitley, D.R., Sadof, C.S., Cranshaw, W., 2014. Insecticide options for protecting ash trees from emerald ash borer. North Central IPM Center Bulletin. 2nd Edition. 16 pp.
- McCullough, D.G., Poland, T.M., Anulewicz, A.C., Cappaert, D., 2009a. Emerald ash borer (Coleoptera: Buprestidae) attraction to stressed or baited ash trees. Environmental Entomology 38, 1668-1679.
- McCullough, D.G., Poland, T.M., Cappaert, D., 2009b. Attraction of the emerald ash borer to ash trees stressed by girdling, herbicide treatment, or wounding. Canadian Journal of Forest Research 39, 1331-1345.
- Poland, T.M., Chen, Y., Koch, J., Pureswaran, D., 2015. Review of the emerald ash borer (Coleoptera: Buprestidae), life history, mating behaviors, host plant selection, and host resistance. Canadian Entomologist 147, 252-262.
- Roberts, C.A., Workman, J., Reeves, J.B. III, (Eds.), 2004. Near-Infrared Spectroscopy in Agriculture. Agronomy, vol. 44, American Societies of Agronomy, Crop and Soil Science, Madison, WI.
- Ryall, K., 2015. Detection and sampling of emerald ash borer (Coleoptera: Buprestidae) infestations. Canadian Entomologist 147, 290-299.
- Schwanninger, M., Rodrigues, J.C., Fackler, K., 2011. A review of band assignments in near infrared spectra of wood and wood components. Journal of Near Infrared Spectroscopy 19, 287-308.
- Speer, J.H., 2010. Fundamentals of tree-ring research. The University of Arizona Press, Tucscon, Arizona.

CHAPTER 1

INTRODUCTION AND LITERATURE REVIEW

1.1. Introduction

The emerald ash borer (EAB) (*Agrilus planipennis* Fairmaire) is a phloem-feeding beetle native to Asia identified in southeast Michigan in 2002 as the cause of extensive decline and mortality of ash (*Fraxinus* spp.) (Anulewicz et al., 2008). Since its recent discovery, emerald ash borer, (Coleoptera: Buprestidae), has killed millions of ash trees (*Fraxinus* spp.) in the eastern U.S. and parts of Canada, and is continuing to spread rapidly (Ryall, 2015). Current methods in detecting emerald ash borer infestation early and at a large scale are limited, restricting the ability to effectively manage for this insect. It is imperative to develop cost-effective approaches in implementing regional scale methods for early detection of EAB. By using cross-dating techniques on cores collected from the initial infestation area of Detroit, Michigan, dendrochronological data has shown that EAB was established for around 10 years before first being detected (Siegert et al., 2014). As of 2015, EAB has killed tens of millions of ash trees in the eastern United States as well as parts of Canada and annually causes billions of dollars' worth of damage (Ryall, 2015; Aukema et al., 2011). EAB is not considered a major pest where it is native in Asia, and does not cause widespread mortality of the more resistant Asian ash species including *Fraxinus mandshurica and F. chinensis* (Poland and McCullough, 2006). Ongoing research efforts are focused on developing methods for early detection of emerald ash borer (Ryall, 2015)

1.2. Detection Techniques for Invasive Insects

Early detection of potentially invasive insect species is a key aspect of preventing these species from causing damage (Parry and Teale, 2011). In practice, this is difficult and often, non-native species are not detected until after they are already established (Parry and Teale, 2011). Studies have indicated that invasion management efforts are typically more feasible and efficient if they are applied as early as possible (Liebhold, 2012; Tobin et al., 2014). Eradication may be possible if new colonies of potentially

invasive insects are detected early when the insect is still in a limited geographic area (Liebhold, 2012). After initial detection, delimitation surveys are implemented to determine where the invasive insect population is distributed in the new environment (Parry and Teale, 2011). Control measures cannot be applied without information of where the insect is located. Detection methods are often specific to the species causing the damage, the life stage under observation and type of damage caused/feeding behavior (Parry and Teale, 2011; Brockerhoff et al., 2006). General survey methods may utilize aerial surveys; observations of the insect itself; the signs, symptoms, or damage caused by the insect; and baited traps (Parry and Teale, 2011).

Insects that feed within trees are typically more difficult to detect than insects that feed on external tree tissues (Tobin et al., 2014). Bark beetle and wood borer detection methods involve ground surveys in well-roaded areas, aerial surveys for large areas, and the use of host volatile or sex pheromone baited traps (Edmonds et al., 2000). Attractants are not available for many insects and their detection is difficult (Brockerhoff et al., 2010). Recent developments include DNA-based methods. DNA "barcodes" for example, identify species with 100% accuracy (Brockerhoff et al., 2006). This method has great potential, but requires the development of global DNA databases for all relevant taxa in order to provide a standardized tool for worldwide use (Brockerhoff et al., 2006). Dendrochronology has also been used to reconstruct past outbreak dynamics and spread of invasive insect species (Siegert et al., 2014; Muzika et al., 1999; Naidoo and Lechowicz, 2001; Rentch et al., 2009).

Spectroscopic and imaging techniques have been applied successfully for plant stress detection, particularly in agriculture and have potential for rapid, non-destructive, and cost-effective detection of damaging insects (Sankaran et al., 2010). Hyperspectral imaging is used in agriculture and some forestry applications by acquiring the spectral reflectance in the visible and infrared regions of the electromagnetic spectrum (Sankaran et al., 2010). In particular, studies have shown that hyperspectral remote sensing can produce detailed maps of forest health conditions and species distribution on a landscape scale (Pontius et al., 2008). There has also been studies looking at the volatile organic compounds (VOC) released by

vegetation which are influenced by humidity, temperature, light, soil conditions, fertilization, growth and developmental stage, and insect presence/damage (Sankaran et al., 2010; Chen et al., 2011).

1.3. Emerald Ash Borer

1.3.1. Life Cycle

The life cycle of an individual emerald ash borer is typically completed in one year, although some individuals may need two years to complete their development (Tluczek et al., 2011). Two year life cycles have been observed on recently infested trees with low population levels of EAB, in areas with cooler climates, or associated with late summer oviposition (Herms and McCullough, 2014; Poland et al., 2015). Adult beetles emerge in May or June leaving behind D-shaped exit holes on the tree and live for about 3 to 6 weeks, during which they feed and mate (Cappaert et al., 2005). The adults are typically more active on warm (>25 °C), sunny days (Poland et al., 2015). After feeding on ash foliage for at least two weeks, mated females lay around 60 to 80 eggs in bark crevices from late June through August, which hatch within 2 weeks when temperatures are around 25 °C (Poland et al., 2015). The larvae then chew their way into the bark and create serpentine shaped galleries packed with frass as they feed in the phloem, cambium, and outer xylem (Poland et al., 2015). Extensive feeding by the larvae disrupts translocation of nutrients, and can girdle and kill a tree in 2-4 years after crown dieback becomes noticeable (Herms and McCullough, 2014). EAB will typically complete 4 instars before overwintering as prepupal larvae in the outer 1-2 cm of sapwood or bark beginning in October (Cappaert et al., 2005; Herms and McCullough, 2014). Two year life cycles occur when the larvae overwinter as early instars, continue to feed a second summer, and overwinter the second year as prepupae (Tluczek et al., 2011). Pupation will take place from the middle of April through May for about 3 weeks, followed by adult emergence (Poland and McCullough, 2006). As the damage is done beneath the bark, infestation is difficult to detect in newly infested trees as there is often a delay between initial infestation and when visual symptoms develop (Ryall, 2015).

1.3.2. Host Species and Spread

Ash is a fast growing woodland tree and has been planted extensively in urban areas which are often unfavorable sites (Poland and McCullough, 2006). The 16 endemic species of ash in North America are susceptible to EAB induced mortality in the United States alone, and potential hosts in the US range from Northern Maine to Southern California (Poland and McCullough, 2006). Where EAB is native, it typically only targets stressed or dying species of Asian ash, but has caused high mortality on North American ash species planted in its native range (Poland et al., 2015). The two most common North American ash species, white (F. americana) and green (F. pennsylvanica) are taxonomically and economically important, but identification is complicated by their ability to hybridize (MacFarlane and Meyer, 2005). While there appears to be strong preference for some species over others, all North American ash species located in its current range have proven to be susceptible to EAB infestation and decline to some extent (DeSantis et al., 2013; Herms and McCullough, 2014; Tanis and McCullough, 2012). The North American species, blue ash (Fraxinus quadrangulata Michx.) can be colonized by EAB but has been shown to have higher resistance compared to other native ash species (Tanis and McCullough, 2012). While females will sometimes oviposit on non-ash species, the larvae have not been observed surviving or developing on any tree that is not in the genus Fraxinus in North America (Anulewicz et al., 2008). The supercooling point for EAB is -35.3 °C: at and below this temperature EAB freezes and dies (DeSantis et al., 2013). It is expected however, that North American EAB distribution will be limited more by host range instead of climate (Herms and McCullough, 2014). EAB adults can fly away from the tree where they emerge, but the spread is primarily facilitated by people moving infested ash into uninfested areas (EAB info, 2013). Human activities as a primary method of dispersal predispose urban forests for introductions and establishment of EAB (Herms and McCullough, 2014). Due to the ability of EAB to spread rapidly, research efforts have focused on identifying and developing new methods for early detection.

Evidence suggests that adult EAB use visual and olfactory cues in locating and selecting hosts (Pureswaran and Poland, 2009). There also appears to be adult preference for rough-barked trees over

smooth-barked trees and will generally target trees grown in open conditions compared to shaded conditions (Anulewicz et al., 2008; McCullough et al., 2009a, 2009b). Adults are also attracted to specific shades of green and purple (Crook et al., 2014). Host volatiles produced by ash are highly attractive to adult beetles and bark sesquiterpenes and green leaf volatiles have been identified (Crook et al., 2008b; Crook et al., 2010; Grant et al., 2010; Ryall, 2015). These volatiles often increase with host stress and girdled ash trees are highly attractive to adult EAB (Grant et al., 2010; Crook et al., 2008b).

1.3.3. Past and Present Detection Methods and Treatment Options

After the discovery of EAB in North America, initial monitoring was based on the visual signs and symptoms of infestation such as D-shaped exit holes left by the emerging adults, longitudinal cracks in the bark over the S-shaped larval galleries, canopy dieback, epicormic shoots and woodpecker damage (Crook and Mastro, 2010). Accurate detection and monitoring methods of EAB populations and newly established infestations have been difficult to develop, which greatly hinders the ability to effectively manage for this pest. In addition to the lengthy amount of time before visual symptoms develop, on the ground detection is further complicated by the fact that adult EAB will typically target the upper portion of a tree during the initial infestation (Poland and McCullough, 2006). Furthermore, there has been an inability to identify a long range sex pheromone (Domingue et al., 2013). Two short range, contact pheromones produced by adult emerald ash borer females have been identified which are antennally attractive to the males and have been used to improve trap captures (Silk et al., 2009; Silk et al., 2015; Poland et al., 2015; Crook and Mastro, 2010). Currently, key survey methods include the use of external signs and symptoms, sticky traps baited with ash volatile lures, green multi-funnel traps, trap logs, and using girdled trap trees which are an expensive and destructive method (Poland and McCullough, 2006; Domingue et al., 2013; McCullough et al., 2011; Crook et al., 2014). Trap trees involve girdling (removing a band of bark and phloem from around the tree) individual trees which become highly attractive to the adult beetles (McCullough et al., 2009a, 2009b). After 1 to 2 years the tree is felled and debarked in autumn to inspect for EAB larvae and S-shaped galleries (McCullough and Siegert, 2007).

Artificial traps include the sticky prism traps (Crook et al., 2014; Francese et al., 2008), double-decker traps (Poland et al., 2011; McCullough et al., 2011), and Lindgren green multi-funnel traps (Francese et al., 2013) (Ryall, 2015). The manufactured sticky prism traps currently used for EAB are visually attractive purple and green made from corrugated plastic covered in sticky glue, which are typically baited with host volatile lures (Crook and Mastro, 2010; Crook et al., 2014). Efforts in the United States include deploying thousands of these baited purple prism traps (McCullough and Mercader, 2012; USDA APHIS PPQ, 2015). Purple traps generally catch more females than males, and green traps (when hung ~13 m in the canopy) will catch more males than females (Crook and Mastro, 2010). Green multi-funnel traps treated with a slippery coating have demonstrated potential as an effective and reusable detection and survey tool (Crook et al., 2014). These green multi-funnel traps have recently started being deployed in the United States in addition to the purple prism traps (USDA APHIS PPQ, 2015). While artificial traps are visually attractive to adult beetles, the effectiveness of traps depends on lure types and combinations and placement of the traps (Ryall, 2015). Improvements to EAB lures are still a focus of EAB detection research and the (Z)-3-hexanol lure is the current recommendation by the USDA APHIS for trap deployment (Crook et al., 2014; Ryall, 2015; USDA APHIS PPQ, 2015). Girdled trap trees are more likely to detect EAB at low populations compared to artificial baited traps (Mercader et al., 2013). The study by Ryall et al. (2011) developed a detection method for urban trees that involves the collection of branches that are subsequently debarked and inspected for EAB feeding activity. Preliminary studies utilizing hyperspectral remote sensing have explored as a potential method for emerald ash borer detection and surveying (Eastman et al., 2005; Pontius et al., 2008; Bartels et al., 2007).

The long-term outlook for North American ash survival does not look promising, but treatment options do exist for high value urban and shade trees and efforts are underway to slow the spread of EAB (Herms et al., 2014). Research has shown that even with large EAB populations, some insecticide options can be highly effective in keeping treated trees alive (Herms et al., 2014). Some estimates have indicated that the cost of treating high value landscape and urban ash trees with systemic insecticides can be less than if the trees were removed (Herms et al., 2014). There are four categories of insecticides that are

currently being used to control EAB: 1) systemic insecticides applied as soil injections; 2) systemic insecticides applied as trunk injections; 3) systemic insecticides applied as lower trunk sprays; and 4) protective cover sprays applied to the trunk, branches, foliage (Herms et al., 2014). These insecticide treatments are most effective when applied as soon as possible to relatively healthy trees, as trees that have lost more than 50% of its crown are usually too far gone to save (Herms et al., 2014). In 2008, a pilot project to slow the impact of EAB, called SLAM (Slow Ash Mortality) was initiated as an integrated strategy for dealing with recently established outlier sites (McCullough and Mercader, 2012). The SLAM pilot project used girdled ash trees, a systemic insecticide, and removed ash trees (McCullough and Mercader, 2012). Long-term conservation of ash and reductions of EAB populations in North America efforts have invested in classical biological control and three parasitoids native to China are currently being released in the United States (USDA-APHIS, 2012). At this time, the long-term impact of the biological control species on EAB populations is uncertain (Herms and McCullough, 2014).

1.4. Dendrochronology

Dendrochronology is the study of tree ring dating to explain surrounding environmental information including climate, disturbance events, stand composition and insect herbivory throughout a tree's lifetime (Speer, 2010). Previous studies have shown the usefulness of dendrochronological methods for observing the impacts of climate, disturbance events, insects and diseases on radial growth (Zhang et al., 1999; Siegert et al., 2014; Chhin et al., 2010). In dendrochronology, valid inferences can be made indirectly about the mechanisms of tree response to their environment (Fritts, 1976). Dendroclimatology (a subfield of dendrochronology) is the study of past and present climates using climatic information and tree ring growth (Fritts, 1971). Trees are highly responsive to their surrounding environments and climatic factors (i.e., temperature and precipitation) in particular have been shown to be primary controlling factors on ring growth (Speer, 2010). Trees growing in different regions are often limited by different forms of climate; for example, trees growing in the American Southwest are typically limited by

moisture availability while at higher latitudes, temperature is the primary limiting factor (Sheppard, 2010; Briffa et al., 1998).

Dendroentomology utilizes tree ring principles to identify the years of outbreak and the dynamics of past insect herbivory on trees. Dendrochronological studies have shown that the mountain pine beetle (*Dendroctonus ponderosae*), a bark beetle native to North America that occurs primarily on lodgepole pine (*Pinus contorta*) shows periodic outbreaks approximately every 40 years in central British Columbia (Taylor et al., 2006). Rentch et al. (2009) used dendrochronology to relate changes in radial growth with crown condition in eastern hemlock (*Tsuga Canadensis*) infested by hemlock woolly adelgid (*Adelges tsugae*). A previous study was conducted on green ash (*Fraxinus pennsylvanica*) to reconstruct the spread of emerald ash borer near the epicenter of initial EAB establishment in North America (southeast Michigan) (Siegert et al. 2014). Using a systematic grid, Siegert et al. (2014) collected samples from a geographic area in southeast Michigan (around 1.5 million ha) in order to reconstruct the initial establishment and spread of EAB. Siegert et al. (2014) concluded that EAB was established in Michigan by the early to mid-1990s, several years before it was officially discovered in 2002.

1.5. Near-Infrared Spectroscopy (NIR)

Near-infrared spectroscopy (NIR) is becoming an increasingly popular technique in a wide range of industries (agricultural, pharmaceutical, industrial, wood-products industry and forestry). NIR is an appealing technique as it investigates the vibrational properties of materials rapidly and nondestructively (Siesler et al., 2002). The near-infrared (NIR) region is located in the 780 to 2500 nm region of the electromagnetic spectrum (EMS) between the visible and infrared regions (Roberts et al., 2004). Modern NIR spectroscopy (post 1960s) incorporates high performance and commercially available spectrometers with multivariate analysis to provide chemical and physical information for both biological and manufactured materials (Roberts et al., 2004). Compared to chemical analysis, which is destructive and costly for relatively small amounts of samples, NIR can non-destructively analyze bulk materials rapidly with minimal sample preparation (Roberts et al., 2004). For NIR studies measuring wood, the spectra are

either collected in diffuse reflectance or transmission modes (Schwanninger et al., 2011). Transmission typically is limited in its application because this method requires more sample preparation such as milling or slicing (Schwanninger et al., 2011). Diffuse reflectance has a wider application as it can measure intact, solid samples in addition to samples whose original state has been altered (although changing the physical state of samples will influence spectra) (Schwanninger et al., 2011). A NIR diffuse reflectance spectrum is a composite of chemical and physical properties of a material (Roberts et al., 2004). Diffuse reflectance works by sending a beam of light to the object being measured, where it interacts with the sample before being reflected back to the spectrometer (Roberts et al., 2004). NIR spectra are unique for every substance, and if two or more samples have similar spectra, it can be assumed that they have similar chemical and physical composition (Roberts et al., 2004). Conversely, if the spectra of multiple samples are different, it can be assumed that the materials are physically and/or chemically different (Roberts et al., 2004).

In NIR studies, multivariate calibrations are often required for spectral analysis. While there are a wide variety of multivariate analytical methods that are used for NIR analysis, they can be separated between two distinct groups, quantitative and qualitative analysis. A qualitative method, discriminant analysis, is used for sorting spectra by sample type and applying the technique to compare the different groups (Burns and Ciurczak, 2008). Discriminant analysis is used for NIR spectroscopic analysis in order to qualitatively determine whether a sample is similar or different compared to samples from one or more predetermined groups (Roberts et al., 2004). Discriminant analysis has been successfully used in several previous NIR studies for classifying spectral samples based on distinct groups (Ertlen et al., 2010; Evans et al., 2008; Watanabe et al., 2012). Ertlen et al. (2010) successfully used multiple discriminant analysis to distinguish between grassland and forest soils. Evans et al. (2008) saw that while discriminant analysis improved the identification of wood from two tree species compared to existing identification methods, classification was still not perfect. Watanabe et al. (2012) were able to successfully identify intact wood compared to wood with wet-pockets using two different variants of discriminant analysis.

The majority of NIR research done for trees is implemented in the wood products industry for wood structural quality and decay; however this technique is increasingly being explored for alternative applications in forestry (So et al., 2004; Schimleck, 2008). NIR studies for assessing various wood properties (i.e., wood density) have been applied to both hardwoods and softwoods (Schimleck et al., 2002). Wood properties are highly influenced by the amount of moisture in the sample, the effects of which can be minimized by oven drying all samples before collecting NIR measurements (Schwanninger et al., 2011). While not extensively, NIR has been successfully used for assessing various forest health concerns and decay in trees (Riggins et al., 2011; Pontius et al., 2008; Fackler and Schwanninger, 2012). The majority of NIR based studies for tree decline due to insect infestation have measured foliage samples, while studies on decay will measure wood samples (Pontius et al., 2005; Pontius et al., 2008; Riggins et al., 2011; Fackler et al., 2007; Green et al., 2012). Field-based NIR spectrometers and satellitebased hyperspectral NIR has the potential to detect early stages of hemlock wooly adelgid induced hemlock decline by measuring foliage (Pontius et al., 2005). Watanabe et al. (2012) reported that spectroscopy in the visible light and near-infrared ranges (VIS-NIR) could discriminate between wood with wet-pockets and wood free of wet-pockets. To assess oak decline due to outbreaks of the insect pest (Enaphalodes rufulus) a handheld NIR spectrometer measured foliage samples to describe plant stress (Riggins et al., 2011).

Several studies have explored the potential of utilizing hyperspectral imaging for detecting and mapping emerald ash borer infestations (Pontius et al., 2008; Eastman et al., 2005; Hallett et al., 2007; Bartels et al., 2007; Zhang et al., 2014). Bartels et al. (2007) found that when using hyperspectral images and LIDAR data for identifying hardwood tree species and EAB declining ash trees, misclassification of different tree species occurred. However, they were able to use hyperspectral imagery for classifying multiple ash health categories with accuracy up to 60-70% (Bartels et al., 2007). Maps created using hyperspectral imagery and vegetation indices were able to identify 5 different ash decline classes (due to EAB infestation) at 97% accuracy (Pontius et al., 2008). A recent case study for EAB detection in Canada using multisourced data (both a variety of commercially available remotely sensed data and archived

maps), highlighted that current challenges prevent effective use of hyperspectral technologies for detection and mapping EAB infestation (Zhang et al., 2014). These challenges include being labor intensive and lengthy manual corrections of segmentations, limited data sources, and timing of image acquisitions (Zhang et al., 2014).

1.6. Study Area and Ash Species of Michigan

All areas sampled in this study took place within Michigan, USA. There are five species of ash that are native to Michigan: white ash (*Fraxinus americana*), black ash (*F. nigra*), green (red) ash (*F. pennsylvanica*), blue ash (*F. quadrangulata*), and pumpkin ash (*F. profunda*) (Dickmann, 2004). This study sampled white ash as it is both economically and ecologically important and found throughout Michigan.

Michigan has diverse soil parent materials and a wide variety of forest cover types that are primarily deciduous but also contain significant coniferous forests (Johnson, 1995). Most of the forested land in Michigan is under private ownership but a significant percentage consists of state and public ownership (Johnson, 1995). Both tourism and the timber are major industries (Johnson, 1995).

Approximately 95% of Michigan's 36.3 million acres was forested prior to European settlement in the 17th century (Dickmann, 2004). Today, approximately 50 percent of the state is still forested, the majority occurring in the northern Lower Peninsula and throughout the Upper Peninsula (Dickmann, 2004). The southern Lower Peninsula only has approximately 21 percent scattered forests and wetlands while the western Upper Peninsula has approximately 88 percent, continuous forested land (Dickmann, 2004).

Starting in the mid-1800s to the early 1900s, the original forests of Michigan underwent widespread logging often followed by intense slash fires (Schulte et al., 2007). Reforestation primarily through natural regeneration occurred due to fire suppression efforts beginning in the 1930s (Schulte et al., 2007). Therefore, the majority of Michigan's forests are relatively young and old-growth forests are rare (Dickmann, 2004). While the forests today are quite different from historic conditions, Michigan has the largest amount of vegetation types of any Midwest state (Dickmann, 2004). The soils and vegetation of

Michigan are strongly influenced by glacial history and the proximity of Michigan to the Great Lakes has created a Lake-effect climate characterized by less severe temperatures extremes and heavy winter snow fall (Schulte et al., 2007).

Tree distributions in Michigan have been shown to be strongly correlated to climatic spatial gradients associated with latitude, longitude, elevation, and proximity to the Great Lakes (Denton and Barnes, 1987). In the Lake States region (i.e. Michigan, Wisconsin and Minnesota), summer precipitation is frequently associated with thunderstorms (Johnson, 1995). A possible natural disturbance of Michigan forests could be a result of the high winds associated with these common summer thunderstorms (Denton and Barnes, 1988). Winter is generally cold and long, and the entire lakes states region is covered by snow from December to April (Johnson, 1995). The study by Denton and Barnes (1988) classified the entire state of Michigan into three regions based on distinct climatic patterns using variables important for tree growth. These regions include (1) the southern half of the Lower Peninsula, (2) the northern half of the Lower Peninsula and the eastern Upper Peninsula, and (3) the western Upper Peninsula. Climatic variables are highly correlated to latitude, particularly in the Lower Peninsula (Denton and Barnes, 1988). The southernmost region (1) is generally warmer with a longer growing season and is less likely to experience spring frost compared to the more northern regions (2 and 3) (Denton and Barnes, 1988). In the southernmost region, urbanization has an equal or greater influence on climate when compared to latitude or proximity to the great lakes (Denton and Barnes, 1988). The more northern regions of Michigan are generally cooler, with more snow and less growing season precipitation, but also with less potential evapotranspiration compared to the southern part of the state (Denton and Barnes, 1988).

White ash is considered one of the most commercially important ash species and its wood is used in products such as baseball bats, furniture and tool handles (Solomon et al., 1993; MacFarlane and Meyer, 2005). It generally grows on upland sites and performs best on well-drained soils with high nitrogen and calcium content and can tolerate a pH range from 5.0 to 7.5 (MacFarlane and Meyer 2005, Burns and Honkala, 1990). Primary associates of white ash include eastern white pine (*Pinus strobus*), northern red oak (*Quercus rubra*), white oak (*Q. alba*), sugar maple (*Acer saccharum*), red maple (*A.*

rubrum), yellow birch (Betula alleghaniensis), American beech (Fagus grandifolia), black cherry (Prunus serotina), American basswood (Tilia americana), eastern hemlock (Tsuga canadensis), American elm (Ulmus americana), and yellow-poplar (Liriodendron tulipifera) (Burns and Honkala, 1990). White ash is dioecious, producing a large seed crop (wind dispersed) every three years at a minimum age of 20 years (Burns and Honkala, 1990). White ash seedlings are shade-tolerant and are highly abundant in the understory of many eastern North American forests, growing into the overstory only when provided with sufficient light (Burns and Honkala, 1990; Hardin et al., 2001). It is a common pioneer species of fertile sites such as abandoned farms, and can reproduce by sprouting readily from stumps (Burns and Honkala, 1990; Hardin et al., 2001). Once it grows past the seedling stage, white ash has intermediate to low shade tolerance (Hardin et al., 2001). Under ideal site conditions, sprouts and young trees can grow rapidly, and in the first year of development, individuals often reach a height of 1.5 meters or greater (Hardin et al., 2001). In less than ideal conditions, it can take an individual 3 to 15 years to reach 1.5 meters (Burns and Honkala, 1990).

In addition to EAB, pollutants as well as native insects and diseases cause damage to white ash (Solomon et al., 1993). For ash trees larger than pole size, it is estimated that one-third contain some heart-rot and up to 90% of the seed crop can be destroyed by seed insects (Solomon et al., 1993). Ashes have been planted as urban trees in the Eastern United States in part due to not being a preferred host of the non-native defoliator, gypsy moth (*Lymantria dispar* L.) (Solomon et al., 1993). Before the discovery of EAB, ash yellows was considered the most serious health concern for white ash (Hardin et al. 2001). Ash yellows causes slow growth, decline, occasionally premature death of ash, and is caused by phytoplasmas (Sinclair and Lyon, 2005). There are several species of insects that feed on ash throughout North America whose populations are often kept in check by natural enemies. The ash borer (*Podosesia syringae*), is a destructive wood boring pest throughout eastern North America, that degrades wood value in timber and can cause tree mortality (Solomon et al., 1993). The carpenterworm (*Prionoxystus robinae*) is another wood boring insect that damages ornamental, shelterbelt, and lumber trees throughout the U.S. and Canada (Solomon et al., 1993). Generally, ash species have intermediate sensitivity to sulfur dioxide

and hydrogen fluoride emissions and are sensitive to ozone (Solomon et al., 1993). The majority of native insects, disease, and abiotic factors do not cause widespread decline and mortality of white ash in North America.

1.7. Thesis Objectives and Structure

The overall objective of this thesis is to explore the potential of utilizing dendrochronology and near infrared spectroscopy (NIR) in determining the presence emerald ash borer infestation in white ash. Chapter 2 explores the utilization of dendrochronological techniques in emerald ash borer detection and radial growth relationships with climatic variables. Chapter 3 examines the use of near infrared spectroscopy as applied on ash bark, phloem and xylem samples for discriminating between EAB infested and healthy tissues. This study took place in both the Lower and Upper Peninsulas of Michigan. Chapter 4 summarizes the findings for chapters two and three and discusses future research options.

REFERENCES

REFERENCES

- Anulewicz, A.C., McCullough, D.G., Cappaert, D. L., Poland, T.M., 2008. Host range of the emerald ash borer (*Agrilus planipennis* Fairmaire) (Coleoptera: Buprestidae) in North America: results of multiple-choice field experiments. Environmental Entomology 37, 230-241.
- Aukema, J.E., Leung, B., Kovacs, K., Chivers, C., Britton, K.O., Englin, J., Frankel, S.J., Haight, R.G., Holmes, T.P., Liebhold, A.M., McCullough, D.G., Von Holle, B. 2011. Economic impacts of non-native forest insects in the Continental United States. Plos One 6 e24587.
- Bartels, D., Williams, D., Ellenwood, J., Sapio, F., 2007. Accuracy assessment of remote sensing imagery for mapping hardwood trees and stressed ash trees. Emerald Ash Borer Research and Development Review Meeting 2007, pp 63-65.
- Briffa, K.R., Schweingruber, F.H., Jones, P.D., Osborn, T.J., Shiyatov, S.G., Vaganov, E.A., 1998. Reduced sensitivity of recent tree-growth to temperature at high northern latitudes. Nature 391, 678-682.
- Brockerhoff, E.G., Liebhold, A.M., Richardson, B., Suckling, D.M. 2010. Eradication of invasive forest insects: concepts, methods, costs and benefits. New Zealand Journal of Forestry Science 40 117-135.
- Brockerhoff, E.G., Liebhold, A.M., Jactel, H. 2006. The ecology of forest insect invasions and advances in their management. Canadian Journal of Forest Research 36, 263-268.
- Burns DA, Ciurczak, EW (Editors). 2008. Handbook of near-infrared analysis (3rd Edition). Practical spectroscopy; 35.
- Burns, Russell M., and Barbara H. Honkala, tech. coords. 1990. Silvics of North America: 1. Conifers; 2. Hardwoods. Agriculture Handbook 654. U.S. Department of Agriculture, Forest Service, Washington, DC. vol.2, 877 p.
- Cappeart, D., McCullough, D.G., Poland, T.M., Siegert, N.W., 2005. Emerald ash borer in North America: a research and regulatory challenge. American Entomologist 51, 152-165.
- Chen, Y., Whitehill, J.G.A., Bonello, P., Poland, T.M. 2011. Feeding by emerald ash borer larvae induces systemic changes in black ash foliar chemistry. Phytochemistry 72, 1990-1998.
- Chhin, S., 2010. Influence of climate on the growth of hybrid poplar in Michigan. Forests 1, 209-229.
- Crook, D.J., Khrimian, A., Francese, J.A., Fraser, I., Poland, T., Sawyer, A.J., Mastro, V.C., 2008b. Development of a host-based semiochemical lure for trapping emerald ash borer *Agrilus planipennis* (Coleoptera: Buprestidae). Environmental Entomology 37, 356-365.
- Crook, D. J., Mastro, V.C., 2010. Chemical ecology of the emerald ash borer Agrilus planipennis. Journal of Chemical Ecology 36, 101–112.
- Crook, D.J., Francese, J.A., Rietz, M.L., Lance, D.R., Hull-Sanders, H.M., Mastro, V.C., Silk, P.J., Ryall, K.L., 2014. Improving detection tools for emerald ash borer (Coleoptera: Buprestidae):

- Comparison of multifunnel traps, prism traps, and lure types at varying population densities. Journal of Economic Entomology 107, 1496-1501.
- Denton, S.R., Barnes, B.V., 1987. Tree species distributions related to climatic patterns in Michigan. Canadian Journal of Forest Research 17, 613-629.
- Denton, S.R., Barnes, B.V., 1988. An ecological climatic classification of Michigan: a quantitative approach. Forest Science 34, 119-138.
- DeSantis, R.D., Moser, W.K., Gormanson, D.D., Bartlett, M.G., Vermunt, B. 2013. Effects of climate on emerald ash borer mortality and the potential for ash survival in North America. Agricultural and Forest Meteorology 178-179, 120-128.
- Dickmann, D.I., 2004. Michigan Forest Communities: A Field Guide and Reference. Michigan State University Extension.
- Domingue, M.J., Lelito, J.P., Fraser, I., Mastro, V.C., Tumlinson, J.H., Baker, T.C. 2013. Visual and chemical cues affecting the detection rate of the emerald ash borer in sticky traps. Journal of Applied Entomology 137, 77-87.
- EAB.info. 2013. Emerald Ash Borer Info. Available at: www.emeraldashborer.info
- Eastman, J.R., Zhu, H., Lazar, A., Williams, D.W., 2005. Progress on remote sensing applications for emerald ash borer survey: analysis of 2004 hyperspectral imagery. Emerald Ash Borer Research and Technology Development Meeting.
- Edmonds, R.L., Agee, J.K., Gara, R.I. 2000. Forest Health and Protection. McGraw-Hill Companies, Inc.
- Ertlen, D., Schwartz, D., Trautmann, M., Webster, R., Brunet, D. 2010. Discriminating between organic matter in soil from grass and forest by near-infrared spectroscopy. European Journal of Soil Science 61, 207-216.
- Evans, P., Heady, R., Cunningham, R., 2008. Identification of yellow stringybark (*Eucalyptus muelleriana*) and silvertop ash (*E. Sieberi*) wood is improved by canonical variate analysis of ray anatomy. Australian Forestry 71, 94-99.
- Fackler, K., Schwanninger, M., 2012. How spectroscopy and microspectroscopy of degraded wood contribute to understand fungal wood decay. Applied Microbiology and Biotechnology 96, 587-599.
- Fackler, K., Schwanninger, M., Gradinger, C., Sreobotnik, E., Hinterstoisser, B., Messner, K., 2007. Fungal decay of spruce and beech wood assessed by near-infrared spectroscopy in combination with uni- and multivariate data analysis. Holzforschung 61, 680-687.
- Francese, J.A., Oliver, J.B., Fraser, I., Lance, D.R., Youssef, N., Sawyer, A.J., Mastro, V.C., 2009. Influence of trap placement and design on capture of the emerald ash borer (Coleoptera: Buprestidae). Journal of Economic Entomology 101, 1831-1837.
- Francese, J.A., Rietz, M.L., Crook, D.J., Fraser, I., Lance, D.R., Mastro, V.C., 2013. Improving detection tools for the emerald ash borer (Coleoptera: Buprestidae): Comparison of prism and multifunnel traps at varying population densities. Journal of Economic Entomology 106, 2407-2414.

- Fritts, H. C., 1971. Dendroclimatology and Dendrocology. Quaternary Research 1, 419-449.
- Fritts, H.C., 1976. Tree Rings and Climate. The Blackburn Press, Caldwell, New Jersey, U.S.A.
- Grant, G.G., Ryall, K.L., Lyons, D.B., Abou-Zaid, M.M., 2010. Differential response of male and female emerald ash borers (Col., Buprestidae) to (Z)-3-hexanol and Manuka oil. Journal of Applied Entomology 134, 1-8.
- Green, B., Jones, P.D., Nicholas, D.D., Schimleck, L.R., Shmulsky, R., Dahlen, J., 2012. Assessment of the early signs of decay of *Populus deltoids* wafers exposed to *Trametes versicolor* by near infrared spectroscopy. Holzforschung 66, 515-520.
- Hallett, R., Pontius, J., Martin, M., Plourde, L., 2007. The practical utility of hyperspectral remote sensing for early detection of emerald ash borer. Emerald Ash Borer Research and Development Review Meeting 2007, pp 67-68.
- Hardin, J.W., Leopold, D.J., White, F.M. 2001. Textbook of Dendrology. Edition 9. McGraw-Hill Higher Education.
- Herms, D.A., McCullough, D.G., 2014. Emerald ash borer invasion of North America: history, biology, ecology, impacts, and management. Annual Reviews of Entomology 59, 13-30.
- Herms, D.A., McCullough, D.G., Smitley, D.R., Sadof, C.S., Cranshaw, W., 2014. Insecticide options for protecting ash trees from emerald ash borer. North Central IPM Center Bulletin. 2nd Edition. 16 pp.
- Johnson, J.E., 1995. The Lake States Region, in: Barrett, J.W., 1995. Regional silviculture of the United States, third edition. John Wiley and Sons Inc. New York, New York, pp. 81 127.
- Liebhold, A.M. 2012. Forest pest management in a changing world. International Journal of Pest Management 58, 289-295.
- Macfarlane, D.W., Meyer, S.P., 2005. Characteristics and distribution of potential ash tree hosts for emerald ash borer. Forest Ecology and Management 213, 15–24.
- McCullough, D.G., Siegert, N.W. 2007. Using girdled trap trees effectively for emerald ash borer detection, delimitation and survey. Michigan State University, USDA Forest Service, Forest Health Protection.
- McCullough, D.G., Poland, T.M., Anulewicz, A.C., Cappaert, D., 2009a. Emerald ash borer (Coleoptera: Buprestidae) attraction to stressed or baited ash trees. Environmental Entomology 38, 1668-1679.
- McCullough, D.G., Poland, T.M., Cappaert, D., 2009b. Attraction of the emerald ash borer to ash trees stressed by girdling, herbicide treatment, or wounding. Canadian Journal of Forest Research 39, 1331-1345.
- McCullough, D.G., Mercader, R.J. 2012. Evaluation of potential strategies to SLow Ash Mortality (SLAM) caused by emerald ash borer (*Agrilus planipennis*): SLAM in an urban forest. International Journal of Pest Management, 58, 9-23.

- McCullough, D.G., Siegert, N.W., Poland, T.M., Pierce, S.J., Ahn, S.Z. 2011. Effects of trap type, placement and ash distribution on emerald ash borer captures in a low density site. Environmental Entomology 40, 1239-1252.
- Mercader, R.J., Siegert, N.W., McCullough, D. G., 2012. Estimating the influence of population density and dispersal behavior on the ability to detect and monitor *Agrilus planipennis* (Coleoptera: Buprestidae) populations. Journal of Economic Entomology 105, 272-281.
- Mercader, R.J., McCullough, D.G., Bedford, J.M., 2013. A comparison of girdled ash detection trees and baited artificial traps for *Agrilus planipennis* (Coleoptera: Buprestidae) detection. Environmental Entomology 42, 1027-1039.
- Muzika, R. M., Liebhold, A. M. 1999. Changes in radial increment of host and nonhost tree species with gypsy moth defoliation. Canadian Journal of Forest Research 29, 1365-1373.
- Naidoo, R., Lechowicz, M.J. 2001. Effects of Gypsy Moth on Radial Growth of Deciduous Trees. Forest Science 47, 338-348.
- Parry, D., Teale, S.A., 2011. Alien invasions: the effects of introduced species on forest structure and function. Castello, J.D., Teale, S.A., (Editors). In Forest Health: An Integrated Perspective . Cambridge University Press. pp 115-162.
- Pontius, J., Hallett, R., Martin, M., 2005. Assessing hemlock decline using visible and near-infrared spectroscopy: indices comparison and algorithm development. Applied Spectroscopy 59, 836-843.
- Pontius, J., Martin, M., Plourde, L., Hallett ,R., 2008. Ash decline assessment in emerald ash borer infested regions: A test of tree-level, hyperspectral technologies. Remote Sensing of Environment 112, 2665–2676
- Poland, T.M., McCullough, D.G., 2006. Emerald ash borer: invasion of the urban forest and the threat to North America's ash resource. Journal of Forestry pp. 118-124.
- Poland, T.M., McCullough, D.G., Anulewicz, A.C., 2011. Evaluation of double-decker traps for emerald ash borer (Coleoptera: Buprestidae). Journal of Economic Entomology 104, 517-531.
- Poland, T.M., Chen, Y., Koch, J., Pureswaran, D., 2015. Review of the emerald ash borer (Coleoptera: Buprestidae), life history, mating behaviors, host plant selection, and host resistance. Canadian Entomologist 147, 252-262.
- Pureswaran, D.S., Poland, T.M., 2009. Host selection and feeding preference of *Agrilus planipennis* (Coleoptera: Buprestidae) on ash (*Fraxinus* spp.) Environmental Entomology, 38,757-765.
- Rentch, J., Fajvan, M.A., Evans, R.A., Onken, B. 2009. Using dendrochronology to model hemlock woolly adelgid effects on eastern hemlock growth and vulnerability. Biological Invasions 11, 551-563.
- Riggins, J.J., Defibaugh y Cha'vez, J. M., Tullis, J.A., Stephen, F.M., 2011. Spectral identification of previsual northern red oak (*Quercus rubra* L.) foliar symptoms related to oak decline and red oak borer (Coleoptera: Cerambycidae) attack. Southern Journal of Applied Forestry, 35, 18-25.

- Roberts, C.A., Workman, J., Reeves, J.B. III, (Eds.), 2004. Near-Infrared Spectroscopy in Agriculture. Agronomy, vol. 44, American Societies of Agronomy, Crop and Soil Science, Madison, WI.
- Ryall, K.L., Fidgen, J.G., Turgeon, J.J. 2011. Detectability of the emerald ash borer (Coleoptera: Buprestidae) in asymptomatic urban trees by using branch samples. Environmental Entomology, 40, 679-688.
- Ryall, K., 2015. Detection and sampling of emerald ash borer (Coleoptera: Buprestidae) infestations. Canadian Entomologist 147, 290-299.
- Sankaran, S., Mishra, A., Ehsani, R., Davis, C., 2010. A review of advanced techniques for detecting plant diseases. Computers and Electronics in Agriculture 72, 1–13.
- Schimleck, L.R., Evans, R., Ilic, J., Matheson, A.C., 2002. Estimation of wood stiffness of increment cores by near-infrared spectroscopy. Canadian Journal of Forest Research 32, 129-135.
- Schimleck, L.R., 2008. Near-infrared spectroscopy: a rapid non-destructive method for measuring wood properties, and its application to tree breeding. New Zealand Journal of Forestry Science 38, 14-35.
- Schulte, L.A., Mladenoff, D.J., Crow, T.R., Merrick, L.C., Cleland, D.T. 2007. Homogenization of northern U.S. Great Lakes forests due to land use. Landscape Ecology 22, 1089-1103.
- Schwanninger, M., Rodrigues, J.C., Fackler, K., 2011. A review of band assignments in near infrared spectra of wood and wood components. Journal of Near Infrared Spectroscopy 19, 287-308.
- Sheppard, P.R., 2010. Dendroclimatology: extracting climate from trees. Dendroclimatology 1, 343-352.
- Silk, P.J., Ryall, K., Lyons, D.B., Sweeney, J., Wu, J., 2009. A contact sex pheromone component of the emerald ash borer, *Agrilus planipennis* Fairmaire (Coleoptera: Buprestidae). Naturwissenschaften 96, 601-608.
- Silk, P.J., Ryall, K., Mayo, P., MaGee, D.I., Leclair, G., Fidgen, J., Lavallee, R., Price, J., McConaghy, J., 2015. A biologically active analog of the sex pheromone of the emerald ash borer, *Agrilus planipennis*. Journal of Chemical Ecology 41, 294-302.
- Siegert, N. W., McCullough, D. G., Liebhold, A. M., Telewski, F. W. 2014. Dendrochronological reconstruction of the epicenter and early spread of emerald ash borer in North America. Diversity and Distributions 20, 847-858.
- Siesler HW, Ozaki Y, Kawata S, Heise HM (Editors). 2002. Near-infrared spectroscopy: principles, instruments, applications. Wiley-VCH.
- Sinclair, W.A., Lyon, H.H. 2005. Diseases of trees and shrubs. Cornell University Press.
- So, C., Via, B.K., Groom, L.H., Schimleck, L.R., Shupe, T.F., Kelley, S.S., Rials, T.G., 2004. Near infrared spectroscopy in the forest products industry. Forest Products Journal, 54, 6-16.
- Solomon, J.D., Leininger, T.D., Wilson, A.D., Anderson, R.L., Thompson, L.C., McCracken, F.I. 1993. Ash pests: a guide to major insects, diseases, air pollution injury, and chemical injury. United

- States Department of Agriculture Forest Serivice, Southern Forest Experiment Station. General Technical Report SO-96.
- Speer, J.H., 2010. Fundamentals of tree-ring research. The University of Arizona Press, Tucscon, Arizona.
- Tanis, S.R., McCullough, D. G., 2012. Differential persistence of blue ash and white ash following emerald ash borer invasion. Canadian Journal of Forestry Research 42, 1542–1550.
- Taylor, S.W., Carroll, A.L., Alfaro, R.I., Safranyik, L. 2006. Forest, climate, and mountain pine beetle outbreak dynamics in western Canada. In: L. Sasfranyik and B. Wilson, eds., The Mountain Pine Beetle: A Synthesis of Biology, Management, and Impacts on Lodgepole Pine. Canadian Forest Service, Pacific Forestry Center. pp. 67-94.
- Tluczek, A.R., McCullough, D.G., Poland, T.M., 2011. Influence of host stress on emerald ash borer (Coleoptera: Buprestidae) adult density, development, and distribution in *Fraxinus pennsylvanica* trees. Environmental Entomology 40, 357-366.
- Tobin, P.C., Kean, J.M., Suckling, D.M., McCullough, D.G., Herms, D.A., Stringer, L.D., 2014. Determinants of successful arthropod eradication programs. Biological Invasions 16, 401-414.
- USDA-APHIS/ARS/FS. 2012. Emerald Ash Borer, *Agrilus planipennis* (Fairmaire), Biological Control Release and Recovery Guidelines. USDA-APHIS-ARS-FS, Riverdale, Maryland.
- USDA APHIS PPQ, 2015. USDA APHIS PPQ: 2015 emerald ash borer survey guidelines. United States Department of Agriculture, Animal and Plant Health Inspection Service, Plant Protection and Quarantine.
- Watanabe, K., Mansfield, S.D., Avramidis, S., 2012. Wet-pocket classification in *Abies lasiocarpa* using spectroscopy in the visible and near infrared range. European Journal of Wood Products 70, 61-67.
- Zhang, K.W., Hu, B.X., Robinson, J., 2014. Early detection of emerald ash borer infestation using multisourced data: a case study in the town of Oakville, Ontario, Canada. Journal of Applied Remote Sensing 8, 083602. doi:10.1117/1.JRS.8.083602.
- Zhang, Q., Alfaro, R.I., Hebda, R.J. 1999. Dendroecological studies of tree growth, climate and spruce beetle outbreaks in Central British Columbia, Canada. Forest Ecology and Management 121, 215-225.

CHAPTER 2

EFFECTS OF CLIMATE ON RADIAL GROWTH OF WHITE ASH INFESTED BY EMERALD ASH BORER ALONG A LATITUDINAL GRADIENT IN MICHIGAN

2.1. Introduction

White ash (*Fraxinus americana*) is a fast growing, upland hardwood, highly valued for its wood quality and is susceptible to EAB induced mortality (Hardin et al., 2001; Herms and McCullough, 2014). Previous dendrochronological evidence indicates that EAB had been established at least 3 to 8 years in southeast Michigan before discovery (Siegert et al., 2014; Herms and McCullough, 2014). Ash has a characteristic ring porous structure where a distinct band of large vessels are formed early in the growing season (before leaf out) using the reserves obtained from the previous growing season (Speer 2010; Siegert et al, 2014). These large water conducting vessels are followed later in the growing season by much smaller pores that end in a distinct boundary (Siegert et al, 2014). Like other ring porous trees, ashes rarely have false or missing rings, but under stressful conditions they can produce very narrow rings with ring boundaries that are difficult to differentiate (Speer 2010; Siegert et al. 2014). Recent studies have shown that in as little as one to two years following infestation ash moisture levels are lowered, causing a degradation of the structural wood properties and an increased risk in branch failure close to the union with the stem (Persad et al., 2013; Persad and Tobin, 2015).

Dendrochronology is used to make valid inferences about the relationship between trees and their environment, without directly measuring the ecophysiological processes themselves (Fritts, 1976). Dendrochronology subfields, dendroclimatology and dendroentomology have been combined and identify relationships between insect herbivores and climate on tree productivity and radial growth. Principles of dendroclimatology and dendroentomology have been combined to examine the relationship between insect herbivory and climate on tree productivity. The study by Haavik et al. (2008) found that past outbreaks of a native woodborer on northern red oak (*Quercus rubra*) in the southeastern U.S. were influenced by drought. In central British Columbia, a possible relationship between moist springs and

outbreaks of spruce beetle (*Dendroctonus rufipennis*) on Douglas-fir was reported (Zhang et al., 1999). In central Canada, dry summers and cool May temperatures were often associated with jack pine budworm outbreaks (Robson, et al., 2015). Rolland and Lemperiere (2004) determined that Norway spruce (*Picea abies*) in France had greater sensitivity to climate variables as a result of infestation by a non-native bark beetle. Limited studies have been conducted on identifying relationships between climate, tree growth and non-native insect herbivory in North America.

Tree growth and response to climate, even within the same species, can vary across broad regional areas and dendroclimatology can be used to explain environmental differences (Tardif and Bergeron, 1997). Multiple studies have been conducted in temperate regions to evaluate tree growth responses to climate across latitudinal gradients (Huang et al., 2010; Chhin et al., 2008; Dillaway and Kruger, 2010; Martin-Benito and Pederson, 2015). Based on previous dendrochronological studies, some tree species growing at their high latitudinal and elevational ranges are limited by cold summer temperature (Martin-Benito and Pederson, 2015) and harsh winters (Chhin et al. 2008). Distinct environments occur along a latitudinal gradient in the eastern half of North America, as both temperature and precipitation increase from north to south (Martin-Benito and Pederson, 2015). Dendrochronological studies on tree growth responses to climate along latitudinal gradients can be important for addressing climate change issues.

Tree growth, climatic responses and overall tree health can vary across different land uses. Trees growing in urban areas are often planted in stressful conditions where they have higher levels of heat stress, compaction, low air humidity, pollution and drought (Poland and McCullough, 2006; Gillner et al., 2014). Trees growing in urban locations therefore have limits on their overall health and vitality (Gillner et al., 2014). Urban trees are particularly predisposed to being exposed to invasive pests and pathogens by human facilitated introduction, transport and spread (Raupp et al., 2006).

The main objective in this study was to examine whether dendrochronological techniques have potential to be used for early detection of emerald ash borer infestation in white ash. The specific objectives include: 1) Identify growth responses to climate in EAB infested and non-symptomatic

(visually healthy) white ash. 2) Identify growth responses to climate across latitudinal regions or land-use categories (natural vs. high impact recreational area).

2.2. Methods

2.2.1. Study Area

This study was conducted on white ash trees selected within the eastern Lower Peninsula and in the western Upper Peninsula of Michigan over two consecutive summers of sampling (2013 and 2014). Since the initial discovery near Detroit, Michigan, EAB has spread throughout the Michigan's Lower Peninsula and is currently moving west in the Upper Peninsula (MDARD, 2015). In the Lower Peninsula, sites with known EAB infestation were selected along a latitudinal gradient starting near Flint, Michigan and extending northward into the Huron-Manistee National Forest area (sampled June-September, 2013) (Fig. 2.1). Three regions along this latitudinal climate gradient were selected. Sites were primarily located using GIS data provided by the Michigan Department of Natural Resources (DNR) and Huron-Manistee National Forest agencies and EAB infestation was determined based on external signs and symptoms. These three regions (from North to South) are: EAB Region 1 (Huron-Manistee National Forest: Iosco and Alcona counties), EAB Region 2 (Gladwin and Arenac Counties), and EAB Region 4 (Lapeer County). Ideally, control sites would have been established in the same latitudes as the EAB infested regions, but this was not possible due to the general presence of EAB in these areas. However, the nearest possible regions for control sites were established. An additional region, north of Huron-Manistee National Forest (Lower Peninsula: Cheboygan and Otsego counties), was selected as a Lower Peninsula control region, and is defined as having healthy crowns with no additional visible signs or symptoms of EAB infestation at the time of site selection.

The second year of field collection (June and July, 2014) took place in the Western Upper Peninsula in the Ontonagon, Iron, and Menominee counties. At the time of sampling, these three counties were outside the Michigan Department of Agriculture and Rural Development (MDARD) EAB quarantined counties. Sampling took place in Ottawa National Forest (Ontonagon County), Crystal Falls State Forest Area (Iron County) and Escanaba River State Forest (Menominee County). The Upper Peninsula control region was further separated by two sub-regions (UPA and UPB) categorized by

different EPA Level IV ecoregions; UPA: Winegar Dead Ice Moraine (ecoregion # 50v), and UPB: Menominee Drumlins and Ground Moraine (ecoregion # 50l) (EPA, 2015).

Soil in the Upper Peninsula control sites generally consisted of well drained sandy loams (Natural Resources Conservation Service, 2015). The Lower Peninsula control region soils ranged from moderately to excessively drained sand/loamy sands (Natural Resources Conservation Service, 2015). The EAB region 1 soils were moderately to well drained sand/fine sandy loams (Natural Resources Conservation Service, 2015). Soil in the EAB region 2 sites ranged from poorly to somewhat excessively drained sand/loamy sands at high impact recreation sites and excessively drained sand at the natural sites (Natural Resources Conservation Service, 2015). EAB region 4 soils were characterized by somewhat poorly drained loam/sandy loam (Natural Resources Conservation Service, 2015).

The average annual temperature from 1992 to 2012 was 5.37 °C in the UP sites and 7.37 °C for all LP sites (Daly et al., 2008;PRISM Climate Group, 2014, http://prism.oregonstate.edu/) (Fig. 2.2). During the same time period, the average, total annual precipitation was 727.5 mm in the UP and 791.2 mm in the LP (Daly et al., 2008;PRISM Climate Group, 2014). The average total annual climatic moisture index (net water availability to trees) (CMI) from 1992 to 2012 was 145.4 mm in the UP and 158.9 mm in the LP (Daly et al., 2008;PRISM Climate Group, 2014; Hogg, 1997). From May to September in the UP and LP respectively, there is a summer drought effect where the actual moisture availability (CMI: precipitation minus potential evapotranspiration) to vegetation is negative (Fig. 2.2 B and D).

2.2.2. Field Sampling

In each of the three Lower Peninsula (LP) EAB infested regions, four plots were sampled with four focal trees per plot (total 16 trees sampled per region) (Fig. 2.1). Fifteen trees were sampled in the LP control region (4 plots sampled with an average 3.75 (range: 3-4) focal trees sampled per plot). In the UP, a total of 22 trees were sampled across five plots, with an average of 4.4 (range: 4-5) focal trees per plot. Focal trees in this study are defined as sampled white ash trees that meet pre-determined, crown vigor

requirements of the specific sampling region. In the three LP EAB regions, two plots from a natural forest and two plots from a high impact recreation use area were chosen to represent potential differences between land-use types. In this study, the recreation use areas were located in a city park, an equestrian trail, and boat launch/hiking trail. Natural forests are defined as trees growing > 2 miles away from human settlements with minimal human impact. The study by Flower et al. (2013) showed that a categorical scale for crown condition classes for ash trees are closely related to tree-level EAB densities and of the percent EAB gallery cover. Similar to the systems used by Pontius et al. (2008) and Flower et al. (2013), within each plot of the EAB infested regions, four t focal trees were chosen based on crown vigor (1 tree per class per plot) (total 16 trees per region). The crown vigor classes included:

- Low decline (10 to 25% crown damage)
- Moderate decline (26 to 50% crown damage)
- Severe decline (> 50% crown damage)
- Dead (dead canopy)

The LP and UP control regions were established in a similar manner to the EAB infested regions, with a few differences. These include: selecting only trees that appear to be healthy and visibly asymptomatic (no major branch mortality or any readily apparent EAB infestation symptoms at the time of site selection), selecting sampling locations in natural areas only (due to a lack of available high impact recreation use sites), and setting up purple prism traps coated with clear Pestick and baited with a Manuka oil lure in each plot to identify a presence of adult EAB in the area (2 traps per plot in LP, 1 trap per plot in UP)(USDA APHIS PPQ, 2013).. Traps were established in the lower canopy from July to August in the Lower Peninsula and June to July in the Upper Peninsula (around 30 days per trap). During the first year of sampling, Manuka oil and (Z)-3-hexanol lures were both recommended as a part of the USDA APHIS PPQ EAB survey guidelines, since then however, the guidelines only recommend using the (Z)-3-hexanol lures (USDA APHIS PPQ, 2013 and 2015). All measurements remained consistent between the EAB infested and control regions. Although the trees sampled in the control regions did not have apparent outward indications of EAB infestation, it is possible that these trees were still infested. To definitively

conclude if non symptomatic trees are infested by EAB, the entire tree would have to be felled and debarked to inspect for the presence of larval galleries in the phloem and outer xylem. As this was not possible due to time, budget and permit constraints, all non-symptomatic control trees sampled in this project were chosen based on crown vigor, with "healthy: crowns (no major branch mortality). The 2 UPA plots sampled were the furthest west (Ontonagon and Iron counties) while the 3 UPB plots were all located in Menominee county.

The regional and plot sampling design for all field work done in the LP is shown in Figure 2.3. Each sample group is denoted by a combination of region (UP = Upper Peninsula Control, LP = Lower Peninsula Control, R1 = Region 1, R2 = Region 2, and R4 = Region 4), land use type (N = Natural, U = Recreation "Use"), and for the EAB infested regions, infestation severity. Infestation severity represents the combination of crown vigor classes (low, moderate, severe and dead), and is denoted by I1 (Infestation level 1) for the combined low and moderate crown decline classes, and I2 (Infestation level 2) for the combined dead and severe crown decline classes. The dead and severe decline trees can justifiably be combined as the dead trees were recently killed (indicated by cross-dating results), and the presence of adult exit holes and additional signs and symptoms of EAB infestation strongly indicate EAB caused mortality. For comparison between tree ring chronologies, there was a total of fifteen "Infestation groups", e.g. R1N-I1 represents the region 1 natural white ash trees of the combined low and moderate decline classes. The fifteen Infestation groups include: UPA, UPB, LP, R1N-I1, R1N-I2, R1U-I1, R1U-I2, R2N-I1, R2N-I2, R2U-I1, R2U-I2, R4N-I1, R4N-I2, R4U-I1, and R4U-I2.

In addition sampling focal trees based on crown vigor, the level of infestation was characterized further by estimating other visual signs and symptoms of EAB for each focal tree including: fine twig mortality, D-shaped adult exit holes, vertical bark splits, visible S-shaped larval galleries, woodpecker activity, and epicormic sprouting (Pontius et al., 2008). The main stem of each focal tree was examined from 0.5 m to 1.5 m above the ground, and the number of D-shaped adult exit holes were counted (if present) (Pontius et al., 2008). Bark splits, woodpecker activity, and epicormic branching were estimated for each tree as: 0 = absent, 1 = few, and 2 = many. Visible S-shaped galleries were recorded as either

present or absent (Note: visible here refers to any galleries that can be seen under bark splits without having to physically remove bark from the stem). One or two live branches were collected (if possible to collect with a rope or 16 foot pole saw) and cut into 40 cm segments closest to the main stem (maximum 3 segments). Before processing branches, the diameter outside bark was measured from both ends of each branch segment to the nearest 0.01 mm. Later, a draw knife was used to carefully strip away the bark and phloem layers to reveal any present EAB larval galleries.

From the north side of each focal tree, one core was collected using an increment borer at stump height (0.3 m). Exceptions were made for these parameters if the tree was growing on a north or south facing slope (to avoid reaction wood) or stump height was impossible to collect. Cores were stored in plastic straws and kept refrigerated before using standard processing techniques (Speer, 2010).

General measurements collected for each focal tree included: diameter at breast height (DBH) (1.37 m) using diameter tape, tree height (m) and height to live crown (m) (live trees only) measured using a laser hypsometer or clinometer, GPS coordinates, and digital pictures from both the north and south direction. Each focal tree sampled in this project became the center of its own sub-plot and was referred to as plot center. To estimate nearby competition and light availability, an expanding radius plot with a minimum (3.6 m) radius or up to a maximum (8.02 m) radius was implemented for each focal tree. The subplot radius size increased until at least 2 nearby trees fell within the plot or the maximum radius length was reached (i.e. if 2 trees were within 3.6 meters of the focal tree, the final radius size was 3.6 meters). The final radius length, DBH, live or dead status, and species of any trees within the subplot were recorded. In addition to recording the nearby competitor trees, light availability was estimated by taking hemispherical photographs from the four cardinal directions at breast height (1.37 m) and a distance of 3 feet (0.91 meter) from each focal tree. To reduce sunlight glare, all hemispherical photographs were taken either before 10 a.m. or after 4 p.m.

2.2.3. Increment Core Processing, Cross-Dating, and Tree-Ring Measurements

Cores were removed from the straws and dried at 80°C for 48-72 hours. After drying, the cores were glued to a grooved wooden mount and sanded up to 600 grit sandpaper in order to achieve clearly visible rings. Cores were glued with the transverse surface facing up so that rings would be visible. Any twisted cores were untwisted using steam and pressure (Speer, 2010).

Using the collection year as an anchor date for the living trees, cores were viewed under a dissecting microscope and calendar dates assigned using the list method of cross-dating by comparing among nearby focal trees (Yamaguchi, 1991). After cross-dating the cores collected from living trees, the dead trees were cross-dated using skeleton plotting and marker years identified from the living trees. Visually cross-dated cores were scanned using a 2400 dpi optical resolution. Scanned images were imported in the program CooRecorder (Larsson, 2008a) for measuring ring widths to an accuracy of \pm 0.001 mm. For each region and land-use class, ring width measurements were combined together. The program COFECHA was used for statistical quality control for both the accuracy of the list-method of cross-dating and ring measurements (Grissino-Mayer, 2001).

2.2.4. Data Analysis

2.2.4.1 Infestation Symptoms

For each tree stem (0.5 to 1.5 m above ground), the surface area (m²) of a conical frustum (McCullough and Siegert, 2007b) was calculated (length 1.0 m). The number of D-shaped exit holes were divided by the surface area sampled to estimate the number of potential EAB per m² for each tree (McCullough and Siegert, 2007b). For the debarked 40 cm branch segments, branches were only included in the analysis if the base diameter was greater than 1.5 cm due to larval feeding requirements (typically require at least 2.5 cm) (McCullough and Siegert, 2007b). The surface area (m²) of a conical frustum was also calculated for the 40 cm branch segments that were stripped of bark to identify any EAB larval galleries. The number of larval galleries was divided by the surface area of each branch segment to

estimate the number of EAB per m² for each branch. Multiple branch segments per tree were averaged together for a single estimate of EAB larval galleries per m² for each tree.

The S-shaped larval galleries are binary data; while the bark splits, woodpecker activity and epicormic sprouting symptoms are ordinal data and as such were all analyzed using the non-parametric Kruskal-Wallis one-way analysis of variance (Systat, 2002). Dead trees almost always had no epicormic sprouting; therefore these trees were removed from the I2 groups' epicormic sprouting statistics. The stem surface area (m²), adult exit holes per surface area (#/m²), percent fine twig mortality, branch segment surface area (m²), and number of larval galleries per surface area for branch segments (#/m²) were tested for normal distributions by visually inspecting histograms and calculating the skewness and standard error of skewness (SES) using SYSTAT (2002). The data was considered normally distributed as the absolute value of skewness/SES was less than 2 (Systat, 2002). A one-way ANOVA Least Significant Difference (LSD) test was used to compare the parametric variables for the fifteen infestation groups (Systat, 2002). Due to a limited number of branches sampled for larval gallery density (insufficient across the fifteen infestation groupings), a one-way ANOVA LSD test was applied over the five crown decline classes (Healthy, Low, Moderate, Severe, and Dead) for the branch segment variables.

2.2.4.2. Tree Level Data

DBH (cm), tree height (m), crown ratio, slenderness coefficient, basal area (m²), and total aboveground biomass (kg) were calculated for each tree and averaged within the fifteen infestation groupings. Crown ratio is the ratio of the length of the live crown (determined by the lowest dominant branch) to the total tree height (Avery and Burkhart, 2002). Slenderness coefficients (dimensionless expression of tree form) are calculated by dividing the tree height by the DBH (in the same units) (Chhin, 2010). Greater values for slenderness represent tall, narrow trees, and any values over 80 indicate a susceptibility to wind-induced stem breakage (Watt et al., 2008; Magruder et al., 2012). Basal area was calculated for each tree using the following formula (Avery and Burkhart, 2002):

$$BA = 0.00007854 * DBH^2$$
 (2.1)

Where

 $BA = basal area (m^2)$

DBH = diameter at breast height (cm)

Total aboveground tree biomass was calculated as a function of DBH using allometric equations developed for all United States tree species (Jenkins et al., 2003). Total aboveground biomass tree biomass was estimated using the following equation (Jenkins et al., 2003):

$$bm = Exp(\beta_0 + \beta_1 \ln DBH)$$
 (2.2)

Where

bm = total aboveground biomass (kg dry weight)

DBH = diameter at breast height (cm)

Exp = exponential function

ln = log base e (2.718282)

 β_0 and β_1 = Parameters specific to species groups for estimating total aboveground biomass and for *F. americana*: β_0 = -2.4800 and β_1 = -2.4835 (Jenkins et al., 2003).

The tree measurement variables were tested for normal distributions by visually inspecting histograms and calculating skewness and standard error of skewness (SES) using SYSTAT (2002). The variables were determined to be normally distributed and a one-way ANOVA LSD test was run to compare between the 15 infestation groups (SYSTAT, 2002).

2.2.4.3. Competition Level Data

For each focal tree, two of the four hemispherical photographs often had glare, therefore only the remaining two photographs (typically from perpendicular sides) were analyzed for light intensity (availability) per tree. Light availability was estimated using the program ImageJ (V1.48) (National Institutes of Health, USA, http://imagej.nih.gov/ij/v) to measure the number of open and closed pixels to calculate the percent light availability for each photograph. The percent openness was then averaged for each tree.

To estimate live competition for each focal tree, the basal area (m²) (equation 2.1) and total aboveground biomass (converted from kg to metric tons) (equation 2.2) were calculated for each living tree present within each subplot on a per hectare basis and summarized together for a single subplot estimate. The focal *F. americana* (i.e. plot center) for each subplot was not included with the competition trees. For the total aboveground biomass calculations, each tree was calculated using the parameters assigned to their species specific groups (Jenkins et al., 2003). The competition variables were tested for normal distributions by visually inspecting histograms and calculating skewness. The data was determined to be normally distributed and a one-way ANOVA LSD test was applied to compare between the fifteen infestation groups.

2.2.5. Dendrochronological Data Analysis

2.2.5.1. Standardization

After cross-dating and statistical quality control, raw ring width measurements were combined together to create the 15 Infestation groupings. To correct for age and site related trends in the raw ring width measurements, the ring width chronologies for each were standardized using the program ARSTAN (Cook, 1985). In ARSTAN, a negative exponential curve or a linear regression line was used for conservatively detrending and standardizing the series and producing a radial growth index for each region (Cook, 1985). This conservative detrending method assumes the age related trend that tree rings decrease in a negative exponential way over time, or if it fails, a linear trend is applied (Cook, 1985). This approach to detrending removes variation in growth due to competition and age while preserving the influence of climate and disturbance (i.e. insects) (Cook, 1985). Radial growth indexes (RGI) are unit-less expressions of ring widths that allow for comparisons for the same year between multiple series. Years of above average growth have RGI values above one and years of below average growth have RGI values less than one. The residual chronology produced by ARSTAN was used for all climatic analysis. Residual chronologies produced in ARSTAN have the autocorrelation removed from each ring-width series.

autocorrelation -meets the necessary statistical assumptions to apply regression analysis. The chronology timelines for each infestation group went as far back to a minimum presence of 50% of the cores in that group.

2.2.5.2. Climate

Spatial weather and climate data was obtained based on the geographical locations of the specific sample sites using the PRISM method developed by Daly et al (2008) provided by the website:

http://prismmap.nacse.org/nn/ (PRISM Climate Group, 2014). The PRISM Climate Group develops and provides spatial climate datasets by utilizing a wide range of United States based weather monitoring networks and incorporating sophisticated quality control. This widely used spatial climate data resource provides averaged monthly weather and climate data based on geographic location as far back as the year 1895 (PRISM Climate Group, 2014). Monthly weather data was collected using this website by entering the GPS coordinates for each plot, downloading the data, and averaging among plots for each region and land-use class group to calculate a geographic average. The weather variables collected were total monthly precipitation (mm) as well as the monthly averages for minimum and maximum temperature (°C) from 1895 to 2014. The mean monthly temperature was calculated by averaging the minimum and maximum monthly temperatures. A climatic moisture index was calculated based on the following equation provided by Hogg (1997) which combines precipitation measurements and the minimum and maximum monthly temperatures to estimate the net water availability to trees.

$$CMI = P - PET (2.3)$$

Where

CMI = climatic moisture index (mm)

P = precipitation (mm)

PET = potential evapotranspiration (mm)

The monthly weather data was averaged for mean temperature and summed for both precipitation and CMI over 3-month periods to account for seasonal trends. As all analysis in this study used weather data over a period of time (21 years) to identify long-term responses, all weather variables will hereafter is referred to as climatic variables. A step-wise multiple regression model with forward stepping using the StepAIC function was used in R to determine relationships between climatic factors and residual growth chronologies (Venables and Ripley, 2002). This regression model used an Akaike information criterion (AIC) to develop parsimonious growth-climate model (Burnham and Anderson 2002). Models were selected based on climatic predictor variables that lowered the Akaike's information criterion (AIC) value by at least 2 if they were added to the model (Burnham and Anderson, 2002). Models with minimum AIC values are preferred and models with too many variables can be penalized (Burnham and Anderson, 2002; Chhin et al., 2008). The climatic variables (months and seasons simultaneously) from April of the previous year (t-1) through October of the current year (t), and the residual chronologies were run through a R program regression model between growth and climate developed by Chhin et al. (2008) which utilizes the stepAIC function. To keep all infestation groupings consistent, the time period used in R was from 1992 to 2012 for a total of 21 years. Regression models with more than one significant climatic predictor variable were ranked by importance using standardized (β) partial regression coefficients (Chhin, 2010; Zar, 1999). The variable with the highest impact on radial growth has the standardized (β) coefficient with the highest absolute value (Zar, 1999).

2.3. Results

2.3.1. Infestation symptoms

The percent fine twig mortality was significantly different across all EAB regions between the I1 and I2 infestation severity groups (p < 0.05) (Table 2.1). The three control region groups had significantly lower fine twig mortality from all of the EAB region infestation groups with the exception of R4U-I1 (p < 0.05) (Table 2.1). With the exception of R1U and R4N, the EAB I1 groups tended to have significantly less adult exit holes per surface area than their corresponding I2 group in the same region and land-use (p < 0.05) (Table 2.1). The R1U-I1 group's average surface area was roughly half the size of R1U-I2 (Table 2.1). When including the control groups in the Kruskal-Wallis tests, the non-parametric variables were all significantly different (p < 0.01) across the fifteen groups so a separate Kruskal-Wallis test was run for only the 12 EAB infested groups (Table 2.1). Visible larval galleries were generally not present in the I1 groups and the Kruskal-Wallis p-value was significant for the 12 EAB groups (p < 0.05) (Table 2.1). Bark splits were significantly different among the EAB groups, and tended to be more severe in the trees with greater crown decline (I2 groups) (p < 0.05) (Table 2.1). Woodpecker damage and epicormic sprouting were not significantly different across the 12 EAB groups (p \geq 0.05) (Table 2.1).

The average surface area of the debarked branch segments was not significantly different across the five crown vigor (decline) classes (healthy, low, moderate, severe and dead) ($p \ge 0.05$) (Table 2.2). No EAB larval galleries were identified on any of the healthy and low crown decline classes' branches (Table 2.2). While the number of positive EAB identifications generally increased with crown decline severity, EAB was not identified on all branch segments. The larval density (# galleries/m²) of the healthy and low decline classes was significantly smaller compared to the severe and dead classes (p < 0.05) (Table 2.2). The moderate decline class had significantly less larval densities compared to the severe class (p < 0.05) (Table 2.2).

In the LP control region, EAB adults were captured in three of the four plots on the baited purple prism traps. There was a maximum 2 adults per trap, minimum 0 adults per trap and an average 0.7 adults per trap in this region. No adults were captured on the purple prism traps in the Upper Peninsula.

2.3.2. Focal Tree Level Data

All of the same region/land use groups except for the two R1U groups were not significantly different in DBH compared to their corresponding infestation severity group ($p \ge 0.05$) (Table 2.3). The recreational use groups generally had the greatest variation in DBH compared to the other groups (Table 2.3). R2U-I1 and R2U-I2 had significantly larger average DBH than the rest of the EAB and control groups (p < 0.05). The tree height for the LP control group was significantly taller compared to the UPA control group (p < 0.05) (Table 2.3). With the exception of R4U-I2, all EAB infestation groups did not have significantly different total tree height (m) compared to each other or to one or more of the control groups ($p \ge 0.05$) (Table 2.3). R4U-I1 and R4U-I2 had significantly smaller total tree height compared to most of the other infestation groups (p < 0.05) (Table 2.3). R1U were the only two groups with significantly different heights within the same region and land-use (p < 0.05) (Table 2.3). R1N-I2 was the only EAB infested group that had a significantly smaller crown ratio compared to the three control groups and the corresponding I1 group in the same region and land-use (p < 0.05) (Table 2.3). UPB, R2U-I1, and R2U-I2 were the only groups with average slenderness values less than 80 (Table 2.3). R2U-II and R2U-I2 had significantly larger basal area (m^2) and total above-ground biomass (kg) than the remaining thirteen infestation groups (p < 0.05) (Table 2.3).

2.3.3. Nearby Tree Competition and Light Availability

In Region 2, the I1 groups had significantly larger basal area (m^2 /ha) of live nearby competitor trees compared to the I2 groups in Region 2 (p < 0.05) (Table 2.4). The average total above-ground biomass (metric ton/ha) of live competitor trees was also significantly greatest in R2U-I1 (p < 0.05) (Table 2.4). Within EAB Region 2, the recreational use groups had significantly more light availability compared to the natural groups (p < 0.05) (Table 2.4). The two R2U groups were also the only two groups within the same region and land use class where there was a significant difference in light

availability between infestation severities, where I2 had greater light availability compared to I1 (Table 2.4).

2.3.4. Tree Ring Chronologies

Trees growing in the control groups tended to be older (longer total (maximum) chronology length) compared to trees growing in the EAB infested groups (Table 2.5). The average total chronology length was 81 years for the three control groups and 38.6 years for the twelve EAB infested groups. The average mean sensitivity for the control and EAB infested groups was 0.232 and 0.246, respectively. The average standard deviation for the control and EAB infested groups was 0.351 and 0.385, respectively. The average mean sensitivities and standard deviations were greater in the I2 infestation groups compared to the I1 groups. Based on the visual cross-dating results and statistical quality control, no absent rings were found in the control groups. The I1 infestation groups had an average of 0.3% in absent rings, while the I2 groups had more absent rings with an average of 2.8%.

The time period for the common interval analysis (a time period of sufficient sample replication) for all 15 chronologies was from 1992 to 2012 (21 years) (Table 2.5). Overall, the control groups had an average (\pm standard deviation) intercorrelation of 0.321 \pm 0.197 while the EAB infested groups was 0.376 \pm .222. Intercorrelation in dendrochronology refers to the average of every tree-ring series compared to the master chronology and higher intercorrelation values are desired (Speer, 2010; Grissino-Mayer, 2001). Among the control groups, the LP chronology had the highest intercorrelation during this time interval at 0.547, while UPA had the lowest at 0.182. The I1 infestation chronologies had a smaller average (\pm standard deviation) intercorrelation at 0.297 \pm 0.178 compared to the I2 chronologies which were 0.455 \pm 0.248. The natural EAB chronologies had a higher average (\pm standard deviation) intercorrelation at 0.445 \pm 0.248 compared to the recreation use chronologies which were 0.307 \pm 0.189. Of the 15 infestation groups, R1N-I2 had the highest intercorrelation of 0.774 while R2U-I1 had the lowest intercorrelation of 0.087.

Basic trends seen across all fifteen groupings were above average growth in the mid to late 1990s and below average growth in the early to mid-2000s (i.e. RGI values above and below 1.0 respectively) (Fig. 2.4). With the exception of R1N-I1, 1996 and/or 1997 were consistently narrower compared to the proceeding years for all chronologies. In 2012, all three control groups had slightly below average radial growth (1.0 > RGI > 0.9). With the exceptions of R1N-I1 and R4U-I1 (RGI > 1.0), all EAB infested groups had RGI values less than 1.0 in 2012. In particular, R1N-I2, R1U-I1, R1U-I2, R2N-I1, R2N-I2, R2U-I2, and R4N-I2 had the smallest RGI values in 2012 compared to the proceeding 20 years.

2.3.5. Growth Climate Relationships

Only seven out of 15 infestation groups had significant relationships between radial growth and mean temperature (Figure 2.5). The control groups had positive monthly associations with temperature in the spring or summer of the current year (t). This positive association with mean temperature in summer of the current year (t) was not seen in any of the EAB infested groups with the exception of R2N-I2. Four groups (UPA, R1N-I1, R1U-I2 and R2U-I1) had negative relationships between mean monthly temperature and radial growth in the summer of the previous year (t-1). The radial growth of R1N-I1 also had a positive association with mean monthly temperature in February of the current year (t). In addition to the positive association in June of the current year (t) between growth and mean temperature for R2N-I2, March had a negative relationship with current year (t) growth. R4U-I1 had a positive relationship between radial growth and mean temperature in April of the previous year (t-1).

Including the three control regions, 12 of the 15 infestation groups had significant associations between radial growth and precipitation (Figure 2.6). With the exception of R1N-I1, all of the 12 groups had significant negative associations with precipitation in the growing season (late spring and/or mid summers) of the previous year (t-1). For any groups with multiple significant precipitation variables, the negative relationships in the growing season of the previous year was the most influential predictor variable in each multiple regression model according to the ranking of the beta regression coefficients. All significant growth relationships with precipitation in the late fall and winter (October-April) were also

negative. UPA also had a negative relationship with precipitation in April of the current year (t) while UPB had a positive relationship with the previous (t-1) September precipitation. The LP control group additionally had negative associations in October-December of the previous year (t-1) and positive in June-August of the current year (t). With the exception of August of the previous year (t-1) for R2N-I1, all significant monthly and seasonal total precipitation relationships with radial growth in the EAB infested groups were negative.

Radial growth responses to climatic moisture index (CMI) showed similar patterns to those seen in precipitation, particularly with a trend in negative growth associations in spring and summer of the previous year (t-1) (Figure 2.7). Unlike precipitation, all significant CMI variables had negative relationships with radial growth. While both UP groups had negative relationships in the spring and summer of the previous year (t-1), the LP control group only had a negative response to CMI in December of the previous year (t-1). Four of the five I2 groups with significant associations to CMI, had negative growth relationships with either September (R1U-I2) or October (R1N-I2, R1U-I2, and R2N-I2) of the current year (t).

2.4. Discussion

2.4.1. Infestation Symptoms

Previous studies have shown that classifying infested ash trees by varying levels of crown mortality is related to EAB density and larval gallery cover (Flower et al., 2013). The particular crown vigor rating system used in this study was adapted from the ones used by Pontius et al. (2008) and Flower et al. (2013). While this study lacks supporting whole tree, larval density data to support the levels of infestation in each tree, the trees sampled were consistently grouped by the level of crown vigor.

EAB will typically first target the upper portion of the stems for larger diameter trees, creating a delay between initial infestation and when adult exit holes are visible, while on smaller diameter trees, exit holes may be visible from the ground much earlier (McCullough and Siegert, 2007a). The surface areas on the stems from 0.5 to 1.5 m above the ground calculated using a conical frustum were generally similar in size with the exception of a few of the larger diameter recreational use groups. In this study, more exit holes per surface area were typically found in the higher infestation severity (I2) groups, compared to the lower infestation severity (I1) groups, particularly within the same region and land-use categories (Pontius et al., 2008; Flower et al., 2013). However, in the two infestation groups in the Region 1, recreation land-use category (R1U), there were significantly more exit holes per surface area in the I1 group compared to the I2 group. This is likely because the average surface area for the R1U-I1 group was less than half that of the R1U-I2 group (McCullough and Siegert, 2007a). Overall, region and land-use category did not appear to influence the numbers of D-shaped exit holes per surface area.

Generally, the additional signs and symptoms of EAB infestation (S-shaped larval galleries, bark splits, and woodpecker damage) quantified in this study were the greatest in trees with more severe crown dieback (I2 groups) than in trees with lower levels of crown dieback (I1 groups). This delay in visible symptoms only after severe infestation is typical of ash decline due to EAB, and the ability to accurately identify infested trees at low population levels using this method is not considered to be reliable (Herms and McCullough, 2014). Region and land-use categories did not appear to influence infestation levels. Due to minimal amounts of bark splits, woodpecker damage, and epicormic sprouting presence in the

control regions, it is probable that some of the control trees had low levels of EAB infestation at the time of sampling.

As EAB will typically target the upper stem and branches before moving towards the base of a tree, a useful detection method for EAB is collecting branch samples that are debarked and inspected for larval galleries (Ryall et al., 2011). The severe crown dieback and dead tree branches both had an average larval density > 20 galleries/m² while the moderate crown dieback had less than 5 galleries/m² and no galleries were identified on the low and control branches. For this EAB detection method, Ryall et al. (2011) recommended sampling at least 2 branches (5-8 cm diameter) from the mid-crown of open-grown urban trees. Due to sampling constraints, the majority of the branches collected was located at the base of the crown and small in diameter, and are likely the reason for the false negatives associated with the low and moderate decline trees (Ryall et al., 2011). However, in addition to quantification of visible signs and symptoms, we are able to provide some estimation of larval density for the five crown decline classes sampled in this study.

As long-range sex pheromones have not been identified for EAB, artificial traps are deployed for adult capture and include green or purple sticky prism traps, or Lindgren green multi-funnel traps baited with manufactured ash volatile lures (Francese et al., 2008; McCullough et al., 2011; USDA APHIS PPQ, 2015). While EAB was captured in most of the Lower Peninsula control plots' traps, this does not indicate which trees are infested, and only proves that EAB adults were present in the area. Ideally, the utilization of multiple trapping methods is recommended for early EAB detection (McCullough et al., 2011). Artificial traps have a lower probability of detecting EAB at low population levels compared to girdled trap trees (Mercader et al., 2013). Therefore, it is possible that the trees sampled were in the early stages of EAB infestation, but without actually observing the signs of EAB development on the trees themselves, we are assuming the trees are relatively healthy compared to the trees sampled in the EAB infested regions.

2.4.2. White Ash Form and Productivity

There were some differences in tree characteristics when comparing between the fifteen infestation groups. For the most part, the infestation groups in the natural land-use category were not significantly different in diameter and height compared to one another. There was the greatest variability in DBH and height in the recreation land-use groups. It has been shown that larger diameter trees can produce more emergent EAB adults per m² and can survive longer compared to smaller diameter trees (McCullough and Siegert, 2007b; Knight et al., 2013). All of the crown ratios of the I1 groups were not significantly different compared to the control groups although some of the I2 groups had significantly smaller crown ratios. Since EAB infested/killed trees have been shown to have compromised structural integrity, the high slenderness values (above 80) for the majority of these groups further increases the chances of stem breakage (Persad and Tobin, 2015; Persad et al., 2013). In particular, trees recreation land-use areas should be considered hazard trees and will likely need to be removed soon to minimize risk of injury or property damage.

2.4.3. Effects of Competition and Light Availability

EAB adults prefer to target and colonize open grown trees with greater light availability (Herms and McCullough, 2014; Chen and Poland, 2009). Overall, there were not significant differences in live tree competition between the majority of the infestation groups. Based on the measurements collected using hemispherical photographs, with the exception of some of the recreational use groups, most trees sampled did not have statistically different low light availability. The exception was that for the Region 2 recreational use groups (R2U), the severe infestation group (I2) had statistically greater light availability compared to the lower infestation group (I1). Previous studies have also documented a preference of adult EAB for sunny conditions (McCullough et al., 2009a, b). While this preference for openly grown trees was observed in R2U, for the most part, there did not appear to be any host preference based on light availability.

2.4.4. White Ash Chronology Characteristics

Changes in radial growth associated with insect herbivory have been successfully identified and used for historical reconstruction of past outbreaks in previous dendroentomological studies (Fierke and Stephen, 2010; Haavik et al., 2008, Siegert et al., 2014). While not all dendroentomological studies employ the use of non-host species for cross-dating purposes (Haavik et al., 2008), others will sample nearby trees of a different (non-host) species to compare with the infested chronologies to help separate the impacts of climate and insect damage on radial growth (Campbell et al., 2005). Future dendrochronological research involving Fraxinus species could possibly benefit from sampling non-host species of EAB at nearby sites. Siegert et al. (2014) used dendrochronology to reconstruct the initial spread of EAB at the epicenter of introduction and colonization of green ash. The average mean sensitivities in the current study for the control (0.232) and EAB infested groups (0.246) are considered to be in the intermediate range and were similar to the previous study on green ash killed by EAB in Michigan (Grissino-Mayer, 2001; Siegert et al., 2014). Intercorrelation values often depend on tree species, region, and climate, but typically are preferred to be greater than 0.5 (Grissino-Mayer, 2001; Siegert et al., 2014). Despite varying levels of EAB infestation almost certainly influencing radial growth in later years, the EAB infested groups' chronologies generally had relatively decent average intercorrelation (0.321 for control groups and 0.376 for EAB infested groups) (Siegert et al., 2014; Grissino-Mayer, 2001). Given the current study's complexity, future multivariate analysis is necessary to properly interpret relationships between the radial growth chronologies, EAB infestation, latitudinal region, and land-use categories.

2.4.5. Growth Climate Relationships

Dendrochronology has been previously used to identify climatic influences on insect herbivory and tree decline. Dendrochronology is also used to make valid, indirect inferences about ecophysiological mechanisms between tree growth and the surrounding environment (Fritts, 1976). As the current study only looked at the relationships between radial growth and climatic variables, the specific responses and

mechanisms for these relationships described in this section are based on general knowledge about how trees respond to climate and disturbance mechanisms (Fritts, 1976). For example, droughts are commonly associated with insect infestations and increased tree susceptibility as they benefit insect populations by weakening the vigor of host trees (Haavik et al., 2008; Haavik and Stephen, 2010; Koprowski and Dunker, 2012). Winters with low snowfall followed by early springs were shown to facilitate *Choristoneura occidentalis* emergence and potentially increase host susceptibility (Campbell et al., 2005). Low precipitation and high temperatures have been shown to improve insect population survival while reducing hosts vigor and increasing predisposition to attack (Fritts, 1976).

Similar to the study by Magruder et al. (2012), also conducted in Michigan, I saw a general trend of negative monthly relationships between temperature and radial growth in the summer of the previous year in all latitudinal regions except for the Lower Peninsula control and EAB region 4 (Figure 2.5). In a study conducted in West Virginia, USA, Pan et al. (1997) also reported a negative relationship between white ash and temperature from June to September in the previous year. Increasing temperatures during the growing season can cause a tree's respiration rate to increase, which in turn reduces radial growth as carbon stores are used up (Adams et al., 2009; Mäkinen et al., 2002). High temperatures in the late summer or early fall can also have a negative impact on radial growth in the following year by prolonging growth of certain tissues, using up stored reserves (Fritts, 1976).

The additional relationships observed with temperature were mostly isolated cases and varied across regions, land-use class and infestation severity (Figure 2.5). The UPA control group and Region 1 natural low severity group (R1N-I1) had positive relationships between growth and mean temperature in April and February of the current year, respectively. Regions further north can experience greater winter harshness and shorter growing seasons compared to the southern regions, so years with colder winter temperatures will have a reduction in growth, where years with warmer winter temperatures will have increased growth (Fritts, 1976; Denton and Barnes, 1988; Hacke and Sauter, 1996). The Region 4, recreational use, low severity group (R4U-I1) had a positive response to temperature in April of the previous year, possibly due to an early start of the growing season, accumulating more carbohydrate

reserves for the following year (Speer, 2010; Fritts, 1976). The Region 2, natural high severity group (R2N-I2) had a negative monthly response to temperature in March of the current year, possibly due to false spring events resulting in early bud break that was subsequently damaged during spring frosts (Denton and Barnes, 1988; Augspurger, 2009). The LP control and Region 2 natural high infestation group (R2N-I2) had positive responses to temperature in July through September and June of the current year, respectively. The radial growth of trees growing near the upper limits of their latitudinal ranges is often positively associated with summer temperatures than trees growing at lower latitudes (Fritts, 1976). Overall, latitude appears to have a greater influence on white ash growth response to temperature compared to land-use or EAB presence in Michigan.

The regression modeling showed a highly consistent pattern of a negative relationship between precipitation and radial growth in the summer of the previous growing season (Figure 2.6). This trend was seen across both land-use types, both infestation levels (I1 and I2), all three EAB infested regions, and in all three of the control groups. A negative response to precipitation was also seen in the summer and fall of the current year for four of the EAB infested groups. This negative response to precipitation was not expected, as precipitation during the growing season generally benefits tree growth (Huang et al., 2010; Huang et al., 2011; Chhin, 2010; Pan et al., 1997; Fritts, 1976). In particular, a study conducted in West Virginia reported a positive growth response to precipitation in the previous summer, previous fall, and current summer for white ash (Pan et al., 1997). Negative relationships between precipitation and growth often occur when precipitation is associated with more limiting factors (Fritts, 1976). A few possible explanations for this inverse relationship with previous summer precipitation include: poor soil drainage, physical damage associated with heavy precipitation and a reduction in direct radiation due to increased cloud cover (Fritts, 1976). Negative associations with precipitation during the growing season often occur at sites with poor drainage, limiting root growth and reducing soil oxygen (Fritts, 1976; Catton et al., 2007). While compaction and poor drainage is often associated with urban or other high impact land-use sites, this negative relationship with summer rainfall was seen across all land-use types and the majority of sites sampled in this study occurred on moderately to well-drained soils (Catton et al., 2007; Natural

Resources Conservation Service, 2015). White ash has also been shown to be able to survive flooding for the entire duration of a growing season (Catton et al., 2007). Another possible explanation for this atypical response is that the canopies may be damaged by wind associated with storm events characteristic of Michigan springs and summers (Everham and Brokaw, 1996; Magruder et al., 2012; Peterson, 2000; Fritts, 1976). Following branch damage, carbohydrate resources would likely be allocated to the crowns in the following growing season, limiting the amount available for radial growth (Chhin, 2010; Fritts, 1976). A similar response of radial growth to precipitation in both the previous and current summers was seen in the study by Magruder et al., (2012) conducted in Michigan on red pine and suggests that a negative response to summer storm events may be a regional characteristic of multiple tree species growing in Michigan. It is possible that this trend was seen in most groups as a result of damage acquired in only the previous year and not the current year, because ash will typically begin ring formation before leaf out, utilizing the carbohydrate reserves obtained from the previous growing season (Speer 2010; Siegert et al. 2014). An increased risk in branch failure has also been documented for EAB infested ash (Persad et al., 2013; Persad and Tobin, 2015). Damage to crowns has been associated with a lagged response in radial growth (Fritts, 1976; Gower, 1995).

The Lower Peninsula control group also showed a positive response to precipitation in the summer of the current year. It is possible that in healthy, uninfested white ash in the Lower Peninsula, higher amounts of precipitation during the current year's growing season will still benefit radial growth, while crown damaging winds during storms of the previous year's growing season will reduce growth in the following year (Pan et al., 1997; Denton and Barnes, 1988; Fritts, 1976). Snow can occur in Michigan through April, and in the UPA group the negative association to precipitation in April of the current year could be a result of late winter snowfall, delaying leaf out or damaging new shoots (Denton and Barnes, 1988; Johnson, 1995; Augspurger, 2009). Any negative relationships to precipitation during winter months are likely due to crown damage associated with heavy snowfalls (Chhin, 2010).

In white ash infested by EAB, there was either no relationship between radial growth and precipitation in the summer of the current year, or the relationship was negative. Previous studies have

shown an increased risk of branch failure in trees infested by EAB (Persad and Tobin 2015; Persad et al., 2013). Therefore, any possible benefits of precipitation in the current summer's growth for EAB infested trees likely no longer occurs due to general crown dieback associated with the disruption of the translocation of water and nutrients, while an increase in branch failure due to summer wind may occur (Poland and McCullough, 2006; Persad et al., 2013; Denton and Barnes, 1988). Moisture levels have also been shown to be important for EAB larval development (ideal between 60 and 80%) (Chen et al., 2011). It is possible that the negative responses seen to precipitation at the end of the growing season may benefit EAB larval development, thereby reducing radial growth (Chen et al., 2011). The responses to precipitation in the EAB infested groups generally did not appear to be influenced by land use type, region or infestation level.

A climatic moisture index (CMI) combines precipitation measurements with the minimum and maximum monthly temperatures to estimate the net water availability to trees (Hogg, 1997). The similar trends observed in the response of radial growth to CMI that also occurred for response precipitation, can generally be explained using the same reasoning (Figure 2.7). Magruder et al. (2012) and Chhin (2015) both saw negative summer relationships to CMI in pine species in Michigan, further supporting a possible regional influence on radial growth possibly due to damaging winds associated with increased summer precipitation (Everham and Brokaw, 1996; Peterson, 2000; Fritts, 1976). The main difference seen between precipitation and CMI was that the LP control no longer had negative relationships in the summer and late fall of the previous year or positive relationships in the summer of the current year. The LP control still had a negative association to CMI in December of the previous year which can be explained by damage associated with heavy snowfall (Chhin, 2010). The three northern control groups were the only groups to have a negative response to winter snowfall, indicating a latitudinal sensitivity. However, four of the five EAB infested I2 groups that had significant relationships to CMI, had negative monthly relationships in either September or October of the current growing season. This indicates a possible benefit of available moisture on larval development and survival. Similar to precipitation, there

did not appear to be large differences in response to CMI due to region or land-use among the twelve EAB infested groups.

2.5. Conclusions

This preliminary study evaluated the potential of dendrochronology as a tool for detection of emerald ash borer in white ash by identifying radial growth responses to climate. The influences of latitude and land-use were also considered. Across all regions, land-use types, EAB presence, and infestation levels, I saw a strong trend in summer precipitation and available moisture (CMI) in the previous summer having an adverse influence on radial growth. This negative relationship with precipitation is possibly an effect of wind damage associated with summer thunderstorms characteristic of Michigan and not a result of EAB infestation. However, the increased risk of branch failure observed for EAB infested ash trees could possibly further exacerbate this negative association with summer precipitation. There was also a negative relationship between radial growth and available moisture (CMI) in autumn of the current year observed only in chronologies categorized with severe infestation. This indicates a possible benefit to larval development and survival due to moisture requirements. However, as these trees were clearly infested (based on visual signs and symptoms), this relationship does not indicate a potential for early detection. The results of this study were inconclusive on the potential for dendrochronology techniques being used for early detection of EAB infestation in Michigan. However, future research is needed in different regions throughout North America to assess current, regional climate response variables of white ash. It is possible that typical radial growth responses to climate may change due to EAB infestation.

APPENDIX

Table 2.1. Average infestation symptoms and tree measurements by infestation groups (standard error in parentheses). Number of trees sampled per infestation group (n). Parametric variables include, percent fine twig mortality, surface area (area of stem inspected for D-shaped exit holes), and adult exit holes per surface area. Non-parametric variables include s-shaped larval galleries (presence/absence), bark splits, woodpecker damage, and epicormic sprouts. All statistical analysis was compared between groups, a one-way ANOVA performed for parametric data and Kruskal-Wallis for non-parametric data (two Kruskal-Wallis tests: one to compare between all groups, and one to compare between only the EAB infested groups). Groups with different letters are significantly different (p < 0.05). P-values < 0.05 indicate significant differences in infestation symptoms between dieback classes (Kruskal-Wallis). For all I2 groups, epicormic sprouting had n = 2.

Group *	n	Percent Fine Twig Mortality	Surface Area (m2)	D-Shaped Exit Holes per Surface Area (#/m2)	S-Shaped Larval Galleries (presence / absence)	Bark Splits	Woodpecker Damage	Epicormic Sprouting
UPA-Control	9	5.6 (0.6) a	0.76 (0.2) bcd	0 (0) a	0 (0)	0.1 (0.1)	0.1 (0.1)	0.4 (0.2)
UPB-Control	13	5.4 (0.4) a	0.76 (0.1) cd	0 (0) a	0 (0)	0.2 (0.1)	0 (0)	0.5 (0.1)
LP-Control	15	6.3 (0.6) a	0.56 (0.04) ab	0 (0) a	0 (0)	0.07 (0.07)	0.07 (0.07)	0.6 (0.2)
R1N-I1	4	26.3 (8) b	0.61 (0.06) abcd	2.81 (2.8) ab	0 (0)	1 (0)	1.3 (0.3)	1 (0)
R1N-I2	4	82.5 (10.3) c	0.54 (0.08) abcd	30.23 (10.6) c	0 (0)	1 (0)	1.5 (0.3)	1.5 (0.5)
R1U-I1	4	22.5 (6) b	0.41 (0.03) a	31.48 (9.2) c	0 (0)	1.3 (0.3)	1.3 (0.3)	1.3 (0.3)
R1U-I2	4	80 (11.6) c	0.86 (0.1) d	17.18 (12.3) bc	0.25 (0.3)	1.3 (0.3)	1.5 (0.3)	1 (0)
R2N-I1	4	27.5 (10.5) b	0.45 (0.05) ab	11.64 (8.2) ab	0 (0)	1 (0)	1 (0)	1.3 (0.3)
R2N-I2	4	77.5 (13.2) c	0.53 (0.03) abcd	59.12 (14.4) d	0.25 (0.3)	1.3 (0.3)	1.8 (0.3)	1.5 (0.5)
R2U-I1	4	26.3 (8.8) b	1.65 (0.1) e	2.71 (1.2) ab	0 (0)	1 (0)	1.5 (0.3)	1.8 (0.3)
R2U-I2	4	91.3 (5.2) c	1.54 (0.3) e	29.03 (9) c	0.25 (0.3)	1.8 (0.3)	1.8 (0.3)	2 (0)
R4N-I1	4	23.8 (6.3) b	0.58 (0.04) abcd	6.36 (2.6) ab	0.5 (0.3)	1.3 (0.3)	1 (0)	1 (0)
R4N-I2	4	80 (11.6) c	0.46 (0.04) abc	14.78 (5.1) bc	0.5 (0.3)	2 (0)	1.5 (0.3)	1 (0)
R4U-I1	4	20 (8.9) ab	0.42 (0.03) a	4.19 (0.6) ab	0 (0)	1.3 (0.3)	1 (0)	1 (0)
R4U-I2	4	91.3 (5.2) c	0.45 (0.01) ab	28.75 (8.7) c	1 (0)	2 (0)	1.8 (0.3)	1 (0)
		Kruskal-Wallis	All groups	p	<.0001	<.0001	<.0001	0.004
			EAB only	p	0.02	0.004	0.17	0.078

^{*} UP = Upper Peninsula Control, LP = Lower Peninsula Control. R1 = EAB Region 1, R2 = EAB Region 2, and R4 = EAB Region 4. Land use type: N = Natural, U = Recreation "Use". I1 = Infestation level 1 (low severity), and I2 = Infestation level 2 (high severity).

Table 2.2. Mean (standard error of the mean) for the surface area (m^2) and larval density (#galleries/m²) of branches (>1.5 cm base diameter) sampled in Michigan separated by crown dieback class. Number of trees with branches sampled (n (trees)). Number of trees with EAB detected on sampled branches (n (EAB)). Crown dieback classes with different letters are significantly different (p < 0.05).

Crown Vigor Class *	n (trees)	n (EAB)	Branch Surface Area (m²)	Larval Density (# galleries/m²)
Healthy	14	0	0.032 (0.0042) a	0 (0) a
Low	4	0	0.034 (0.0076) a	0 (0) a
Moderate	5	1	0.027 (0.0059) a	4.84 (4.84) ab
Severe	5	4	0.03 (0.0032) a	24.22 (11.98) c
Dead	5	3	0.033 (0.0089) a	21.71 (11.67) bc

^{*} Healthy = no major branch mortality; Low = (10-25% crown mortality); Moderate = (26-50% crown mortality); Severe = (>50% crown mortality); Dead = (dead crown)

Table 2.3. Tree level productivity for white ash sampled in Michigan based on 15 infestation groups. Number of trees sampled per infestation group (n). Average (SEM) tree level productivity variables: DBH, tree height, crown ratio, slenderness, basal area, total aboveground biomass, and total stem biomass. Significant difference between infestation groupings is designated by different letters (p < 0.05). For all I2 groups, crown ratio has n = 2.

Infestation Group *	n	DBH (cm)	Tree Height (m)	Crown Ratio	Slenderness	Basal Area (m²)	Total Above- Ground Biomass (kg)
UPA-Control	9	25.53 (6.08) bc	15.85 (2.04) bc	0.48 (0.05) bc	82.81 (7.77) b	0.0667 (0.0325) b	446.8 (253.97) a
UPB-Control	13	23.5 (2.24) bc	17.92 (1.42) cd	0.51 (0.05) c	79.67 (4.38) b	0.0481 (0.0081) ab	255.21 (49.91) a
LP-Control	15	17.12 (1.27) abc	19.44 (0.88) de	0.57 (0.04) c	117.5 (5.5) d	0.0248 (0.0041) ab	111.51 (24.22) a
R1N-I1	4	18.66 (1.84) abc	17.75 (1.57) cde	0.54 (0.04) c	95.79 (3.43) bc	0.0281 (0.005) ab	126.24 (26.07) a
R1N-I2	4	16.48 (2.54) abc	18.25 (1.69) cde	0.25 (0.06) a	114.46 (8.44) cd	0.0228 (0.0065) ab	99.62 (33.69) a
R1U-I1	4	12.6 (1) a	13.88 (1.14) abc	0.43 (0.04) abc	110.51 (6.71) cd	0.0127 (0.002) a	46.88 (9.11) a
R1U-I2	4	26.35 (3.64) c	23.39 (2.6) e	0.42 (0.07) abc	90.26 (3.61) bc	0.0576 (0.0133) ab	311.36 (82.26) a
R2N-I1	4	13.55 (1.58) a	16.5 (1.23) bcd	0.54 (0.04) c	123.56 (6.7) d	0.015 (0.0036) ab	58.4 (17.71) a
R2N-I2	4	15.97 (0.76) abc	17.56 (1.34) cd	0.5 (0.03) bc	110.58 (8.82) cd	0.0202 (0.0019) ab	82.57 (9.62) a
R2U-I1	4	51.09 (3.14) d	18.52 (3.72) cde	0.55 (0.04) c	37.03 (7.92) a	0.2073 (0.0238) c	1494.29 (205.86) b
R2U-I2	4	46.29 (8.41) d	16.95 (1.77) bcd	0.53 (0.13) c	40.96 (8.94) a	0.1849 (0.0546) c	1345.95 (451.53) b
R4N-I1	4	17.78 (1.12) abc	16.95 (0.48) bcd	0.5 (0.07) bc	96.5 (6.81) bc	0.0251 (0.0033) ab	108.81 (17.7) a
R4N-I2	4	13.93 (1.21) ab	13.22 (0.27) abc	0.28 (0.1) ab	97.23 (8.95) bc	0.0156 (0.0028) ab	60.48 (13.69) a
R4U-I1	4	12.38 (0.84) a	11.24 (0.25) ab	0.63 (0.05) c	92.28 (7.39) bc	0.0122 (0.0017) a	44.4 (7.94) a
R4U-I2	4	13.3 (0.38) a	10.78 (0.21) a	0.64 (0.02) c	81.31 (3.08) b	0.0139 (0.0008) ab	51.97 (3.74) a

^{*} UP = Upper Peninsula Control, LP = Lower Peninsula Control. R1 = EAB Region 1, R2 = EAB Region 2, and R4 = EAB Region 4. Land use type: N = Natural, U = Recreation "Use". I1 = Infestation level 1 (low severity), and I2 = Infestation level 2 (high severity).

Table 2.4. Nearby live competition productivity and light availability for white ash focal trees sampled in Michigan. Number of focal trees sampled per infestation group (n). Mean (standard error of the mean in parentheses) for live competition productivity (basal area (m^2/ha), total aboveground biomass (ton/ha), and light availability (percent openness)) of focal white ash trees in fifteen infestation groups. Groupings with different letters are significantly different (p < 0.05).

Infestation Group *	n	Basal Area (m²/ha)	Total Above-ground Biomass (Metric ton/ha)	Light Availability (Percent openness)
UPA - Control	9	20.4 (5.36) ab	135.8 (39.98) ab	6.4 (0.3) a
UPB - Control	13	25.4 (4.48) ab	132.7 (22.15) ab	9.6 (0.6) abc
LP - Control	15	20.5 (3.62) ab	95.8 (18.21) ab	7.5 (0.1) ab
R1N-I1	4	18.2 (3.71) ab	80.4 (14.86) ab	7.2 (0.3) ab
R1N-I2	4	18.5 (2.14) ab	87.8 (9.85) ab	7.2 (0.3) ab
R1U-I1	4	33.9 (7.8) bcd	190.3 (38.19) ab	8.9 (0.4) abc
R1U-I2	4	24.7 (12.92) abc	135.8 (78.73) ab	9 (0.8) abc
R2N-I1	4	50.4 (8.73) cd	229.4 (50.26) bc	7.7 (0.6) abc
R2N-I2	4	17.8 (5.66) ab	73.3 (26.24) ab	7.5 (0.4) abc
R2U-I1	4	56.4 (35.88) d	410.2 (259.44) c	19 (5.5) d
R2U-I2	4	6.3 (3.65) a	44.9 (25.98) ab	34.5 (8.4) e
R4N-I1	4	14.9 (4.6) ab	58.2 (15.8) ab	8.8 (0.4) abc
R4N-I2	4	13 (3.63) ab	49.8 (13.98) ab	8.1 (0.1) abc
R4U-I1	4	2.7 (1.63) a	10.1 (6.29) a	13.4 (1.5) cd
R4U-I2	4	3 (0.89) a	13.5 (4.84) a	11.7 (0.8) bc

^{*} UP = Upper Peninsula Control, LP = Lower Peninsula Control. R1 = EAB Region 1, R2 = EAB Region 2, and R4 = EAB Region 4. Land use type: N = Natural, U = Recreation "Use". I1 = Infestation level 1 (low severity), and I2 = Infestation level 2 (high severity).

Table 2.5. General statistics of the standard chronologies of white ash sampled in Michigan for each of the 15 Infestation groups.

Common Interval Analysis (1992-2012)**Total** No. of No. of Infestation Mean Standard Absent Intercore Chronology Group * sensitivity ŧ deviation ŧ trees rings (%) trees correlation • Length 9 0 8 **UPA - Control** 1916-2013 0.251 0.406 0.182 **UPB** - Control 1921-2013 13 0.196 0.330 0 11 0.234 0.249 1958-2012 15 0.316 0 15 0.547 LP - Control 2 **R1N-I1** 1979-2012 4 0.216 0.356 0 0.163 0.774 **R1N-I2** 1986-2012 4 0.248 0.389 3.125 3 **R1U-I1** 1963-2012 4 0.259 0.432 0 4 0.332 **R1U-I2** 1969-2012 0.285 4 0.435 1.33 4 0.647 **R2N-I1** 4 0 4 1968-2012 0.195 0.285 0.508 **R2N-I2** 1967-2012 4 0.24 0.517 0.595 4 0.587 **R2U-I1** 1978-2012 4 0.218 0.224 0 4 0.087 R2U-I2 1954-2012 4 0.235 0.331 0 4 0.296 **R4N-I1** 1984-2012 4 0.248 0.350 1.587 4 0.497 0.270 **R4N-I2** 1978-2012 4 0.398 5.43 4 0.141 0 **R4U-I1** 1972-2012 4 0.255 0.445 4 0.195 **R4U-I2** 0.280 3 1983-2012 4 0.463 6.52 0.287

^{*} UP = Upper Peninsula Control, LP = Lower Peninsula Control. R1 = EAB Region 1, R2 = EAB Region 2, and R4 = EAB Region 4. Land use type: N = Natural, U = Recreation "Use". I1 = Infestation level 1 (low severity), and I2 = Infestation level 2 (high severity). t Produced by ARSTAN using the detrended chronologies.

[†] Produced using detrended chronologies in SYSTAT using a pairwise Pearson correlation.

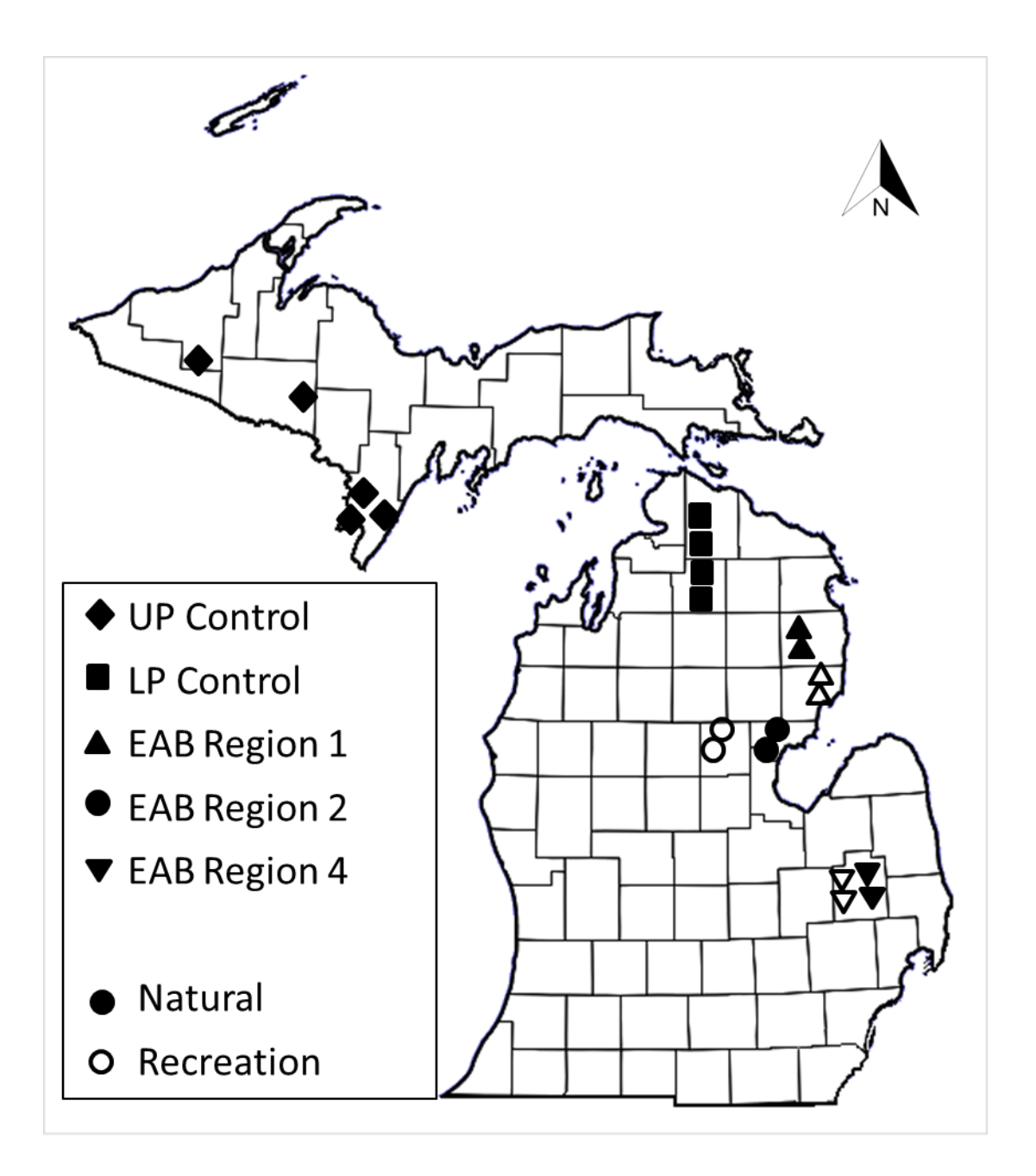


Figure 2.1. Site map representing general locations of white ash sample sites in Michigan. UP = Upper Peninsula Control, LP = Lower Peninsula Control, Control = non-symptomatic sites, EAB = emerald ash borer infested regions (R1, R2 and R4). Solid shapes represent "natural" sites while open shapes represent recreation "use" sites.

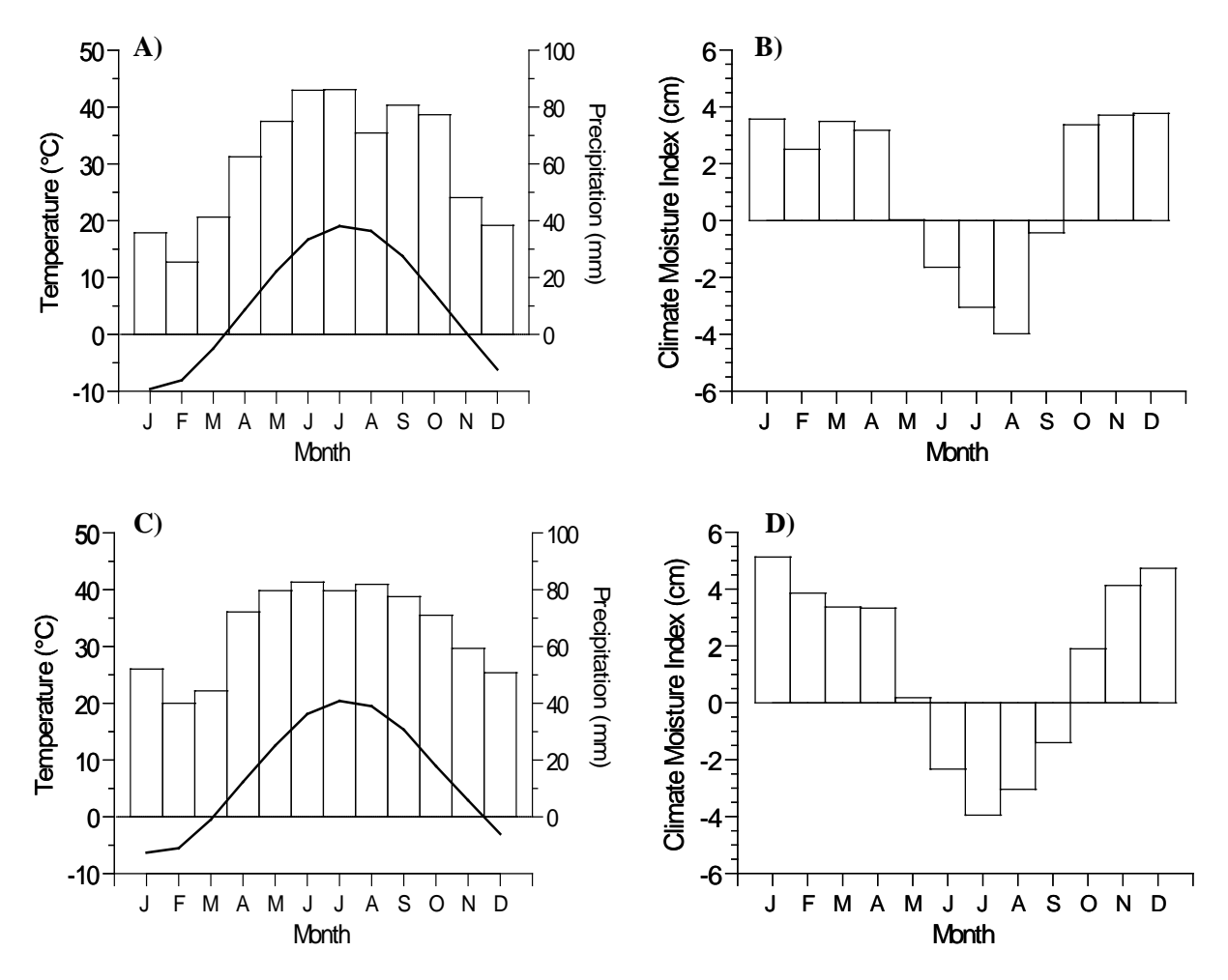


Figure 2.2. A) Mean monthly temperature and mean total monthly precipitation were averaged from 1992 - 2012 for the six plot locations in the UP (western UP). Line represents temperature and bars represent precipitation. B) Mean monthly climatic moisture index averaged from 1992 - 2012 for the six plot locations in the UP. C) Mean monthly temperature and mean total monthly precipitation average from 1992-2012 for all plot locations in the Lower Peninsula. Line represents temperature and bars represent precipitation. D) Mean monthly climatic moisture index averaged from 1992-2012 for all plot locations in the Lower Peninsula.

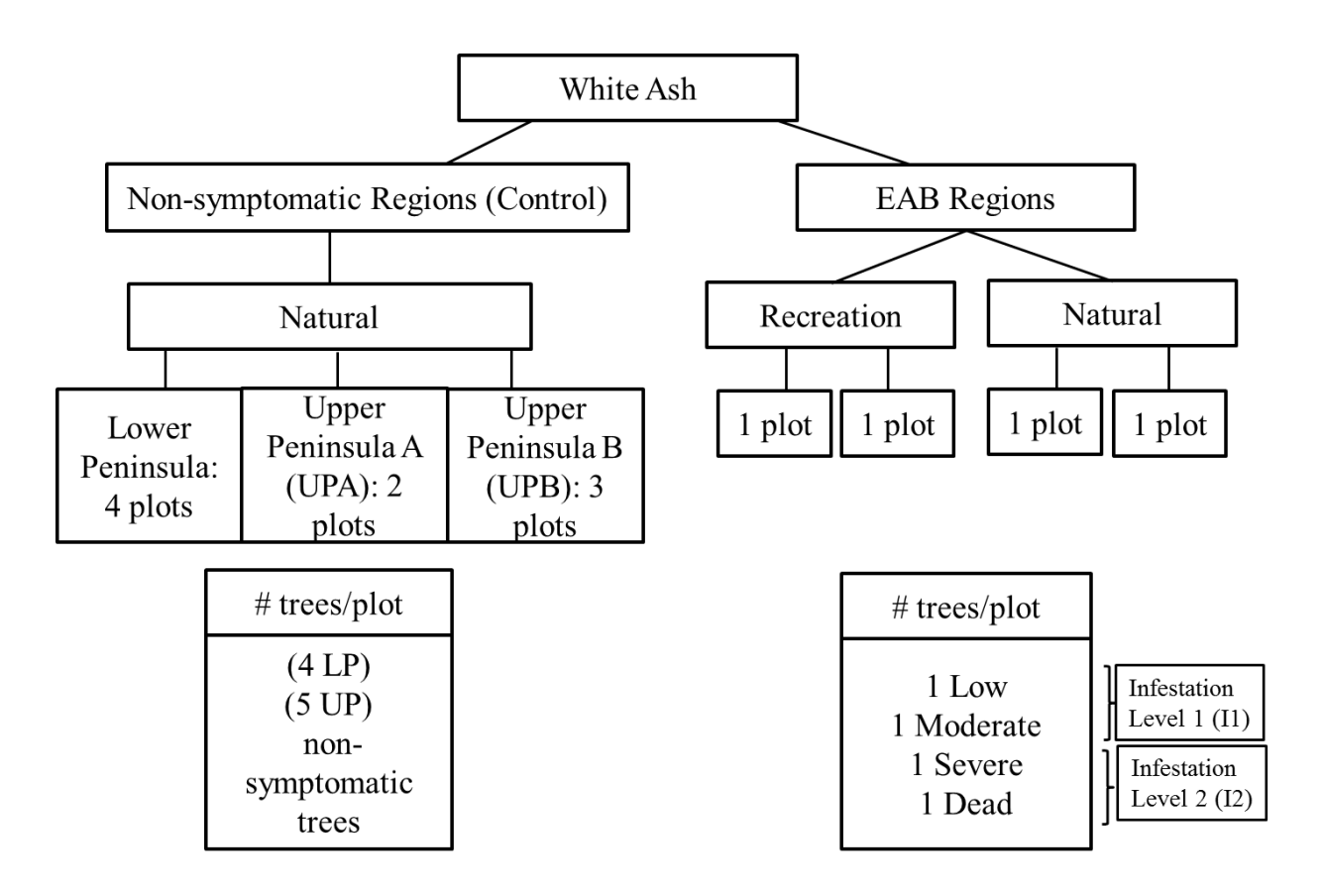


Figure 2.3. Sampling design of the regions sampled in Michigan's (3 control regions, 3 EAB regions). Each EAB infested region sampled had 16 trees for a total of 48 infested trees sampled. The LP control region had four plots with only non-symptomatic white ash sampled in natural stands. Each of the three EAB infested regions was separated between two land-use classes (recreational use and natural). There were two plots sampled in each land-use class with four trees per plot. In the EAB region plots, trees were selected so that there was one tree representing one of four crown dieback classes. Later in the dendrochronology analysis, these four dieback classes were further consolidated into two infestation levels (I1 represents both the low and moderate dieback classes and I2 represents the combined severe and dead dieback classes).

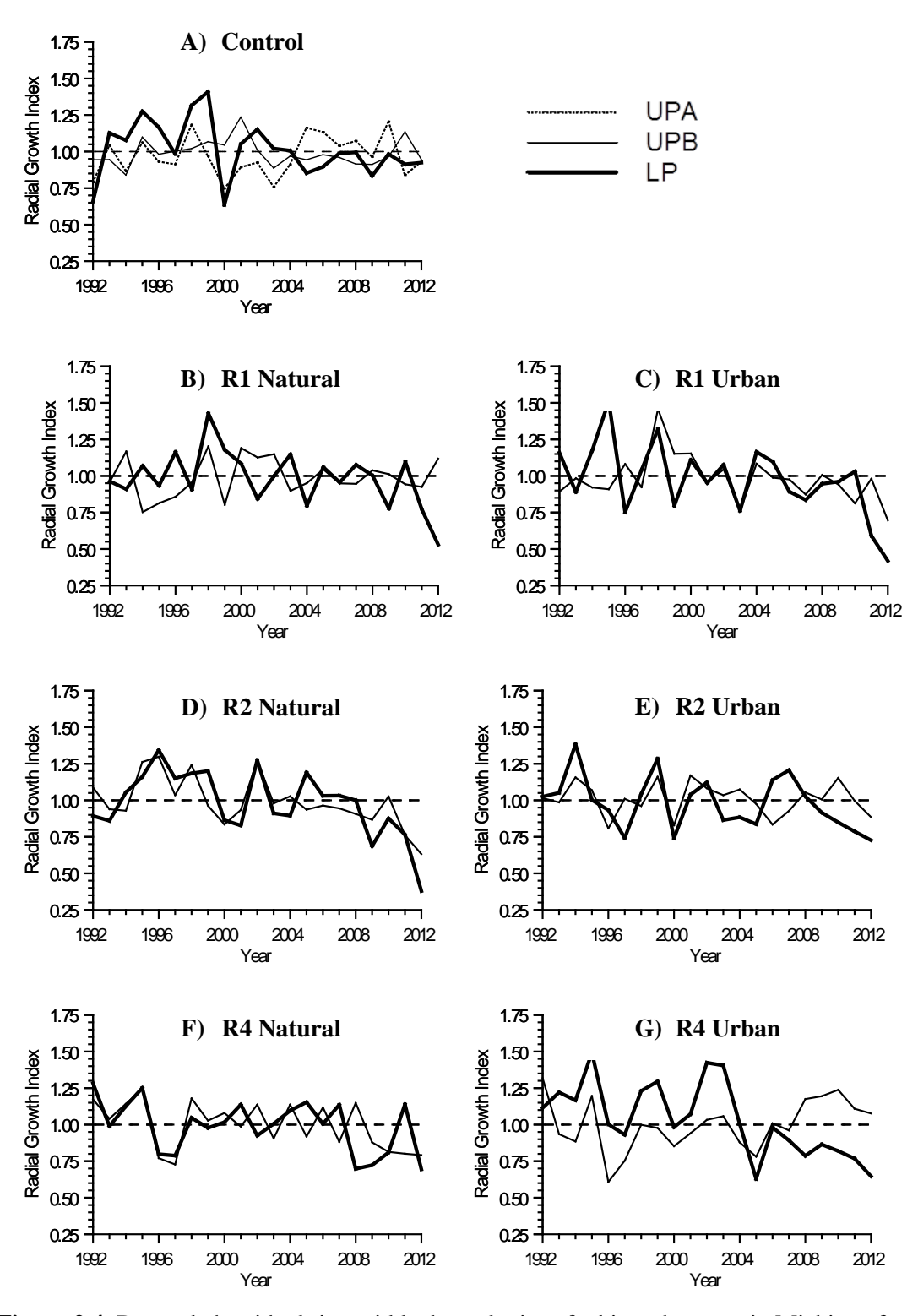


Figure 2.4. Detrended residual ring width chronologies of white ash grown in Michigan from 1992 to 2012. The thin solid line represents Infestation group "I1" (lower severity crown dieback) and the thick solid line represents Infestation group "I2" (higher severity crown dieback).

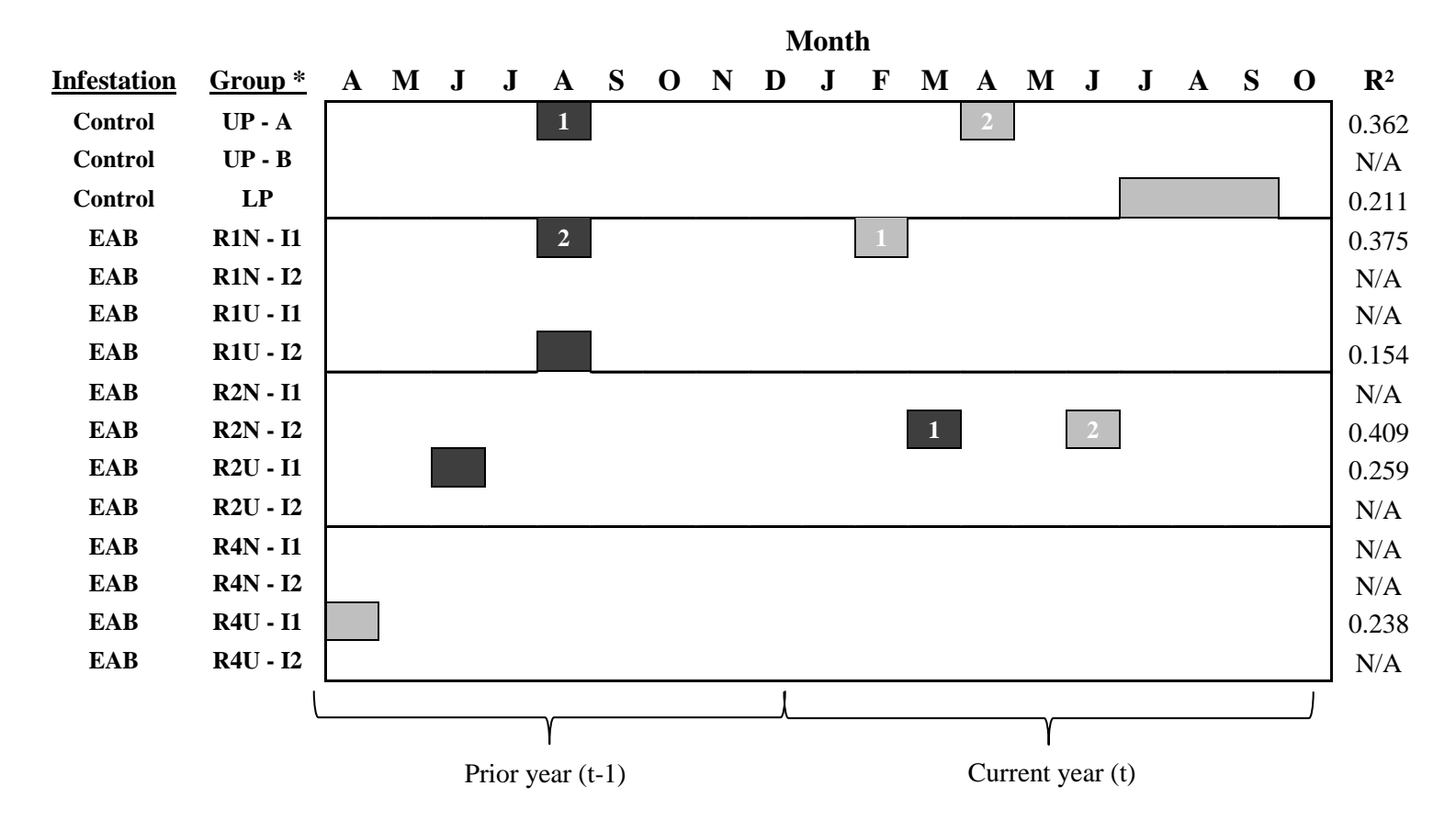


Figure 2.5. Regression models representing monthly and/or seasonal mean monthly temperature influences on growth and the associated adjusted r^2 value for white ash in Michigan's Lower Peninsula and Upper Peninsula. Regression models presented are all statistically significant (p < 0.05). For each model, the climate variables that have a positive influence on growth are represented by light gray boxes, and climate variables with a negative influence on growth are represented by the darker boxes. Infestation groups with R^2 denoted by N/A have no significant growth response to mean monthly temperature. Groups with multiple significant variables are ranked in order of importance using Beta regression coefficients (i.e., a rank of 1 is the most influential predictor variable in the regression model).

^{*} UP = Upper Peninsula Control, LP = Lower Peninsula Control. R1 = EAB Region 1, R2 = EAB Region 2, and R4 = EAB Region 4. Land use type: N = Natural, U = Recreation "Use". I1 = Infestation level 1 (low severity), and I2 = Infestation level 2 (high severity).

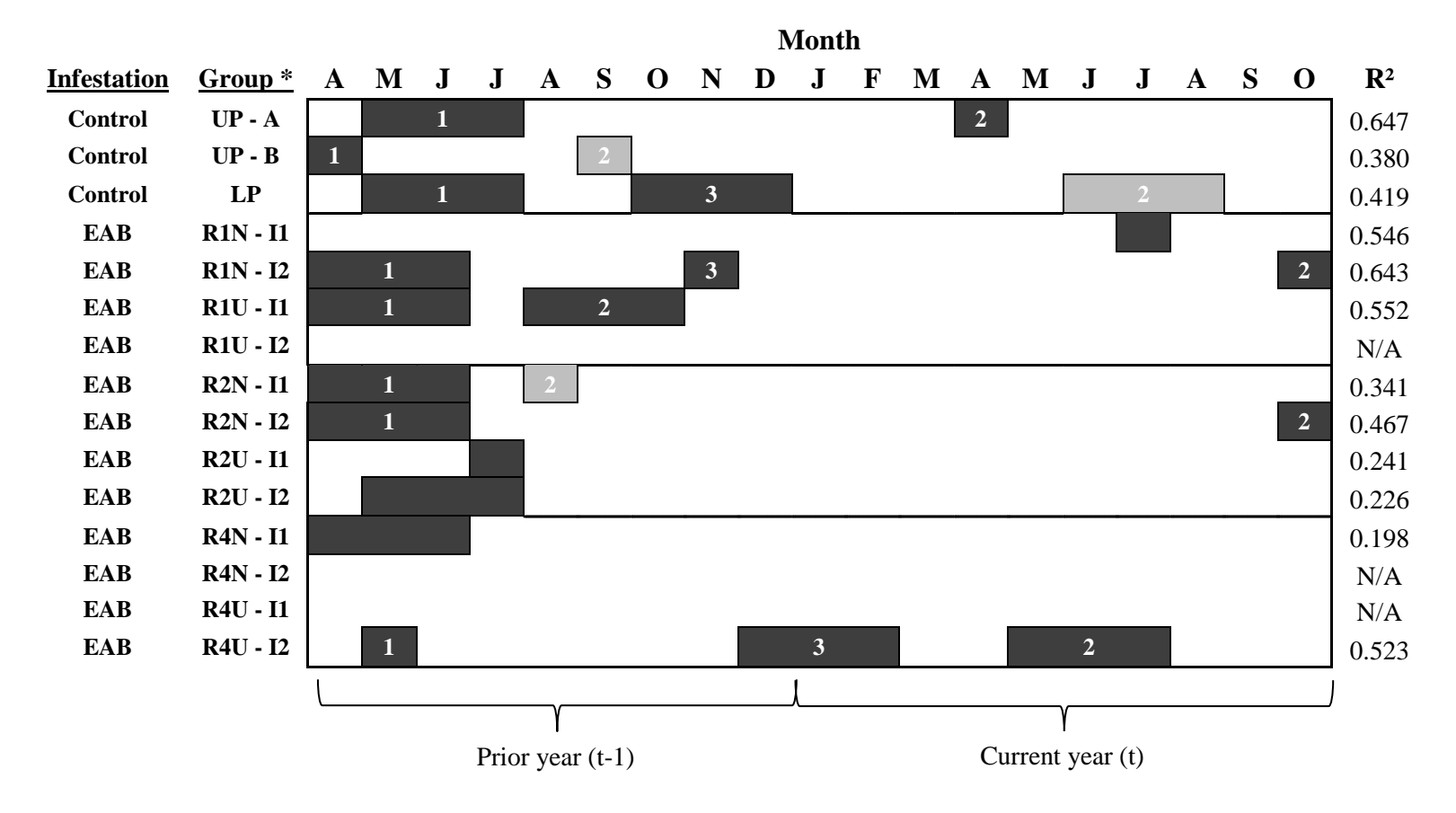


Figure 2.6. Regression models representing monthly and/or seasonal total precipitation influences on growth and the associated adjusted r^2 value for white ash in Michigan's Lower Peninsula and Upper Peninsula. Regression models presented are all statistically significant (p < 0.05). For each model, the climate variables that have a positive influence on growth are represented by light gray boxes, and climate variables with a negative influence on growth are represented by the darker boxes. Groups with R^2 denoted by N/A have no significant growth response to total monthly precipitation. Groups with multiple significant variables are ranked in order of importance using Beta regression coefficients (i.e., a rank of 1 is the most influential predictor variable in the regression model).

^{*} UP = Upper Peninsula Control, LP = Lower Peninsula Control. R1 = EAB Region 1, R2 = EAB Region 2, and R4 = EAB Region 4. Land use type: N = Natural, U = Recreation "Use". I1 = Infestation level 1 (low severity), and I2 = Infestation level 2 (high severity).

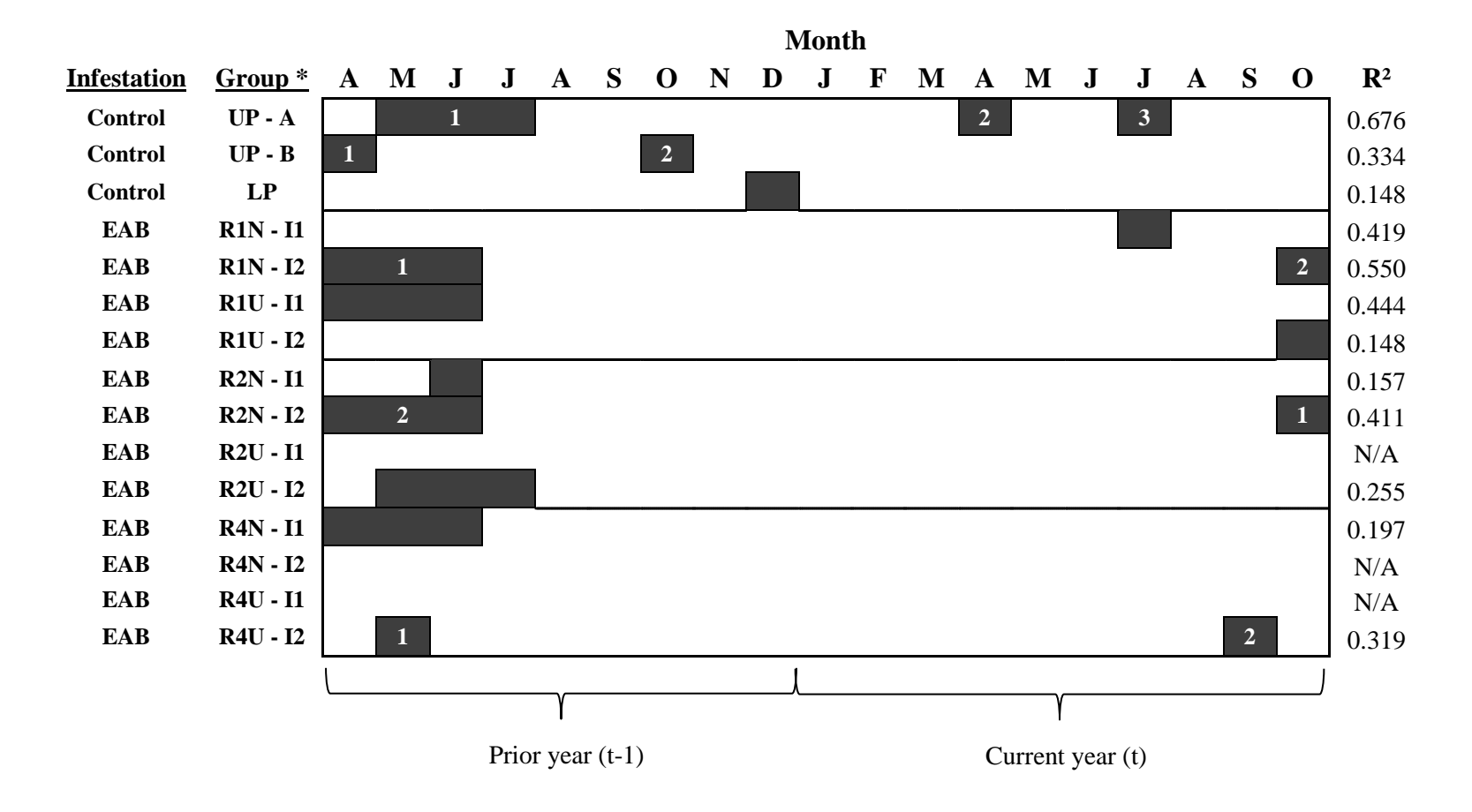


Figure 2.7. Regression models representing monthly and/or seasonal total climatic moisture index (CMI) influences on growth and the associated adjusted r^2 value for white ash in Michigan's Lower Peninsula and Upper Peninsula. Regression models presented are all statistically significant (p < 0.05). For each model, the climate variables that have a positive influence on growth are represented by light gray boxes, and climate variables with a negative influence on growth are represented by the darker boxes. Groups with R^2 denoted by N/A have no significant growth response to total monthly CMI. Groups with multiple significant variables are ranked in order of importance using Beta regression coefficients (i.e., a rank of 1 is the most influential predictor variable in the regression model).

^{*} UP = Upper Peninsula Control, LP = Lower Peninsula Control. R1 = EAB Region 1, R2 = EAB Region 2, and R4 = EAB Region 4. Land use type: N = Natural, U = Recreation "Use". I1 = Infestation level 1 (low severity), and I2 = Infestation level 2 (high severity).

REFERENCES

REFERENCES

- Adams, H.D., Guardiola-Claramonte, M., Barron-Gafford, G.A., Villegas, J.C., Breshears, D.D., Zou, C.B., Troch, P.A., Huxman, T.E., 2009. Temperature sensitivity of drought induced tree mortality portends increased regional die-off under global-change-type drought. Proceedings of the National Academy of Science 106, 7063-7066.
- Augspurger, C.K., 2009. Spring 2007 warmth and frost: phenology, damage and refoliation in a temperate deciduous forest. Functional Ecology 23, 1031-1039.
- Avery, T.E., Burkhart, H.E., 2002. Forest measurements. 5th edition. New York, NY: McGraw-Hill.
- Burnham, K.P., Anderson, D.R., 2002. Model selection and multimodel inference: a practical information-theoretic approach. Springer-Verlag, New York, NY. 488 pp.
- Campbell, R., Smith, D. J., Arsenault, A. 2005. Dendroentomological and forest management implications in the interior Douglas-fir zone of British Columbia, Canada. Dendrochronologia 22, 135-140.
- Catton, H.A., St.George, S., Remphrey, W.R., 2007. An evaluation of bur oak (Quercus macrocarpa) decline in the urban forest of Winnipeg, Manitoba, Canada. Arboriculture and Urban Forestry 33, 22-30.
- Chen, Y., Ciaramitaro, T., Poland, T.M., 2011. Moisture content and nutrition as selection forces for emerald ash borer larval feeding behavior. Ecological Entomology 36, 344-354.
- Chen, Y., Poland, T.M., 2009. Biotic and abiotic factors affect green ash volatile production and emerald ash borer adult feeding preference. Environmental Entomology 38, 1756-1764.
- Chhin, S., 2010. Influence of climate on the growth of hybrid poplar in Michigan. Forests 1, 209-229.
- Chhin, S., 2015. Impact of future climate change on a genetic plantation of hybrid pine. Botany 93, 397-404.
- Chhin, S., Hogg, E.H., Lieffers, V.J., Huang, S., 2008. Potential effects of climate change on the growth of lodgepole pine across diameter size classes and ecological regions. Forest Ecology and Management 256, 1692-1703.
- Cook, E.R., 1985. A time series analysis approach to tree-ring standardization. PhD Thesis. University of Arizona, Tucson, AZ, USA.
- Daly, C., Halbleib, M., Smith, J.I., Gibson, W.P., Doggett, M.K., Taylor, G.H., Curtis, J., Pasteris, P.P., 2008. Physiographically sensitive mapping of climatological temperature and precipitation across the conterminous United States. International Journal of Climatology DOI: 10.1002/joc.1688.
- Denton, S.R., Barnes, B.V., 1988. An ecological climatic classification of Michigan: a quantitative approach. Forest Science 34, 119-138.
- Dillaway, D.N., Kruger, E.L., 2010. Thermal acclimation of photosynthesis: a comparison of boreal and temperate tree species along a latitudinal transect. Plant, Cell and Environment 33, 888-899.

- EPA, 2015. Level III and IV ecoregions of the continental United States. http://www.epa.gov/wed/pages/ecoregions/level_iii_iv.htm
- Everham III, E.M.Brokaw, N.V.L., 1996. Forest damage and recovery from catastrophic wind. Botanical Review 62, 113-185.
- Fierke, M. K., Stephen, F. M., 2010. Dendroentomological evidence associated with an outbreak of the native wood-boring beetle *Enaphalodes rufulus*. Canadian Journal of Forest Research 40, 679-686.
- Flower, C.E., Knight, K.S., Rebbeck, J., Gonzalez-Meler, M.A., 2013. The relationship between the emerald ash borer (*Agrilus planipennis*) and ash (*Fraxinus* spp.) tree decline: Using visual canopy condition assessments and leaf isotope measurements to assess pest damage. Forest Ecology and Management 303, 143-147.
- Francese, J.A., Oliver, J.B., Fraser, I., Lance, D.R., Youssef, N., Sawyer, A.J., Mastro, V.C., 2008. Influence of trap placement and design on capture of the emerald ash borer (Coleoptera: Buprestidae). Journal of Economic Entomology 101, 1831-1837.
- Fritts, H.C., 1976. Tree Rings and Climate. The Blackburn Press, Caldwell, New Jersey, U.S.A.
- Gillner, S., Brauning, A., Roloff, A., 2014. Dendrochronological analysis of urban trees: climatic response and impact of drought on frequently used tree species. Trees 28, 1079-1093.
- Gower S.T., Isebrands J.G., Sheriff D.W. 1995. Carbon allocation and accumulation in conifers. In: Smith W.K., Hinckley T.M., editors. Resource Physiology of Conifers. San Diego: Academic Press; pp. 217-254.
- Grissino-Mayer, H. D. 2001. Research Report, Evaluating crossdating accuracy: a manual and tutorial for the computer program COFECHA. Tree-Ring Research 57, 205-221.
- Haavik, L. J., Stephen, F. M., Fierke, M. K., Salisbury, V. B., Leavitt, S. W., Billings, S. A. 2008. Dendrochronological parameters of northern red oak (*Quercus rubra* L. (Fagaceae)) infested with red oak borer (*Enaphalodes rufulus* (Haldeman) (Coleoptera: Cerambycidae)). Forest Ecology and Management 255, 1501-1509.
- Haavik, L. J., Stephen, F. M. 2010. Historical dynamics of a native cerambycid, *Enaphalodes rufulus*, in relation to climate in the Ozark and Ouachita Mountains of Arkansas. Ecological Entomology 35, 673-683.
- Hacke, U., Sauter, J.J., 1996. Xylem dysfunction during winter and recovery of hydraulic conductivity in diffuse-porous and ring-porous trees. Oecologia 105, 435-439.
- Hardin, J.W., Leopold, D.J., White, F.M. 2001. Textbook of Dendrology. Edition 9. McGraw-Hill Higher Education.
- Herms, D.A., McCullough, D.G., 2014. Emerald ash borer invasion of North America: history, biology, ecology, impacts, and management. Annual Reviews of Entomology 59, 13-30.

- Hogg, E.H., 1997. Temporal scaling of moisture and the forest-grassland boundary in western Canada. Agricultural and Forest Meteorology 84, 115-122.
- Huang, J., Tardif, J.C., Bergeron, Y., Denneler, B., Berninger, F., Girardin, M.P. 2010. Radial growth response of four dominant boreal tree species to climate along a latitudinal gradient in the eastern Canadian boreal forest. Global Change Biology 16, 711-731.
- Huang, J., Bergeron, Y., Zhai, L., Denneler, B., 2011. Variation in intra-annual radial growth (xylem formation) of *Picea mariana* (Pinaceae) along a latitudinal gradient in western Quebec, Canada. American Journal of Botany 98, 792-800.
- Jenkins, J.C., Chojnack, D.C., Heath, L.S., Birdsey, R.A., 2003. National-scale biomass estimators for United States tree species. Forest Science 49, 12-35.
- Johnson, J.E., 1995. The Lake States Region, in: Barrett, J.W., 1995. Regional Silviculture of the United States, third edition. John Wiley and Sons Inc. New York, New York, pp. 81 127.
- Knight, K.S., Brown, J.P., Long, R.P. 2013. Factors affecting the survival of ash (*Fraxinus* spp.) trees infested by emerald ash borer (*Agrilus planipennis*). Biological Invasions 15, 371-383.
- Koprowski, M., Duncker, P. 2012. Tree ring width and wood density as the indicators of climatic factors and insect outbreaks affecting spruce growth. Ecological Indicators 23, 332-337.
- Larsson, L., 2008a. CooRecorder program of the CDendro package. Version 7.1. http://www.cybis.se
- Magruder, M., Chhin, S., Monks, A., O'Brien, J., 2012. Effects of initial stand density and climate on red pine productivity within Huron National Forest, Michigan, USA. Forests 3, 1086-1103.
- Mäkinen, H., Nöjd, P., Isomäki, A., 2002. Radial, height and volume increment variation in *Picea abies* (L.) Karst. stands with varying thinning intensities. Scandinavian Journal of Forest Research 17, 304-316.
- Martin-Benito, D., Pederson, N., 2015. Convergence in drought stress, but a divergence of climatic drivers across a latitudinal gradient in a temperate broadleaf forest. Journal of Biogeography 42, 925-937.
- McCullough, D.G., and Siegert, N.W. 2007a. Using girdled trap trees effectively for emerald ash borer detection, delimitation and survey. Michigan State University; Michigan Technological University; USDA Forest Service, Forest Health Protection.
- McCullough, D.G., Siegert, N.W., 2007b. Estimating potential emerald ash borer (Coleoptera: Buprestidae) populations using ash inventory data. Entomological Society of America 100, 1577-1586.
- McCullough, D.G., Siegert, N.W., Poland, T.M., Pierce, S.J., Ahn, S.Z. 2011. Effects of trap type, placement and ash distribution on emerald ash borer captures in a low density site. Environmental Entomology 40, 1239-1252.
- MDARD (Michigan Department of Agriculture and Rural Development), 2015. Emerald Ash Borer: State of Michigan. http://www.michigan.gov/mdard/0,4610,7-125-1568_2390_18298---,00.html

- Mercader, R.J., McCullough, D.G., Bedford, J.M., 2013. A comparison of girdled ash detection trees and baited artificial traps for Agrilus planipennis (Coleoptera: Buprestidae) detection. Environmental Entomology 42, 1027-1039.
- Natural Resources Conservation Service, 2015. Web Soil Survey. United States Department of Agriculture, Natural Resources Conservation Service, Soil Survey Staff. http://websoilsurvey.nrcs.usda.gov/. Accessed June 17, 2015
- Pan, C., Tajchman, S.J., Kochenderfer, J.N. 1997. Dendroclimatological analysis of major forest species of the central Appalachians. Forest Ecology and Management 98, 77-87.
- Persad, A.B., Tobin, P.C., 2015. Evaluation of ash tree symptoms associated with emerald ash borer infestation in urban forests. Arboriculture and Urban Forestry 41, 103-109.
- Persad, A.B., Siefer, J., Montan, R., Kirby, S., Rocha, O.J., Redding, M.E., Ranger, C.M., Jones, A.W., 2013. Effects of emerald ash borer infestation on the structure and material properties of ash trees. Arboriculture and Urban Forestry 39, 11-16.
- Peterson, C.J., 2000. Catastrophic wind damage to North American forests and the potential impact of climate change. The Science of the Total Environment 262, 287-311.
- Poland, T.M., McCullough, D.G., 2006. Emerald ash borer: invasion of the urban forest and the threat to North America's ash resource. Journal of Forestry pp. 118-124.
- Pontius, J., Martin, M., Plourde, L., Hallet, R., 2008. Ash decline assessment in emerald ash borer-infested regions: a test of tree-level, hyperspectral technologies. Remote Sensing of Environment 112, 2665–2676
- PRISM Climate Group, Oregon State University, Accessed 2014. http://prism.oregonstate.edu
- Raupp, M.J., Cumming, A.B., Raupp, E.C., 2006. Street tree diversity in eastern North America and its potential for tree loss to exotic borers. Arboriculture and Urban Forestry 32, 297-304.
- Robson, J.R.M., Conciatori, F., Tardif, J.C., Knowles, K., 2015. Tree-ring response of jack pine and scots pine to budworm defoliation in central Canada. Forest Ecology and Management 347, 83-95.
- Rolland, C., Lemperiere, G. 2004. Effects of climate on radial growth of Norway spruce and interactions with attacks by the bark beetle *Dendroctonus micans* (Kug., Coleoptera: Scolytidae): a dendroecological study in the French Massif Central. Forest Ecology and Management 201, 89-104.
- Ryall, K.L., Fidgen, J.G., Turgeon, J.J. 2011. Detectability of the Emerald Ash Borer (Coleoptera: Buprestidae) in Asymptomatic Urban Trees by using Branch Samples. Environmental Entomology 40, 679-688.
- Siegert, N. W., McCullough, D. G., Liebhold, A. M., Telewski, F. W. 2014. Dendrochronological reconstruction of the epicenter and early spread of emerald ash borer in North America. Diversity and Distributions 20, 847-858.
- Speer, J.H., 2010. Fundamentals of tree-ring research. The University of Arizona Press, Tucscon Arizona.

- SYSTAT Software Incorporated, 2002. SYSTAT 10.2 Statistics 1, Richmond, CA.
- Tardif, J., Bergeron, Y. 1997. Comparative dendroclimatological analysis of two black ash and two white cedar populations from contrasting sites in the Lake Duparquet region, northwestern Quebec. Canadian Journal of Forest Research 27, 108-116.
- USDA APHIS PPQ, 2013. USDA APHIS PPQ: 2013 emerald ash borer survey guidelines. United States Department of Agriculture, Animal and Plant Health Inspection Service, Plant Protection and Quarantine.
- USDA APHIS PPQ, 2015. USDA APHIS PPQ: 2015 emerald ash borer survey guidelines. United States Department of Agriculture, Animal and Plant Health Inspection Service, Plant Protection and Ouarantine.
- Venables, W.N., Ripley, B.D., 2002. Modern applied statistics with S, 4th edition. Springer, New York.
- Watt, M.S., D'Ath, R., Leckie, A.C., Clinton, P.W., Coker, G., Davis, M.R., Simcock, R., Parfitt, R.L., Dando, J., Mason, E.G., 2008. Modelling the influences of stand structural, edaphic and climatic influences on juvenile *Pinus radiat*a fibre length. Forest Ecology and Management 254, 166-177.
- Yamaguchi, D.K. 1991. A simple method for cross-dating increment cores from living trees. Canadian Journal of Forest Research 21, 414-416.
- Zar, J.H., 1999. Biostatistical analysis, 4th edition. Prentice Hall, Upper Saddle River.
- Zhang, Q., Alfaro, R.I., Hebda, R.J. 1999. Dendroecological studies of tree growth, climate and spruce beetle outbreaks in Central British Columbia, Canada. Forest Ecology and Management 121, 215-225.

CHAPTER 3

USE OF NEAR-INFRARED SPECTROSCOPY (NIR) AS AN INDICATOR OF EMERALD ASH BORER INFESTATION IN WHITE ASH IN MICHIGAN

3.1. Introduction

Since the initial discovery of emerald ash borer (EAB) (*Agrilus planipennis* Fairmaire) (Coleoptera: Buprestidae), the previously limited knowledge about its biology has greatly been expanded through significant research in little over a decade (Herms and McCullough, 2014). Initial detection methods relied on the visual signs and symptoms of infestation which tend to appear after populations have expanded in an area and further dispersal has already occurred (Herms and McCullough, 2014). Research efforts and funding are focused on developing new methods for the detection and monitoring the spread of EAB in order to mitigate damage (Pontius et al., 2008). Research utilizing satellite-based hyperspectral imaging specifically in the NIR range to monitor EAB induced ash decline has been conducted with some success and limitations in assessing infestation levels using tree foliage (Pontius et al., 2008; Eastman et al., 2005; Zhang et al., 2014).

Induced systemic plant resistance results when insect herbivory (or other forms of damage) on plants stimulates a signal that is translocated from the damaged tissue to other parts of the plant, resulting in chemical or physical changes in tissues away from the damaged area (Ananthakrishnan, 2001; Leon et al., 2001). Studies have shown that ash trees become stressed and are highly attractive to adult EAB beetles after bark and phloem girdling a tree, leading to the effectiveness of utilizing girdled trap trees for EAB detection (McCullough et al., 2009a, 2009b). Increases in bark sesquiterpenes have been measured in the bark and phloem from girdled green ash (*Fraxinus pennsylvanica*) compared to non-girdled trees (Crook and Mastro, 2010; Crook et al., 2008b). Six phenolics were shown to decrease in the phloem of EAB infested trees, but the phenolic concentrations themselves did not vary significantly along the stem of 3 m tall black (*F. nigra* Marshall) and Manchurian (*F. mandschurica* Ruprecht) ash when sampled from the crown towards the soil line (Chakraborty et al., 2014). While limited studies have been

conducted on the changes of sapwood quality for girdled trees, physical and chemical responses in the sapwood below phloem-girdles have been identified (Taylor and Cooper, 2002; Parkin, 1938).

Near-infrared spectroscopy (NIR) (wavelength range 780-2500 nm) has been previously used in forestry and the wood products industry for rapidly and non-destructively measuring the physical and chemical properties of tree tissues (Axrup et al., 2000; So et al., 2004; Schimleck, 2002). For forest health studies focused on detection and monitoring, the majority have measured foliage samples (either field based or using hyperspectral imaging) (Pontius et al., 2005; Pontius et al., 2008; Riggins et al., 2011; Eastman et al., 2005). Studies focused on wood properties and decay have measured wood tissues using NIR (Watanabe et al., 2012; Fackler and Schwanninger, 2012; Axrup et al., 2000). Available spectrometers come in a wide selection of wavelength range options and models that cover wider portions of the electromagnetic spectrum (up to 2500 nm) are generally more expensive than lower range models, many of which only go up to 1700 nm wavelengths. A nondestructive, field based method for sampling trees using NIR is the collection of increment cores, which preserves the trees for later research or product utilization (Roberts et al., 2004; Schimleck et al., 2002). Sampling trees from a height of 1.1 to 2.2 meters has been shown to provide a good representation of the entire tree in NIR studies (Roberts et al., 2004).

This preliminary study explores the potential application of ground based, near-infrared spectroscopy (NIR) for early detection of EAB by collecting spectral measurements for white ash bark, phloem and xylem tissue sampled from breast height. The main objective of this first stage project is to investigate the ability of NIR spectroscopy to differentiate between white ash with known EAB infestation and non-symptomatic (assumed uninfested) white ash throughout the state of Michigan. I hypothesize that the physical and/or chemical changes in the bark, phloem and xylem (associated with EAB infestation) can be measured using NIR spectroscopy. Although the specific response mechanisms will not be measured in this study, changes associated with infestation can possibly be indicated using this technology. To address the main objective, the study will answer three questions: (1) Using qualitative analytical methods (stepwise, linear discriminant analysis), can NIR spectroscopy differentiate between white ash tissues with known EAB infestation and non-symptomatic trees of the same species? (2) Do

different spectral pretreatment methods influence the ability of stepwise linear discriminant analysis to classify samples into predetermined groups? (3) Does reducing the spectral range change the accuracy in classification of EAB infested trees?

3.2. Methods

3.2.1. Study Site and Field Sampling

The same site locations and white ash trees were sampled for both Chapters 2 and 3 with a few exceptions. Three latitudinal regions in the Lower Peninsula of Michigan were sampled in the summer of 2013, with four plots per region with three trees with known EAB infestation sampled per plot. Each tree per plot represented a different level of crown vigor (low decline (10-25% crown damage), moderate decline (26 to 50% crown damage), and severe decline (> 50% crown damage)), with one tree in each class (crown vigor classes adapted from Pontius et al., (2008)). To avoid potential effects of decay, the dead trees sampled in Chapter 2 were not included in any analysis in this particular study. A total of thirty six, live EAB infested trees were sampled. As NIR is a highly site specific technology, when using NIR over a broad geographical range, it is recommended to sample over a variety of site conditions (Burns and Ciurczak, 2008). Therefore, plots were selected in high impact recreational sites as well as in natural (minimal human impact) areas to improve the robustness of the sample set. Additionally in 2013, an average of 3.75 (range: 3-4 trees) non-symptomatic, with no major branch mortality (control) trees per plot were sampled in four plots (fifteen trees total) in the Lower Peninsula, north of Huron-Manistee National Forest (Cheboygan and Otsego counties). An average of 4.7 (range: 4-5 trees) non-symptomatic trees per plot were sampled in the summer of 2014 in six plots in the Ontonagon, Iron, Menominee and Delta counties of the Upper Peninsula of Michigan (total of twenty eight trees). There were a combined total of forty-three control trees sampled in the Lower and Upper Peninsulas. The general locations of all plots included in this study can be seen in Figure 3.1. For a further detailed description of site selection and site characteristics, please see Chapter 2.2.1.

Four short increment cores of the bark, phloem and outermost xylem (approximately 4-5 cm in length) were collected from the trunk of each tree at breast height (1.37 m) from the four cardinal directions using an increment borer. Cores were stored in plastic straws and kept on ice until returning to East Lansing, MI, where they were kept refrigerated (5°C). Additional field sampling procedures for

supplemental EAB infestation symptoms, tree characteristics and competition information can be found in Chapter 2.2.2.

3.2.2. Sample Preparation

The stem increments were dried in the plastic straws (with a hole cut in each straw) for 24 - 48 hours at 80 °C before collecting NIR spectra. Previous studies have shown that moisture influences NIR spectrum, so all stem samples were dried to prevent fluctuations due to water content (Schwanninger et al., 2011; Henery et al., 2008). Since temperature of the samples can also influence the spectrum, all samples were allowed to cool to room temperature before collecting measurements (Schwanninger et al., 2011; Henery et al., 2008). After drying, a single-edged razor blade was used to slice the phloem and bark from the xylem along the tangential plane (Figure 3.2). If possible, the bark and phloem were kept in one piece as bark segments had a tendency to break into multiple pieces during collection. The outermost 20 mm of the xylem (closest to the bark) was separated from any excess wood and used for all NIR measurements (Figure 3.2).

3.2.3. Acquisition of NIR Diffuse Reflectance Spectra

NIR diffuse reflectance spectra were collected using a NIR spectrometer (AvaSpec-NIR256-2.5 TEC (Avantes, Colorado, USA)), a tungsten halogen light source SPL-2H (Photon Control, British Columbia, Canada), and a reflectance probe (SPA-RP-SMA-200-V) (Photon Control). Avasoft (version 8.1) software (Avantes, Colorado, USA) was used for all spectra collection and specifying spectrometer settings (Avantes, 2012). Before taking measurements, the light source was allowed to warm up for at least fifteen minutes. As the stem samples have a matte surface, for diffuse reflectance it was sufficient to set the reflectance probe at a 90° angle in a probe holder to maximize the amount of light striking the samples. For all measurements, the Integration time was set to 17 ms and the averaging was set to 30; therefore every spectrum saved is an average of 30 measurements. Using the white reference standard tile, the light source, and position of the probe in the probe holder was adjusted until the maximum ADC

(analog-to-digital converter) counts were around 50,000: this is done to prevent saturation while optimizing maximum light intensity. A reference spectrum (light and dark spectra) was reset using the standard tile every 5 to 10 minutes to control for any fluctuations from the light source and/or the spectrometer. White reference standard tiles are commonly used to create a baseline reference of 100% reflectance before collecting NIR reflectance measurements (Photon Control, British Columbia, Canada).

The NIR spectrometer measured diffuse reflectance in 256 spectral bands (1053 - 2577 nm) with varying bandwidth of minimum 5.5 nm to as high as 6.8 nm in the near infrared region (same wavelengths measured for all samples) (Dutta et al. 2015). In Avasoft 8.1, the reflectance at wavelength n is calculated using the following equation:

$$R_n = 100 * ((sample_n - dark_n) / (reference_n - dark_n))$$
(3.1)

Where

 R_n = reflectance at wavelength n

sample_n = reflectance of the current sample at wavelength n

 $dark_n = dark$ reflectance at wavelength n (white reference tile)

reference_n = reference reflectance at wavelength n (white reference tile)

For this particular NIR spectrometer and reflectance probe set-up, it is crucial to maintain the same distance of the probe to the reference tile with the same distance of the probe to samples measured after the reference spectrum is saved (the probe and probe holder must be situated perpendicular over the sample). When collecting bark and phloem NIR spectra, one measurement was taken from both the bark and from the phloem, the sample was rotated 180° and the measurements were repeated (4 total measurements: 2 bark and 2 phloem) (Fig. 3.2). In a few samples, the bark/phloem segment was too short and only the bark was measured. The outer 20 mm xylem samples were measured in two locations on one side, the sample was rotated 180° and the two measurements were repeated (4 measurements per xylem sample) (Fig. 3.2). All measurements were taken from the radial surface of the wood (i.e. when looking at the tangential surface, the wood fibers are horizontal).

3.2.4. Spectral Pretreatment

For each tissue type, all subsamples were averaged together to obtain a single reflectance measurement for each tree (480 measurements per tree for xylem, 240 measurements per tree for bark and phloem (if possible to collect)). The 1053 – 1059 nm and 2252 – 2577 nm spectral ranges were removed because they were visually noisy and therefore unreliable (Sandak et al., 2011; Carvalho et al., 2013). The spectral range (1066 – 2246 nm) for further analysis was the same for all three tissue types with 190 wavelength measurements.

A common problem associated with raw NIR spectral measurements is additive baseline effects, where the spectra have the same or similar slopes but are slightly offset from one another along the y-axis (i.e. % reflectance) (Rinnan et al., 2009). Some of the common sources of spectral variation include: a lack of consistency in the measurement process, variable distances from the probe to the sample, or fluctuations caused by the hardware and are often unavoidable (Heise and Winzen, 2002). To help resolve this issue, many NIR studies apply preprocessing techniques without compromising or changing the spectroscopic information, where the raw spectral measurements are transformed using smoothing filters and derivative transformations (Heise and Winzen, 2002; Roberts et al., 2004). Smoothing filters are applied in an effort to reduce noise, while preserving signal-to-noise ratio, with several different methods that can be used (Heise and Winzen, 2002). A more advanced method, the Savitzky-Golay smoothing filter, applies a specified degree polynomial (typically 2nd degree) to the spectral data points in a moving gap size (Heise and Winzen, 2002). Smoothing filters can be calculated alone (without derivative calculations), but are often applied before derivative transformations (Rinnan et al., 2009). Derivatives are calculated in order to remove or minimize background signaling in spectral data and have been used for decades in spectroscopy (Heise and Winzen, 2002; Rinnan et al., 2009). A commonly used method for calculating spectral derivatives is the Savitzky-Golay algorithm which uses a smoothing filter before calculating derivatives (Rinnan et al., 2009). The Savitzky-Golay algorithm uses a localized segment at each wavelength (with a specified number of points on each side) to calculate the derivative

for that wavelength (Roberts et al., 2004; Savitzky and Golay, 1964). The Savitzky-Golay derivative method requires the number of points in the local window size to be the same for each center point and consequently reduces the number of data points at both ends of the spectrum by the number of points used in the smoothing gap size minus one (Rinnan et al., 2009).

Unscrambler software (version 10.3, CAMO, Corvallis, OR, USA) was used for calculating three data pre-processing data transformations. First, the Savitzky-Golay second-order polynomial smoothing filter was applied using a 21-point segment window (10 points to the left and 10 points to the right of each wavelength) without calculating any derivatives. First and second derivatives were also obtained using the Savitzky-Golay algorithm with the 21-point smoothing filter and second-order polynomial (Savitzky and Golay 1964). Calculating derivative transformations in the Unscrambler software with a 21 point window results in a loss of measurements by 10 points at each end of the spectrum, reducing the total number of wavelength measurements for analysis to 170 (final wavelength range: 1134 to 2190 nm) (Rinnan et al., 2009). The three pre-processing transformations used in this study were: Savitzky-Golay (SG) Smoothing filter, SG smoothing filter with a first derivative (hereafter referred to simply as first derivative), and SG smoothing filter with a second derivative (hereafter referred to simply as second derivative).

3.2.5. Data Analysis

3.2.5.1. Infestation Symptoms, Competition, and White Ash Form and Productivity

The infestation symptoms: percent fine twig mortality, the surface area of the stem (m²) from 0.5 to 1.5 m, the number of exit holes per surface area on the stem (#/m²) from 0.5 to 1.5 m, the larval galleries per surface area on available branch segments (#/m²), light availability (percent openness measured using a hemispherical camera), the live surrounding competitor trees basal area (m²/ha), S-shaped larval galleries (presence/absence), bark splits, woodpecker damage, and epicormic sprouting were calculated using the same methods described in Chapter 2.2.4.1 and 2.2.4.3. The previously listed symptoms and measurements were averaged for both the control and EAB trees. The parametric variables

(percent fine twig mortality, stem surface area, number of exit holes per surface area (stem), number of larval galleries per surface area (branch), live competition basal area, and light availability) were tested for normality using histograms and by calculating skewness and standard error of skewness (SES) (SYSTAT, 2002). All parametric variables were determined to be skewed (skewness/SES > 2) and logarithmically transformed (using ln(x) or ln(x+1) if values of 0 were present). The transformed variables were retested for normality using (skewness/SES) (SYSTAT, 2002). The logarithmically transformed number of exit holes per surface area (stem), number of larval galleries per surface area (branch), and live competition basal area were determined to be normally distributed (skewness/SES < 2) and a one-way ANOVA Least Significant Difference test was applied (SYSTAT, 2002). A Kruskal-Wallis one-way analysis of variance was applied for the non-parametric and not normally distributed variables (SYSTAT, 2002). All means and 95% confidence limits were reported in their original measurement scales as the logarithmically transformed data were back-transformed using the antilogs (e^x or e^x -1).

The tree characteristic variables measured in this study (DBH (cm), tree height (m), crown ratio, slenderness, basal area (m²), and total aboveground biomass (kg)) were calculated using the same methods described in Chapter 2.2.4.2. The tree level variables were averaged for both the control and EAB trees. Variables were tested for normal distributions by visually inspecting histograms and calculating the skewness and standard error of skewness (SES) using SYSTAT (2002). With the exception of crown ratio, all variables were not normally distributed (absolute value of skewness/SES was greater than 2) and subsequently logarithmically transformed using ln(x) (SYSTAT, 2002). The logarithmically transformed variables were all determined to still not have normal distributions and a Kruskal-Wallis one-way analysis of variance was applied for these variables using the untransformed data (SYSTAT, 2002). A one-way ANOVA Least Significant Difference test was run for the crown ratio (SYSTAT, 2002).

3.2.5.2. Discriminant Analysis and Classification

Since EAB is not localized to a small geographic range, it is important to address the potential of NIR in being applied across a broad area and different site conditions. NIR spectroscopy is a highly sensitive technique, and can detect subtle differences in chemical composition of trees grown in different locations (Sandak et al., 2011). Wide-ranging calibration datasets are necessary to ensure maximum variation and can reduce population error (Burns and Ciurczak 2008). To ensure a wide-ranging calibration dataset the EAB infested samples were pooled together across the three latitudinal regions, the three crown dieback classes (low, moderate and severe) and land-use type (high impact recreational and natural). While high impact recreational control sites were not available, the control samples were pooled together across a wide geographical area from multiple sampling locations.

A stepwise linear discriminant analysis (LDA) was performed for each of the three pretreatment methods (Savitzky-Golay (SG) Smoothing filter, first derivative, and second derivative) for each sample using the SYSTAT 10.2 software (Engelman, 2002). All discriminant analysis conducted in this study used automatic, forward stepping with a probability F-to-enter specified at 0.05 and F-to-remove of 0.10 (Engelman, 2002). When forward automatic stepping is specified in SYSTAT 10.2, variables (i.e. wavelength bands) with the highest F-to-enter are entered into the model while variables with the lowest F-to-remove are removed from the model (Engelman, 2002).

Discriminant analysis is a comparable method to multivariate analysis of variance and multiple regression (Engelman, 2002). Discriminant analysis has been successfully used as a qualitative classification method where variables (in this case, wavelength bands) are identified that best separate cases of predefined groups (Engelman, 2002; Burns and Ciurczak, 2008). This particular method can be categorized as a supervised classification method, because specific groups are known beforehand (Burns and Ciurczak 2008). In addition to calculating canonical scores for each group, discriminant analysis produces a classification matrix table where each sample is classified into the group where its classification function value is the largest. These classification matrix tables provide the percentage correct classification for each group as well as the total percent correct classification for all samples. In an

attempt to approximate cross-validation we present the jackknifed classification matrix. Jackknifed classification removes and replaces one sample at a time for the current samples in the discriminant analysis (Engelman, 2002)

As this study collected measurements for three different tissue types, I first ran a stepwise discriminant analysis for all tissues with a matrix of 231 rows (number of samples) and 170 columns (number of spectral values) with the tissue types (xylem, bark, and phloem) as the grouping variable. For each tissue type the mean percent reflectance from 1134 to 2190 nm was calculated for both the first and second derivatives. SYSTAT (version 10.2) identified specific wavelength bands that contributed the most to the separation between EAB and control spectra (i.e. F-to-enter below 0.05) (Engelman, 2002).

Stepwise discriminant analyses were run for the individual tissue types (for each pre-treatment method) and the jackknifed classification (i.e. approximate cross-validation of the current sample set) between the EAB and control spectra was reported. Additionally, the mean percent reflectance of the control and EAB infested trees was calculated for both the first and second derivatives of each tissue type (xylem, bark, and phloem) in the wavelength range from 1134 to 2190 nm. For each tissue type, samples were pooled together across regions and land-use classes so that the only two grouping variables were EAB infested white ash and control (non-symptomatic) white ash. Using the infestation type (EAB vs control) as the grouping variable, individual stepwise discriminant analysis was run for each tissue type and pretreatment methods for the full wavelength range (1134 – 2190 nm) as well as for two reduced wavelength ranges (1134 – 1696 nm (lower NIR) and 1703 – 2190 nm (upper NIR)). The reduced wavelength ranges were chosen with 1700 nm as the separating wavelength to take into account the fact that most lower-cost NIR spectrometers only go up to 1700 nm wavelengths and any models above this range are typically more expensive. The xylem spectra ended up with a total of 79 samples, while the bark and phloem had 76 samples. The full wavelength range had 170 spectral values, the lower NIR range had 87 spectral values, and the upper NIR range had 83 spectral data points. The wavelength bands that contributed the most to the separation between EAB and control spectra are only reported for the discriminant analyses run for the full wavelength range (1134 – 2190 nm).

3.3. Results

3.3.1. Infestation Symptoms, Competition, and White Ash Form and Productivity

The average percent fine twig mortality was statistically higher in EAB infested trees than the control trees (Table 3.1) (p < 0.05). No adult exit holes were found on the stems of control trees from 0.5 to 1.5 m while the EAB infested trees had an average 16.4 exit holes per m^2 . The average percent light availability (openness) was significantly greater for EAB trees compared to control trees (p< 0.05). As the control trees were selectively sampled as non-symptomatic, the S-shaped larval galleries, bark splits, woodpecker damage, and epicormic sprouting were significantly greater in the EAB infested trees compared to the control trees (p < 0.05). The average stem surface area (m^2) and live competition basal area (m^2 /ha) were not significantly different between the control and EAB trees ($p \ge 0.05$).

The white ash form and productivity variables were averaged across the combined EAB infested trees and for the combined control trees (Table 3.2). White ash form and productivity was not statistically different between the control and EAB infested trees ($p \ge 0.05$).

3.3.2. Discriminant Analysis and Classification of Tissue

The canonical scores plots produced by the discriminant analysis show clear separation between the three tissue types for both the first and second derivative spectra (Fig. 3.3). For the first derivatives, the jackknifed discriminant analysis had 96% correct classification for the phloem, 97% correct for the bark, and 100% correct classification for the xylem (Table 3.3). The total percent correct classification (all three tissue types) for the first derivative discriminant analysis was 98 % (Table 3.3). Of the misclassified bark and phloem samples, none were classified as xylem. The higher the eigenvalue and Mahalanobis distances are in discriminant analysis, the better the separation between groups (Engelman, 2002). Again, none of the misclassified bark and phloem spectra were classified as xylem for the second derivative discriminant analysis (Table 3.3). The significant wavelength bands that contributed to separation between tissue types were different between the first and second derivatives (Fig. 3.4).

3.3.3. Discriminant Analysis and Classification of EAB Infestation

While EAB and control samples were clearly separated from one another, classification was not perfect (i.e. 100 %) for any discriminant analysis (Fig. 3.5). Generally, for each tissue type, spectral pretreatment, and wavelength range, the discriminant analysis was more accurate in classifying the control samples than it was with the EAB samples. The single exception was for the discriminant analysis of the first derivative of bark over the full wavelength range, where EAB was correctly classified at 88% and the control at 86% (Fig 3.5). The xylem samples typically had the strongest classification between EAB and control spectra compared to the bark and phloem (Fig. 3.5). The total classification accuracy for the phloem was generally consistent across pretreatment methods and wavelength ranges (Table 3.4). However, the discriminant analysis that was run for the phloem using the smoothing filter in the upper wavelength range (1703-2190 nm), was unable to classify between EAB and control spectra (no variables in the model) (Table 3.4). The phloem discriminant analyses also typically had the largest discrepancies between the two infestation types compared to the other tissues, with the control groups having much higher classification (often above 95%) compared to the EAB groups (mostly under 80%). For the bark samples, the classification accuracy in the three wavelength ranges was similar between the smoothing filter and 1st derivative and generally the lowest in the 2nd derivative (Table 3.4). Of the three tissue types, the bark spectra typically had the lowest total classification accuracy. Of the different discriminant analyses (Fig. 3.5 and Table 3.4), the xylem, first derivative over the full wavelength range had the highest classification accuracy, with 100% classification of the control samples, 94% for the EAB samples, and an overall accuracy of 97% (Fig. 3.5).

For all three tissue types, the smoothing filter pretreatment had the lowest eigenvalues, canonical correlations and Mahalanobis distances with overall lower classification accuracy (Table 3.4). For this pretreatment type, the full wavelength range discriminant analyses for xylem and inner bark were the highest with Mahalanobis distances of 2.84 and 2.92, respectively.

The mean EAB and control spectra of the first and second derivatives for xylem samples are presented for the full wavelength range measured (1134 - 2190 nm) (Fig. 3.6). The significant

wavelengths that contributed towards the group classification changed between the first and second derivatives (Fig. 3.6). For the xylem first derivative spectra, the five wavelengths that separated xylem samples between the EAB and control groups were linked to literature bands assigned to lignin, aromatics, hemicellulose and cellulose (Table 3.5). Wavelength bands that significantly contributed to xylem sample separation using the second derivative pretreatment were linked to starch, cellulose, CH₂-groups, aromatics/extractives, lignin and hemicellulose (Table 3.6).

Average bark spectrum in the full wavelength range (1134-2190 nm) for first and second derivative pretreatments both showed visual separation in limited wavelength ranges between EAB infested samples and control samples (Fig. 3.7). Specific wavelengths that contributed the most towards classification between EAB and control samples changed between derivative treatments (Fig. 3.7). Previously assigned lignin, hemicellulose, and starch wavelength bands corresponded with the bands that contributed towards separation of first derivative bark spectra between the EAB and control groups (Table 3.5). When the bark spectra were transformed using the second derivative pretreatment, cellulose corresponded to one of the significant bands (Table 3.6).

The average spectrum for the phloem first and second derivative spectra also showed some visual separation between the EAB and control groups (Fig. 3.8). Of the two significant bands for the phloem first derivative spectra, only one corresponded with cellulose and hemicellulose literature assignments (Table 3.5). The second derivative phloem spectra were also significantly classified with two bands, which were linked to literature band assignments for aromatics, lignin/extractives, and protein (Table 3.6).

3.4. Discussion

3.4.1. White Ash Tissue Type Classification

There have been limited studies that have specifically looked at differences between bark, phloem and xylem using NIR spectroscopy. Many studies conducted for wood properties using NIR often look at localized sections of the wood or mill wood samples together for further analysis (Shimleck and Evans, 2004; Cooper et al., 2012; Jones et al., 2008). It is understood that there are chemical differences between non-living outer bark and living inner bark (phloem) (So and Eberhardt, 2006). NIR spectroscopy has previously been used to differentiate between the outer bark and phloem of southern yellow pine bark samples (So and Eberhardt, 2006). Based on the results for the discriminant analysis conducted for the first and second derivative spectra, the ability to classify living white ash tissue types (bark, phloem, and xylem) was highly accurate in this study. The bark and phloem samples did have minimal overlap between the two groups. No bark or phloem samples were misclassified as xylem, and all xylem samples were correctly classified. The xylem was clearly highly separated from bark and phloem based on the canonical scores plots. The Mahalanobis distance between the bark and phloem was much smaller than the Mahalanobis distances between the xylem and the other two tissues. A previous study used NIR diffuse reflectance to clearly differentiate between the epidermis, phloem, and xylem of ginseng using principle components analysis (PCA) (Wu et al., 2011). It has been shown that NIR spectra collected from small, specific regions of wood can provide excellent wood property calibration statistics (Jones et al., 2008). Based on the high classification accuracy between tissue types and to avoid potential influences of differences in the physical and chemical properties of the multiple tissues, it was decided not to combine tissues together and to analyze them separately.

3.4.2. Classification of EAB Infested White Ash

The primary objective of this study was to determine if NIR spectroscopy can be used to differentiate between white ash tissues from trees with known EAB infestation and trees that are visually healthy (but possibly infested). A fundamental principle of NIR spectroscopy is that the physical and

chemical properties of an object are measured and are specific to that object based on these properties. Despite the tendency of EAB to target the upper stem and crown in early stages of infestation, it was expected in this study that systemic induced response mechanisms stimulated by phloem girdling resulting from larval feeding elicits a physical and/or chemical change throughout the entire tree (Ananthakrishnan, 2001, Leon et al., 2001; Taylor and Cooper, 2002). Chakraborty et al. (2014) saw reductions in phenolics in the phloem of 3 m tall, EAB infested trees but the actual concentrations did not vary along the stem. However, it is unknown at this time how phenolic concentrations differ along the stems of larger ash trees due to EAB infestation (Chakraborty et al., 2014). While this current study did not identify the specific physical and chemical properties associated with EAB infested trees, it was hypothesized that the systemic changes in the bark, phloem and xylem chemistry and physical properties could be measured using NIR. For example, bark-phloem girdling has shown to increase levels of phenolic compounds in the sapwood of soft maple (*Acer rubrum*) below the girdle compared to above the girdle and in un-girdled trees (Taylor and Cooper, 2002). Also in girdled trees, parenchyma viability and moisture content in sapwood of pines have shown a reduction beneath a girdle (Taylor and Cooper, 2002).

NIR spectroscopy has been successfully used to identify trees with early insect infestation stages by measuring tree tissues (Ismail and Mutanga, 2011; Riggins et al., 2011). Using stepwise discriminant analysis for a qualitative analysis, this study was able to classify tissue samples between EAB infested and visually healthy trees. Previous studies have also successfully used discriminant analysis to classify wood properties (Tsuchikawa et al., 2003; Watanabe et al., 2012). Tsuchikawa et al. (2003) was able to discriminate the NIR spectra of different species of wood. Wet pockets of green *Abies lasiocarpa* wood were separated from normal wood (98% correct) using discriminant analysis (Watanabe et al., 2012). The study by Riggins et al. (2011) used machine learning techniques to accurately predict (90%) of assigned stress rankings to northern red oak foliage from trees with varying levels of infestation due to red oak borer. While the samples clearly belonged to two distinct groups, the total correct classification was never 100% for any of the tissue types, pretreatment methods, or wavelength ranges (Table 3.3). The discriminant analysis in this study with the best classification of EAB and control samples (97% correct

classification) was for the xylem transformed using the Savitzky-Golay 1st derivative over the full wavelength range (1134-2190 nm). The first derivative xylem at the full wavelength range also had the highest eigenvalue and Mahalanobis distances at 2.78 and 3.30, respectively.

An important aspect of NIR spectroscopy is pre-processing treatment of the spectral data (Rinnan et al., 2009). Savitzky-Golay smoothing filters and derivatives are commonly used methods for preprocessing spectral data in NIR spectral analysis (Rinnan et al., 2009). In many studies, pre-treatment methods are often compared based on the calibration dataset's performance (Rinnan et al., 2009). Using discriminant analysis, a previous study saw an improvement in the ability to classify soils from different vegetation types by using first and second derivatives (Ertlen et al., 2010). Differences in the classification accuracy between EAB infested and control spectra among the different pretreatment methods applied in this study were different among the three tissue types. For the xylem, classification accuracy was higher using the derivatives pretreatments compared to the smoothing filter (Table 3.3). A study on early detection of fungal decay also saw that first derivative spectra had the strongest calibration and prediction ability (Green et al., 2012). The smoothing filter classification accuracy in my study was often comparable or slightly less accurate compared to the two derivative pretreatments for the bark and phloem (Table 3.3). The exception was the phloem transformed using the smoothing filter in the upper NIR range (1703-2190 nm) where it was unable to classify groups, whereas it was able to successfully classify samples using the derivative pre-treatments (Table 3.3). The only discriminant analysis for tissue type, pretreatment method or wavelength range with total classification accuracy above 95% was the full spectrum range (1134-2190 nm) for the first derivative of xylem tissue with a 97% correct classification.

Many studies focused on wood properties often use the full NIR wavelength range (typically 1000-2500 nm) as this range has the best spectral information (Kelley et al., 2004). More studies are beginning to use reduced spectral ranges as this could potentially reduce the time and cost associated with sampling (Kelley et al., 2004). The chemical composition of wood and bark chips used for pulping being transported on a conveyor belt was successfully measured using NIR spectroscopy in the range between 800 and 1100 nm (Axrup et al., 2000). Axrup et al. (2000) were able to measure water content, extractive

content, Klason lignin, and wood chip size distribution with water content, wood content and bark coarseness using the reduced spectral range. The eigenvalues and Mahalanobis distances for the two reduced wavelength ranges utilized in the current study (1134 - 1696 and 1703 – 2190 nm) were always lower compared to the full wavelength range (1134 - 2190 nm) when discriminant analysis was used to classify control and EAB spectra. However, the total classification accuracy was generally similar among the three wavelength ranges, with the full wavelength range almost always having the highest accuracy. Similar classification results were seen for reduced wavelength ranges for NIR classification of wet-wood pockets compared to normal wood using second derivative spectra (Watanabe et al., 2012). For the first derivative discriminant analyses of the three tissue types, the lower NIR (1134-1696 nm) range always had the lowest percent classification, while the 1703 – 2190 nm range was either the same or within a few percent accuracy compared to the full wavelength range. For the second derivatives of the three tissue types, the total classification accuracy for the reduced wavelength ranges were either the same or within 1-2% of the full wavelength range classification accuracy. The reduced wavelength ranges still showed clear separation between EAB and control spectra in the current study. This indicates that cheaper NIR spectrometers (up to 1700 nm) could potentially be calibrated for early detection of EAB with a minimal loss of accuracy compared to the full range spectrometers (up to 2500 nm). It was observed in a previous study that a shorter NIR range (800-1400nm) actually had better classification information for woodbased materials compared to a longer wavelength range (1400-2500 nm) (Tsuchikawa et al., 2003). Based on the results of the current study, the second derivative pretreatment had a slightly higher overall accuracy at reduced wavelength ranges compared to the first derivative.

To the best of my knowledge, no other study has specifically used NIR spectroscopy for identification of insect infestation in trees by measuring the xylem, bark or phloem. The majority of NIR studies looking at tree stress and mortality due to insect infestation either use remote sensing data (Fassnacht et al., 2014), sub-canopy hyperspectral imagery (Lawrence and Labus, 2003), or directly measure foliage samples in the field or in the lab (Riggins et al., 2011; Pontius et al., 2008). The collection of increment cores has been previously utilized as a nondestructive, field based method for

sampling trees using NIR to measure wood properties (Schimleck et al., 2002; Tsuchikawa and Schwanninger, 2013).

3.4.2.1. Previously Assigned Wavelength Bands of Wood Defense Components

There is a general understanding of the interactions between herbivores and plant chemical defenses for conifers and bark beetles, and in foliage (Cipollini et al., 2011). While there is less of an understanding about how angiosperms withstand herbivory by wood-boring insects, plant defense mechanisms likely include phenolics in the wood, phloem defense proteins and the ability to heal wounds (Cipollini et al., 2011). Several previous studies have examined the chemical and nutritional characteristics of ash phloem, the primary feeding substrate for emerald ash borer and the possible response mechanisms in ash (Eyles et al., 2007; Cipollini et al., 2011; Chen et al., 2012; Hill et al., 2012; Crook et al., 2008b; Chakraborty et al., 2014). Although EAB studies typically focus on the nutritional and chemical characteristics of phloem and foliage, changes bark volatiles in the bark and phloem of girdled ash have been identified (Crook et al., 2008b). Chen et al. (2012) found that EAB larvae were able to convert phenolics to non-phenolics better in white ash compared to green and black ash. Differences in phenolic compounds (hydroxycoumarins, a monolignol, lignans, phenylethanoids, and secoiridoids) in the phloem of three species of ash (F. americana, F. pennsylvanica, F. mandshurica) were observed and have been suggested as possible mechanisms of defense against EAB (Eyles et al., 2007). Cipollini et al. (2011) found similar differences in phenolic compounds between ash species as well as additional compounds either present or absent when comparing the resistant F. mandshurica with the EAB susceptible F. americana, cv. Autumn Purple and F. pennsylvanica, cv. Patmore.

Cellulose, hemicellulose, aromatic compounds (phenols), starch, lignin and protein are important structural or induced chemical defense compounds found in wood and can be associated with resistance to insect herbivory (Eaton and Hale, 1993; Eyles et al., 2010; Hill et al., 2012). Many specific wavelengths in the NIR spectrum have been assigned to these compounds in previous studies. The 1452, 1480, 1490, 1608, 1730, 1780, 1820, 1900, 1930, 2100, 2276, 2336, 2352, and 2488 nm wavelengths have been

assigned to cellulose (Shimleck et al., 2004; Jones et al., 2006; Ertlen et al., 2010; Burns and Ciurczak, 2008). Wavelength bands that have been assigned to hemicellulose include: 1157, 1171, 1350, 1471, 1493, 1666, 1681, 1705, 1710, 1720, 1724, 1907, 1910, 2086, 2134, 2170, and 2178 (Schwanninger et al., 2011). Wavelength bands associated with aromatic compounds are 1143, 1417, 1446, 1668, 1685, and 2132 (Jones et al., 2006; Burns and Ciurczak, 2008). Bands assigned to starch include 1450, 1540, 1930, 1960, and 2100 nm wavelengths (Burns and Ciurczak, 2008). The 1130, 1132, 1292, 1294, 1312, 1704, and 1714 nm wavelengths were assigned to lignin in the study by Jones et al. (2006). Wavelengths assigned to protein include 1510, 2055, 2060, and 2180 nm (Burns and Ciurczak, 2008). The above listed wavelength bands are not necessarily the only bands to be assigned to their respective chemicals, but they have been documented from previous NIR and chemical calibration research.

Many previous NIR studies involve chemical analysis to assign specific wavelengths of the near infrared spectrum to chemicals, compounds or physical properties of interest (Schwanninger et al., 2011). However, because of vibration combinations and overtone overlap, there is still a limited understanding about wavelength band assignments in the NIR spectrum (Tsuchikawa, 2007). Comparison of results among different studies can be complicated by the fact that wavelength bands can possibly shift position along the spectrum when second derivatives are applied to raw reflectance measurements (Schwanninger et al., 2011). While the current study did not calibrate the NIR spectra with chemical measurements, the specific wavelength bands that contributed the most towards separation between the EAB and control groups were identified as a result of the discriminant analysis (Tables 3.5 and 3.6). A literature review of near infrared band assignments for the previously mentioned wood components, identified wavelength bands within ± 10 nm of the significant wavelength bands in this study and their corresponding wood components (cellulose, hemicellulose, aromatic compounds, starch, lignin, and proteins) (Tables 3.5 and 3.6). The significant wavelength bands that contributed for classification of EAB and control groups changed for each tissue type when different pretreatment transformation methods were used. It was seen that when the smoothing filter was applied without derivatives, the 1930 nm (associated with cellulose and starch) band contributed to the classification of EAB and control samples for all three tissue types

(Shenk et al., 2008). A reduction in starch in the sapwood of bark-phloem girdled trees located below the girdle has also been previously measured in maple, pine and oak species (Taylor and Cooper, 2002; Parkin, 1938). While the specific wavelength bands and their associated chemical components changed among different tissue types and pretreatment methods, in Tables 3.5 and 3.6, starch, cellulose and lignin were often associated with the significant wavelength bands for both the first and second derivative spectra. In particular, increases in lignin have been associated with plant defense against insect herbivory (Hill et al., 2012). While the different pretreatment methods were all able to discriminate between EAB and control samples, there is likely a shift in wavelength bands along the near-infrared spectrum among the different methods (Schwanninger et al., 2011).

3.5. Conclusions

Overall, the results of this preliminary study are promising for using NIR spectroscopy as an indicator of emerald ash borer infestation. Using multiple white ash tissue types (bark, phloem, and xylem), I was successfully able to use stepwise discriminant analysis to distinguish NIR spectra between known EAB infested trees and visually healthy trees in Michigan. This preliminary study only showed the ability of NIR to indicate EAB infestation, and future development of calibrations is required before this technology can be used as a detection method. While there was a minor degree of misclassification in the discriminate analysis, the samples were clearly from two distinct populations. The discrimination between the two groups was never 100%; with typically more EAB samples being misclassified as control (this was consistent for all three tissue types and wavelength ranges). This indicates potential limitations for early detection of EAB infestation using this technology if trees of known infestation are being misclassified as visually healthy trees. Another possibility is that the misclassified, EAB infested trees could potentially have greater resistance and could be studied in future genetic analysis. The xylem spectra transformed using a Savitzky-Golay, 1st derivative smoothing filter over the full NIR wavelength range observed in this study (1134-2190 nm) had the highest discriminating power at 97% correct classification accuracy. Comparisons between the different tissues showed high classification accuracy, with particularly high separation between the bark and phloem compared to the xylem. As NIR is a highly site specific technology, this study was robust in that the calibration dataset was collected from trees grown in a wide geographical area and a variety of site conditions (Burns and Ciurczak, 2008). Increment borers are a common tool in forestry for sampling trees non-destructively. This study shows that by combining this efficient sampling process with near-infrared spectroscopy, NIR can be used as an indicator of emerald ash borer infestation. There is potential for future research in possibly developing NIR spectroscopy as a cost-effective method of early detection of emerald ash borer in support of current detection methods.

APPENDIX

Table 3.1. Average infestation symptoms and tree measurements by group. The lower and upper limits of a 95% confidence interval of the mean are shown in parentheses. Number of trees sampled per group (n). For the branch segments: Control n = 16 and EAB n = 14. The adult exit holes per surface area on the stem (#/m²), branch larval galleries (#/m²), and the live competition basal area (m²/ha) were the only comparisons made based on log transformed data. Groups with different letters are significantly different (p < 0.05).

Group	Control	EAB
n	43	36
Percent Fine Twig Mortality	5.7 (5.2, 6.2) a	38.8 (30.4, 47.1) b
Stem: Surface Area (m²)	0.7 (0.6, 0.8) a	0.7 (0.6, 0.9) a
Stem: D-Exit Hole per Surface Area (#/m²)	0 (0, 0) a	16.4 (9.4, 23.4) b
Branch: Larval Galleries (#/m²)	0 (0, 0) a	10.4 (-0.8, 21.6) b
Live Competition: Basal Area (m²/ha)	31.8 (25.4, 38.1) a	29.4 (18.2, 40.6) a
Percent Open (Hemispherical)	8.3 (7.7, 9) a	12 (8.9, 15) b
S-Shaped Larval Galleries (presence / absence)	0 (0, 0) a	0.2 (0, 0.3) b
Bark Splits	0.1 (0.0165, 0.2) a	1.3 (1.1, 1.4) b
Woodpecker Damage	0 (0, 0.1) a	1.3 (1.2, 1.5) b
Epicormic Sprouting	0.6 (0.4, 0.8) a	1.3 (1.1, 1.4) b

Table: 3.2. Average tree growth and form characteristics (standard error in parentheses). Number of trees sampled per group (n). Significance difference between group is designated by different letters (p < 0.05).

Group	n	DBH (cm)	Tree Height (m)	Crown Ratio	Slenderness	Basal Area (m²)	Total Above- Ground Biomass (kg)
Control	43	21.94 (1.65) a	17.82 (0.78) a	0.54 (0.024) a	90.55 (4.35) a	0.0467 (0.0079) a	264.66 (59.04) a
EAB	36	21.96 (2.5) a	16.24 (0.74) a	0.5 (0.022) a	91.67 (5.16) a	0.0551 (0.0134) a	352.22 (103.64) a

Table 3.3. Summary of discriminant analysis on reflectance spectra for living white ash comparing the three tissue types using the Savitzky-Golay first derivative, and second derivative. Results of the discriminant analysis are reported for the full wavelength range (Full NIR: 1134-2190 nm.

	Eigenvalue		Canonical Correlations		Mahalanobis D		% Correct Classification				
Treatment Type	Principle Component	Principle Component 2	Principle Component	Principle Component 2	Bark- Phloem	Phloem- Xylem	Bark- Xylem	Bark	Phloem	Xylem	Total
1st Derivative	25.07	3.41	0.98	0.88	2.03	9.33	11.36	97	96	100	98
2nd Derivative	28.41	3.43	0.98	0.88	1.77	10.18	11.94	96	96	100	97

Table 3.4. Summary of discriminant analysis on reflectance spectra for living white ash for the three tissue types using the Savitzky-Golay smoothing filter, first derivative, and second derivative. Results of the discriminant analysis are reported for the full wavelength range (Full NIR: 1134-2190 nm), and the reduced wavelength ranges (Lower NIR: 1134-1696 nm and Upper NIR: 1703-2190 nm) for each tissue and pretreatment type. Xylem: Control n = 43, EAB n = 36. Outer bark: Control n = 43, EAB n = 33.

-						Canonical Sc	ores of group	
						me	ans	% Correct
				Canonical				
Tissue	Pretreatment Type	Wavelength Range	Eigenvalue	Correlations	Mahalanobis D	Control	EAB	Total
Xylem	Smoothing	Full NIR	2.06	0.82	2.84	1.30	-1.55	85
Xylem	Smoothing	Lower NIR	1.22	0.74	2.19	-1.00	1.19	87
Xylem	Smoothing	Upper NIR	1.87	0.81	2.71	-1.24	1.48	86
Bark	Smoothing	Full NIR	1.61	0.79	2.53	-1.10	1.43	88
Bark	Smoothing	Lower NIR	0.46	0.56	1.35	0.59	-0.76	70
Bark	Smoothing	Upper NIR	1.33	0.76	2.29	1.00	-1.30	88
Phloem	Smoothing	Full NIR	2.16	0.83	2.92	1.27	-1.65	89
Phloem	Smoothing	Lower NIR	1.11	0.73	2.10	0.91	-1.19	86
Phloem	Smoothing	Upper NIR	no variables	no variables	no variables	no variables	no variables	no variables
Xylem	1st Derivative	Full NIR	2.78	0.86	3.30	1.51	-1.80	97
Xylem	1st Derivative	Lower NIR	1.14	0.73	2.12	-0.96	1.15	86
Xylem	1st Derivative	Upper NIR	1.65	0.79	2.54	1.16	-1.38	91
Bark	1st Derivative	Full NIR	1.58	0.78	2.50	1.09	-1.42	87
Bark	1st Derivative	Lower NIR	0.96	0.70	1.95	0.85	-1.10	79
Bark	1st Derivative	Upper NIR	1.22	0.74	2.20	-0.96	1.24	88
Phloem	1st Derivative	Full NIR	1.40	0.76	2.35	-1.02	1.33	88
Phloem	1st Derivative	Lower NIR	1.09	0.72	2.08	0.90	-1.18	84
Phloem	1st Derivative	Upper NIR	1.22	0.74	2.20	-0.96	1.24	88
Xylem	2nd Derivative	Full NIR	2.25	0.83	2.97	-1.36	1.62	90
Xylem	2nd Derivative	Lower NIR	1.47	0.77	2.40	-1.10	1.31	90
Xylem	2nd Derivative	Upper NIR	2.03	0.82	2.83	-1.29	1.54	90
Bark	2nd Derivative	Full NIR	1.30	0.75	2.27	-0.99	1.29	84
Bark	2nd Derivative	Lower NIR	1.12	0.73	2.11	0.92	-1.19	84
Bark	2nd Derivative	Upper NIR	1.24	0.74	2.22	-0.96	1.26	82
Phloem	2nd Derivative	Full NIR	1.54	0.78	2.47	-1.07	1.40	89
Phloem	2nd Derivative	Lower NIR	1.51	0.78	2.44	-1.06	1.38	88
Phloem	2nd Derivative	Upper NIR	1.49	0.77	2.43	1.06	-1.37	87

Table 3.5. Summary of significant wavelengths identified by Stepwise Discriminant Analysis (Full NIR: 1134 - 2190 nm) that best separated between EAB infested and control spectra using the first derivative pre-treatment method. Wavelengths are separated tissue type (xylem, bark and phloem). Wavelengths from the literature that have been assigned to wood components within ± 10 nm of the measured significant wavelengths are included.

Tissue	Wavelength (nm)	Wood Components (Literature Wavelengths nm)	Sources
Xylem	1134	Lignin (1130, 1132)	Jones et al. (2006)
	1255	None	
	1407	Aromatic (1417), Lignin/Extractives (1410)	Shenk et al. (2008); Schwanninger et al. (2011)
	1918	Hemicellulose (1910)	Schwanninger et al. (2011)
	2071	Cellulose (2080)	Schwanninger et al. (2011)
Bark	1174	Lignin (1170), Hemicellulose (1171)	Schwanninger et al. (2011)
	1295	Lignin (1294)	Jones et al. (2006)
	1965	Starch (1960)	Shenk et al. (2008)
Phloem	1492	Cellulose (1490), Hemicellulose (1493)	Shenk et al. (2008); Schwanninger et al. (2011)
	1971	None	

Table 3.6. Summary of significant wavelengths identified by Stepwise Discriminant Analysis (Full NIR: 1134 - 2190 nm) that best separated between EAB infested and control spectra using the second derivative pre-treatment method. Wavelengths are separated tissue type (xylem, bark and phloem). Wavelengths from the literature that have been assigned to wood components within ± 10 nm of the measured significant wavelengths are included.

Tissue	Wavelength (nm)	Wood Components (Literature Wavelengths nm)	Sources
Xylem	1550	Starch (1540), Cellulose (1548)	Shenk et al. (2008); Schwanninger et al. (2011)
	1765	CH2-groups	Schwanninger et al. (2011)
	1948	None	
	2024	None	
	2140	Aromatic (2132), Lignin, Extractives, and Hemicellulose (2134)	Jones et al. (2006), Schwanninger et al. (2011)
Bark	1582	Cellulose (1580)	Schwanninger et al. (2011)
	1948	None	
Phloem	1407	Aromatic (1417), Lignin/Extractives (1410)	Shenk et al. (2008); Schwanninger et al. (2011)
	2054	Protein (2055)	Shenk et al. (2008)

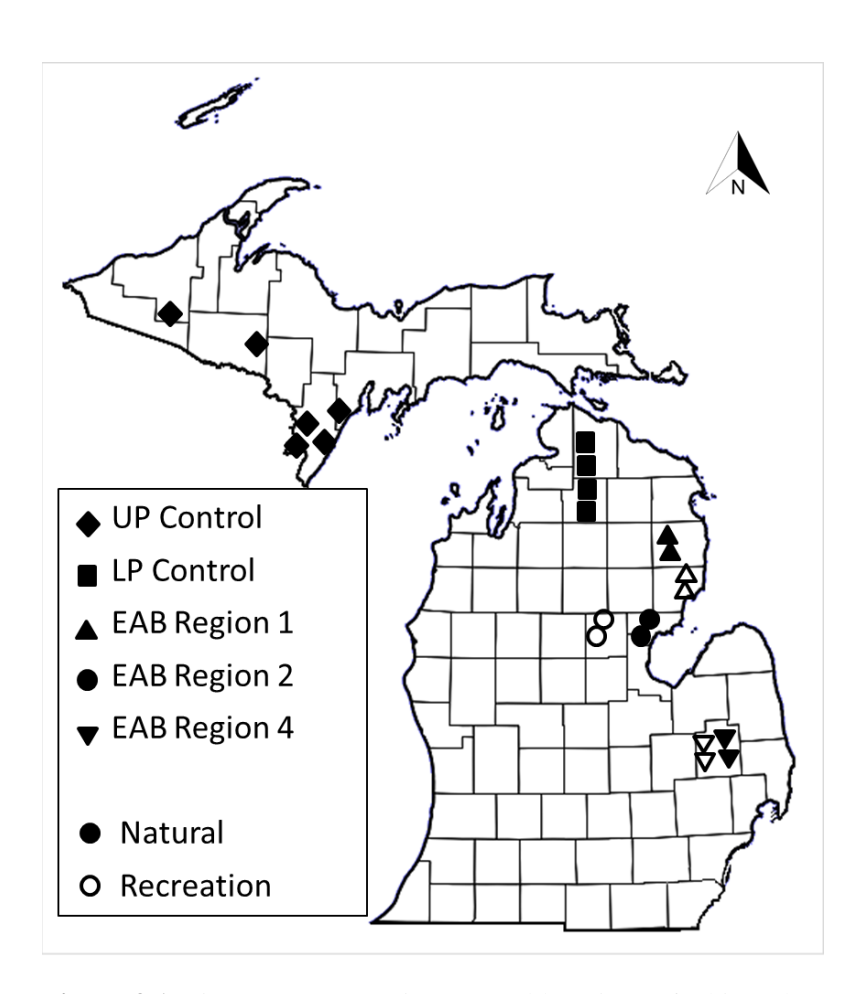


Figure 3.1. Site map representing general locations of white ash sample sites in Michigan. UP = Upper Peninsula Control, LP = Lower Peninsula Control, Control = non-symptomatic sites, EAB = emerald ash borer infested regions (R1, R2 and R4). Solid shapes represent "natural" sites while open shapes represent high impact "recreation" sites.

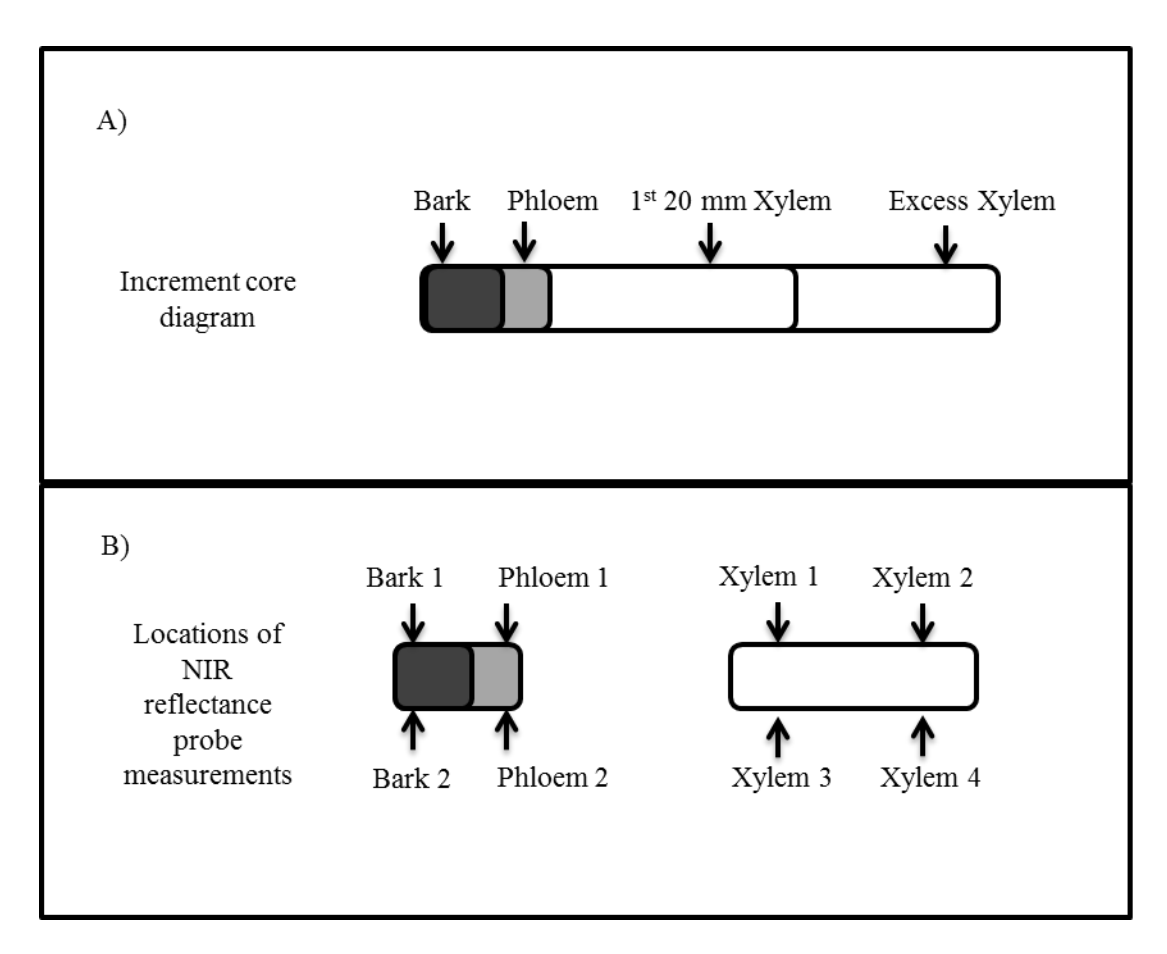
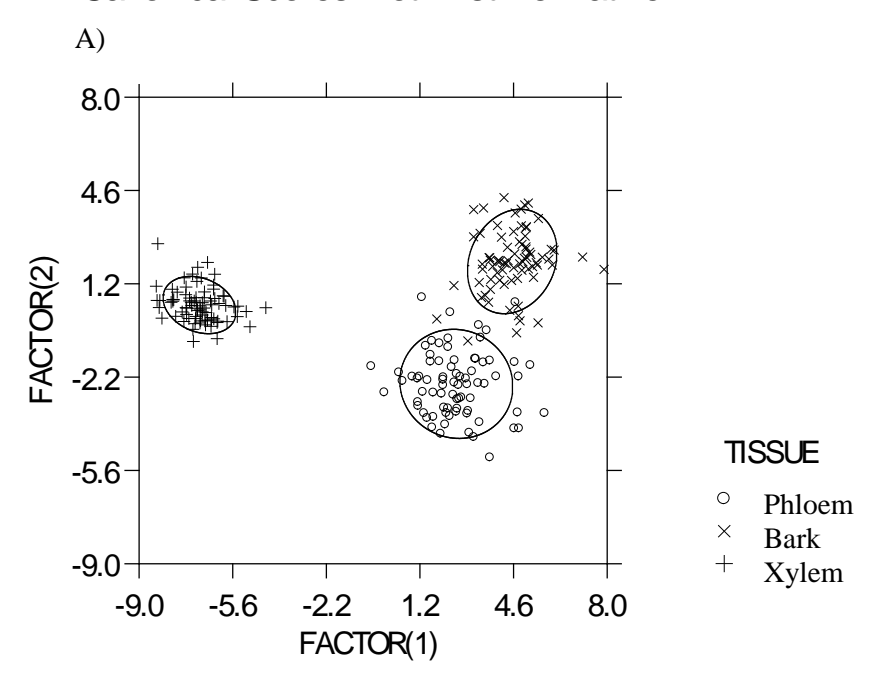


Figure 3.2. A) Diagram of increment core samples and B) reflectance probe positioning for NIR measurement collection for bark, phloem and outermost 20 mm of the xylem.

Canonical Scores Plot - 1st Derivative



Canonical Scores Plot - 2nd Derivative

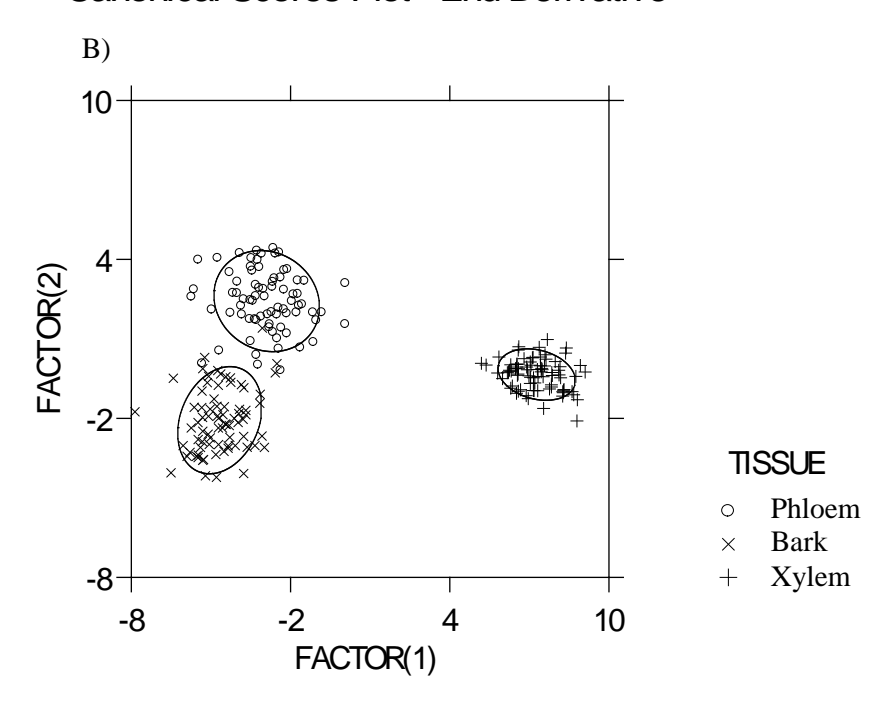


Figure 3.3. Canonical Scores Plots combined live white ash sampled in Michigan using discriminant analysis for 1134 - 2190 nm wavelengths to classify between tissue types (bark, phloem, xylem): A) 1^{st} Derivative, B) 2^{nd} Derivative. Xylem: n = 79, bark: n = 76, phloem: n = 76.

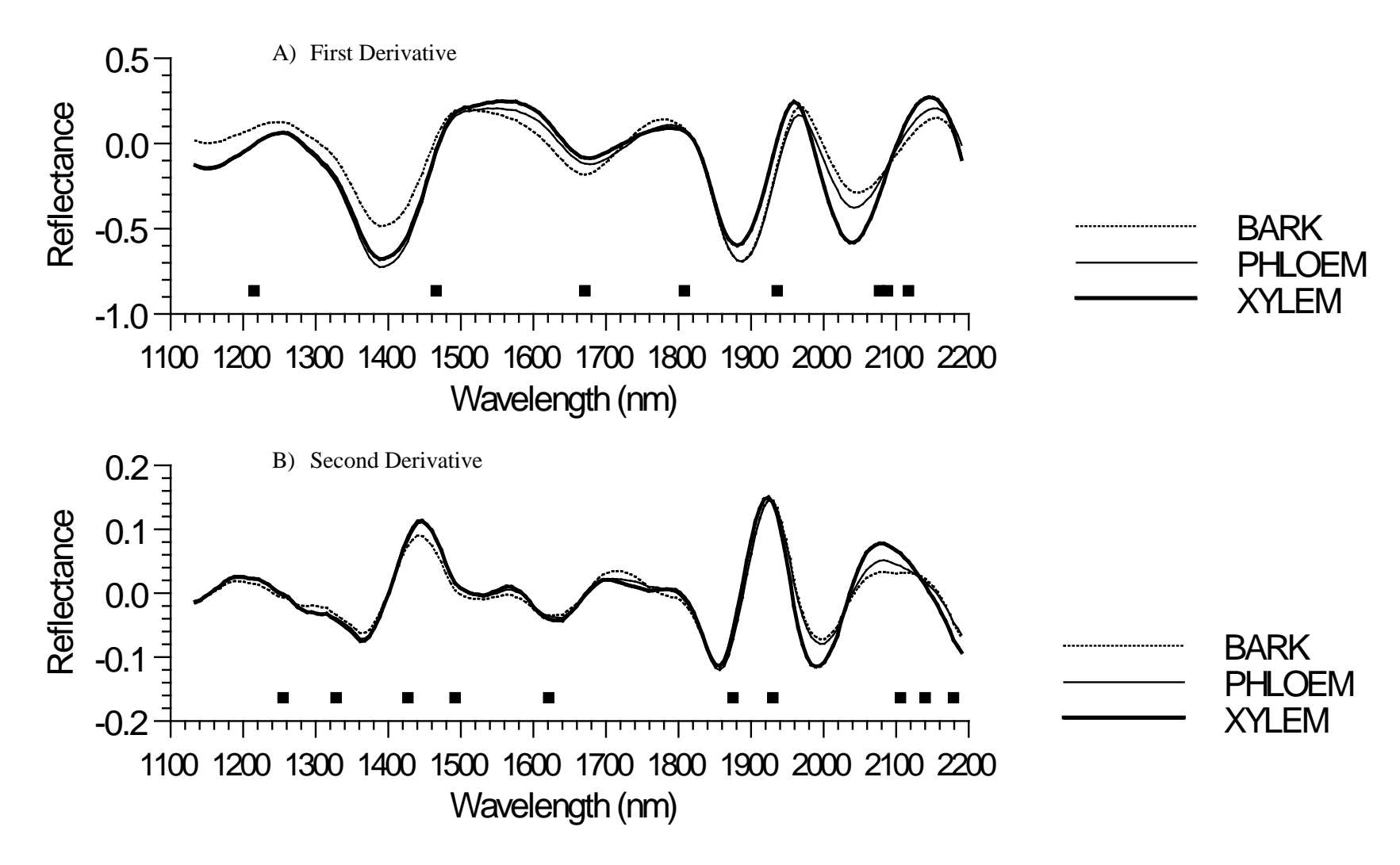


Figure 3.4. NIR reflectance mean spectra by tissue type (bark, phloem, xylem) from 1134 to 2190 nm wavelengths. A) presents spectra of living trees transformed using the SG-1st derivative, B) presents spectra of living trees transformed using the SG-2nd derivative. Xylem: n = 76, Phloem: n = 76. Solid squares denote wavelength bands that allowed for significant separation between the spectra of the three tissue types during stepwise discriminant analysis.

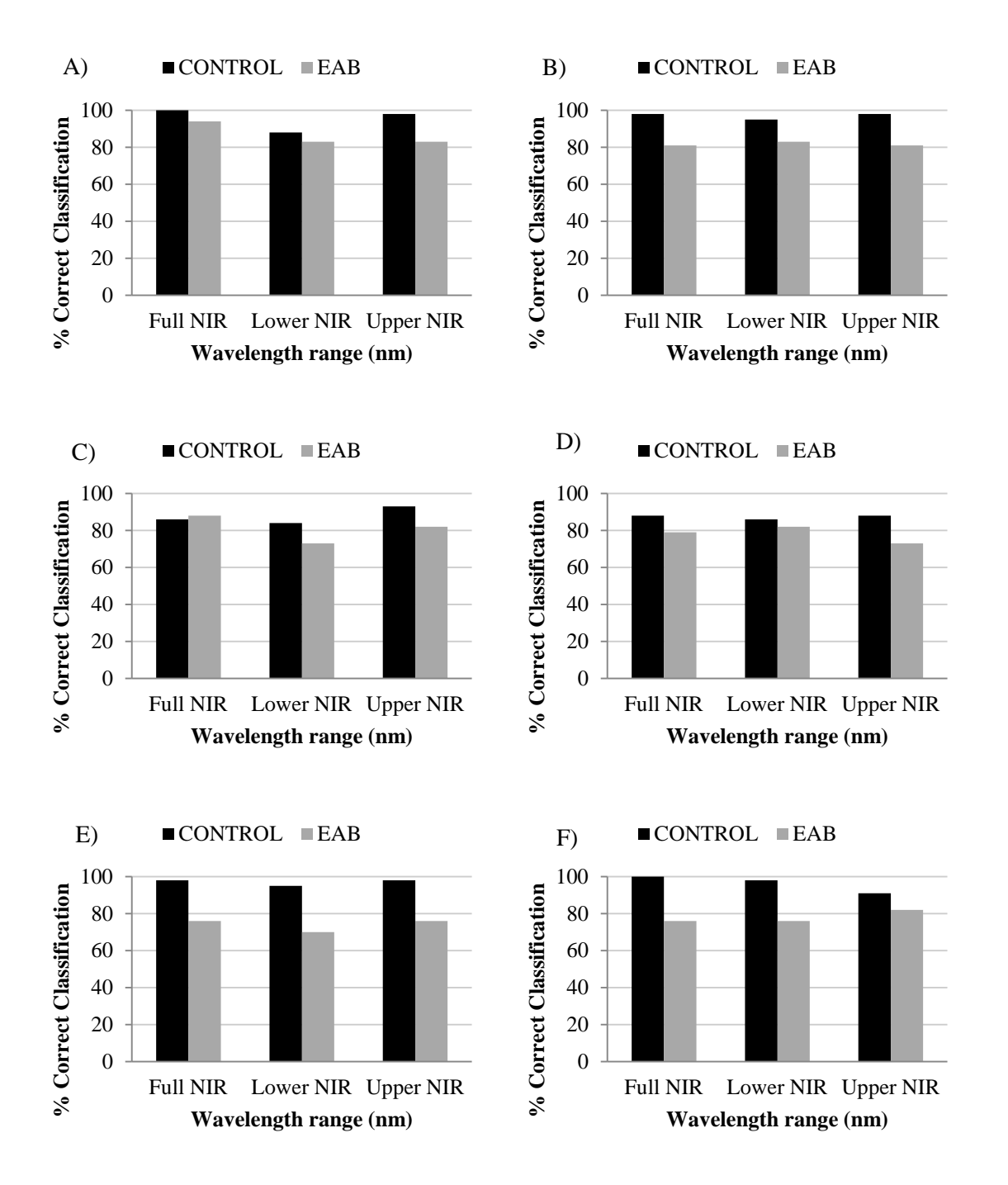
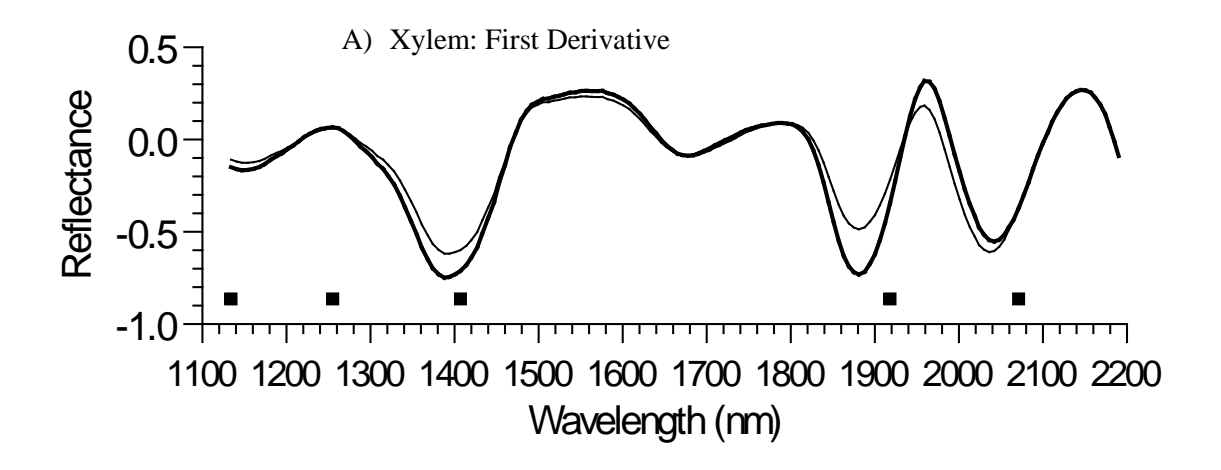


Figure 3.5. Percentage correct classifications of non-symptomatic (control) and EAB infested reflectance spectra: A) xylem first derivative, B) xylem second derivative, C) bark first derivative, D) bark second derivative, E) phloem first derivative, F) phloem, second derivative. Black bars represents control, light grey bars represents EAB. Xylem: Control n = 43, EAB n = 36. Bark: Control n = 43, EAB n = 33. Phloem: Control n = 43, EAB n = 33.



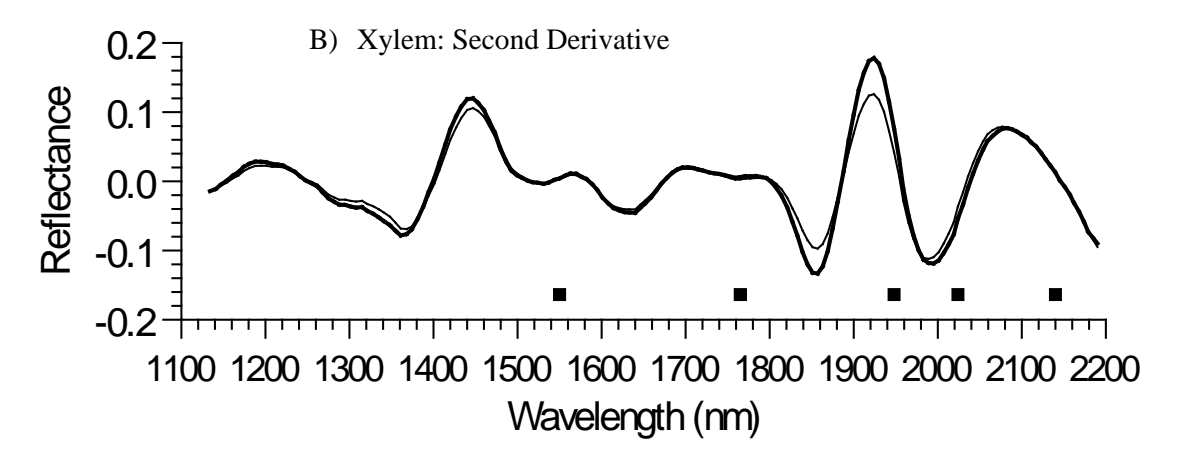
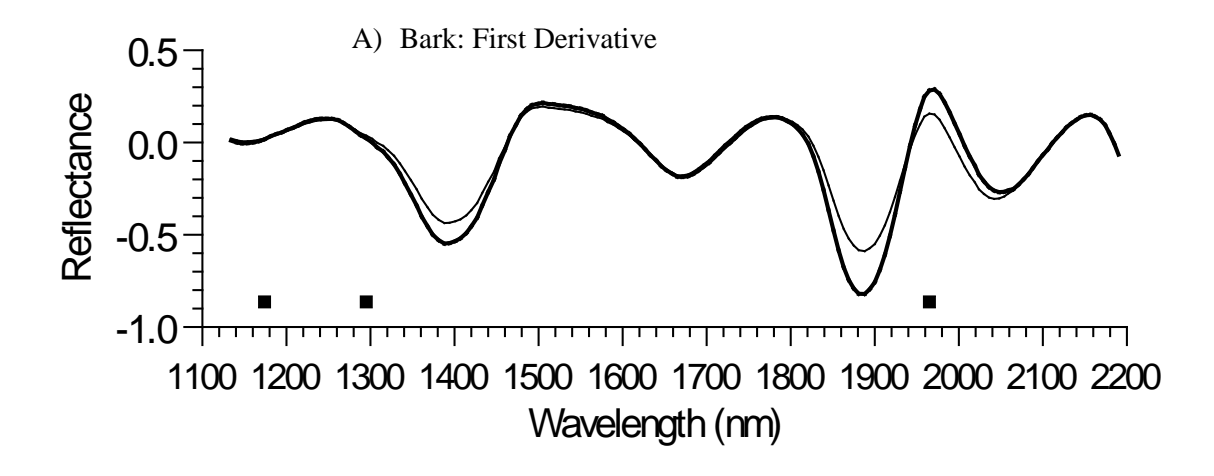


Figure 3.6. Means of xylem spectra derivatives for control (thin line) and EAB (bold line) samples from 1134 to 2190 nm wavelengths: A) first derivative, B) second derivative. Control n = 43, EAB n = 36. Solid squares denote wavelength bands that allowed for significant separation between the Control and EAB spectra during Stepwise Discriminant Analysis.



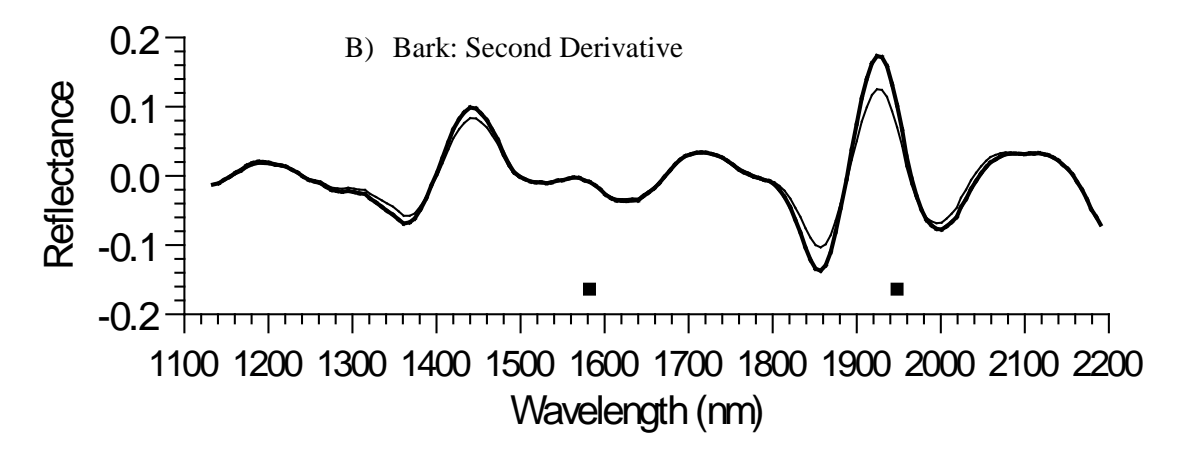
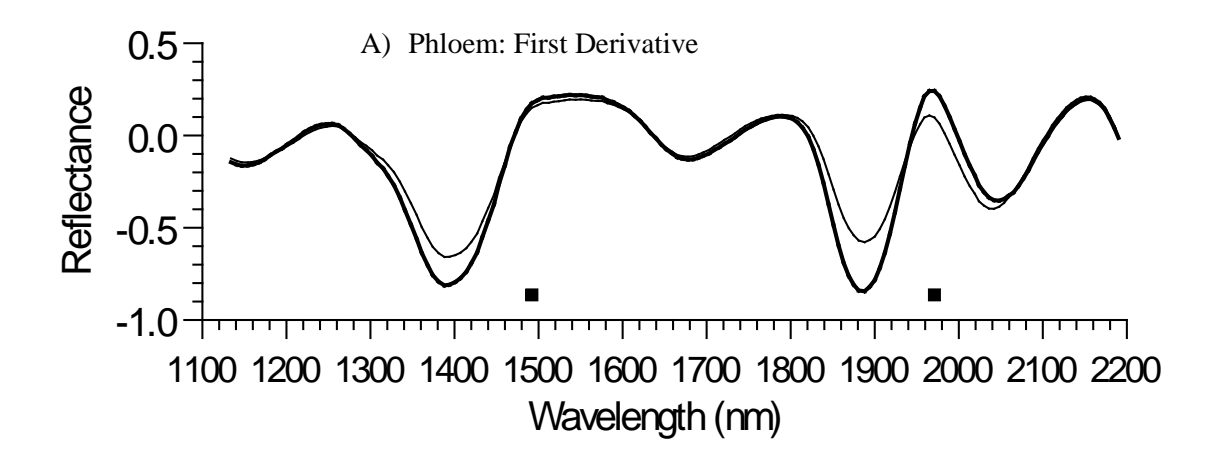


Figure 3.7. Means of bark spectra derivatives for control (thin line) and EAB (bold line) samples from 1134 to 2190 nm wavelengths: A) first derivative, B) second derivative. Control n = 43, EAB n = 33. Solid squares denote wavelength bands that allowed for significant separation between the Control and EAB spectra during Stepwise Discriminant Analysis.



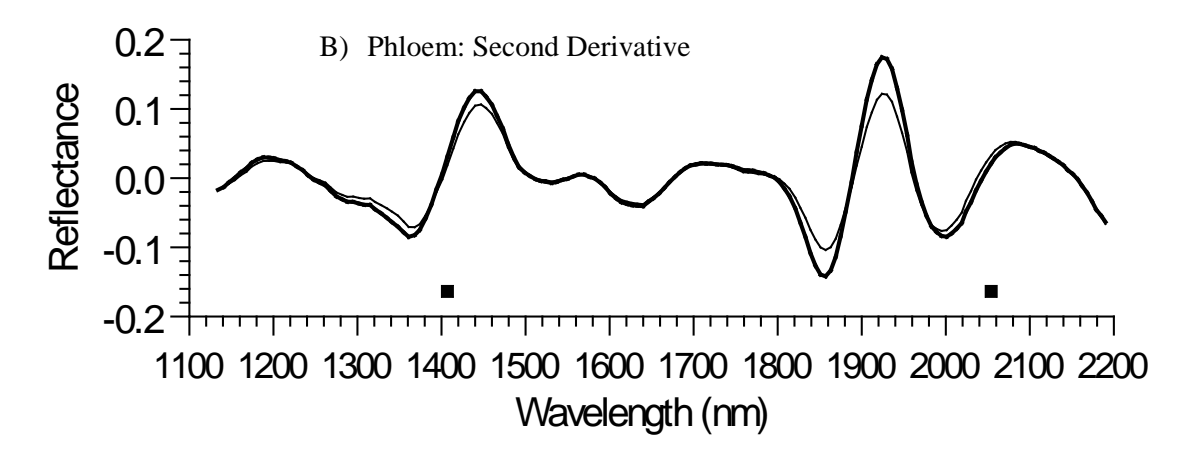


Figure 3.8. Means of phloem spectra derivatives for control (thin line) and EAB (bold line) samples from 1134 to 2190 nm wavelengths: A) first derivative, B) second derivative. Control n=43, EAB n=33. Solid squares denote wavelength bands that allowed for significant separation between the Control and EAB spectra during Stepwise Discriminant Analysis.

REFERENCES

REFERENCES

- Ananthakrishnan, T.N. (Editor)., 2001. Insects and plant defense dynamics. Science Publishers, Inc., Enfield, NH, USA.
- Avantes, 2012. AvaSoft for AvaSpec-USB2, User's Manual (Version 8.0). Broomfield, CO, USA, Avantes Inc. www.avantes.com
- Axrup, L., Markides, K., Nilsson, T., 2000. Using miniature diode array NIR spectrometers for analysis wood chips and bark samples in motion. Journal of Chemometrics 14, 561-572.
- Burns DA, Ciurczak, EW (Editors). 2008. Handbook of near-infrared analysis (3rd Edition). Practical spectroscopy; pp 1-808.
- Dutta, D., Das, P.K., Bhunia, U.K., Singh, U., Singh, S., Sharma, J.R., Dadhwal, V.K., 2015. Retrieval of tea polyphenol at leaf level using spectral transformation and multi-variate statistical approach. International Journal of Applied Earth Observation and Geoinformation 36, 22-29.
- Carvalho, S., Macel, M., Schlerf, M., Moghaddam, F.E., Mulder, P.P.J., Skidmore, A.K., van der Putten, W.H. 2013. Changes in plant defense chemistry (pyrrolizidine alkaloids) revealed through high-resolution spectroscopy. ISPRS Journal of Photogrammetry and Remote Sensing 80, 51-60.
- Chakraborty, S., Whitehill, J.G.A., Hill, A.L., Opiyo, S.O., Cipollini, D., Herms, D.A., Bonello, P., 2014. Effects of water availability on emerald ash borer larval performance and phloem phenolics of Manchurian and black ash. Plant, Cell and Environment 37, 1009-1021.
- Chen, Y., Ulyshen, M.D., Poland, T.M., 2012. Differential utilization of ash phloem by emerald ash borer larvae: ash species and larval stage effects. Agricultural and Forest Entomology 14, 324–330.
- Cipollini, D., Wang, Q., Whitehill, J.G.A., Powell, J. R., Bonello, P., Herms, D.A., 2011. Distinguishing defensive characteristics in the phloem of ash species resistant and susceptible to emerald ash borer. Journal of Chemical Ecology 37,450–459.
- Cooper, P.A., Jeremic, D., Radivojevic, S., Ung, Y.T., Leblon, B., 2012. Potential of near-infrared spectroscopy to characterize wood products. Canadian Journal of Forest Research 41, 2150-2157
- Crook, D.J., Khrimian, A., Francese, J.A., Fraser, I., Poland, T., Sawyer, A.J., Mastro, V.C., 2008b. Development of a host-based semiochemical lure for trapping emerald ash borer *Agrilus planipennis* (Coleoptera: Buprestidae). Environmental Entomology 37, 356-365.
- Crook, D.J., Mastro, V.C., 2010. Chemical ecology of the emerald ash borer Agrilus planipennis. Journal of Chemical Ecology, 36,101–112.
- Eastman, J.R., Zhu, H., Lazar, A., Williams, D.W., 2005. Progress on remote sensing applications for emerald ash borer survey: analysis of 2004 hyperspectral imagery. Emerald Ash Borer Research and Technology Development Meeting.
- Eaton, R.A., Hale, M.D.C., 1993. Wood: Decay, Pests, and Protection. 546 pp. Chapman and Hall, London, UK.

- Engelman, L., 2002. Discriminant Analysis. In: SYSTAT 10.2, Statistics I. Richmond, CA.
- Ertlen, D., Schwartz, D., Trautmann, M., Webster, R., Brunet, D. 2010. Discriminating between organic matter in soil from grass and forest by near-infrared spectroscopy. European Journal of Soil Science 61, 207-216.
- Eyles, A., Jones, W., Riedl, K., Cipollini, D., Schwartz, S., Chan, K., Herms, D.A., Bonello, P. 2007. Comparative Phloem Chemistry of Manchurian (*Fraxinus mandshurica*) and Two North American Ash Species (*Fraxinus americana* and *Fraxinus pennsylvanica*). Journal of Chemical Ecology 33, 1430-1448
- Eyles, A., Bonello, P., Ganley, R., Mohammed, C., 2010. Induced resistance to pests and pathogens in trees. New Phytologist 185, 893-908. doi: 10.1111/j.1469-8137.2009.03127.x.
- Fackler, K., Schwanninger, M., 2012. How spectroscopy and microspectroscopy of degraded wood contribute to understand fungal wood decay. Applied Microbiology and Biotechnology 96, 587-599.
- Fassnacht, F.E., Latifi, H., Ghosh, A., Joshi, P.K., Koch, B., 2014. Assessing the potential of hyperspectral imagery to map bark beetle-induced tree mortality. Remote Sensing of Environment 140, 533-548.
- Green, B., Jones, P.D., Nicholas, D.D., Schimleck, L.R., Shmulsky, R., Dahlen, J., 2012. Assessment of the early signs of decay of *Populus deltoids* wafers exposed to *Trametes versicolor* by near infrared spectroscopy. Holzforschung 66, 515-520.
- Henery, M.L., Henson, M., Wallis, I.R., Stone, C., Foley, W.J., 2008. Predicting crown damage to *Eucalyptus grandis* by *Paropsis atomaria* with direct and indirect measures of leaf composition. Forest Ecology and Management 255, 3642-3651.
- Herms, D.A., McCullough, D.G., 2014. Emerald ash borer invasion of North America: history, biology, ecology impacts, and management. Annual Review of Entomology 59, 13-30.
- Heise, H.M., Winzen, R., 2002. Chemometrics in near-infrared spectroscopy. In: near-infrared spectroscopy: principles, instruments, applications (Eds: Siesler HW, Ozaki Y, Kawata S, Heise HM), pp 125-162. Wiley-VCH, Germany.
- Hill, A.L., Whitehill, J.G.A., Opiyo, S.O., Phelan, P.L., Bonello, P. 2012. Nutritional attributes of ash (*Fraxinus* spp.) outer bark and phloem and their relationships to resistance against the emerald ash borer. Tree Physiology 32, 1522-1532.
- Ismail, R., Mutanga, O. 2011. Discriminating the early stages of *Sirex noctilio* infestation using classification tree ensembles and shortwave infrared bands. International Journal of Remote Sensing 32, 4249-4266.
- Jones, P.D., Schimleck, L.R., Peter, G.F., Daneils, R.F., Clark III, A., 2006. Nondestructive estimation of wood chemical composition of sections of radial wood strips by diffuse reflectance near infrared spectroscopy. Wood Science and Technology 40, 709-720.

- Jones, P.D., Schimleck, L.R., Daniels, R.F., Clark III, A., Purnell, R.C., 2008. Comparison of *Pinus taeda* L. whole-tree wood property calibrations using diffuse reflectance near infrared spectra obtained using a variety of sampling options. Wood Science and Technology 42, 385-400.
- Kelley, S.S., Rials, T.G., Snell, R., Groom, L.H., Sluiter, A., 2004. Use of near infrared spectroscopy to measure the chemical and mechanical properties of solid wood. Wood Science and Technology 38, 257-276.
- Lawrence, R., Labus, M., 2003. Early detection of Douglas-fir beetle infestation with subcanopy resolution hyperspectral imager. Western Journal of Applied Forestry 18, 202-206.
- Leon, J., Rojo, E., Sanchez-Serrano, J.J., 2001. Wound signaling in plants. Journal of Experimental Botany, 52 1-9.
- McCullough, D.G., Poland, T.M., Anulewicz, A.C., Cappaert, D., 2009a. Emerald ash borer (Coleoptera: Buprestidae) attraction to stressed or baited ash trees. Environmental Entomology 38, 1668-1679.
- McCullough, D.G., Poland, T.M., Cappaert, D., 2009b. Attraction of the emerald ash borer to ash trees stressed by girdling, herbicide treatment, or wounding. Canadian Journal of Forest Research 39, 1331-1345.
- Parkin, E.A., 1938. The depletion of starch from timber in relation to attack by Luctus beetles II: A preliminary experiment upon the effect of girdling standing oak trees. Forestry 12, 30-37.
- Poland, T.M., McCullough, D.G., 2006. Emerald ash borer: invasion of the urban forest and the threat to North America's ash resource. Journal of Forestry pp 118-124.
- Pontius, J., Hallett, R., Martin, M., 2005. Assessing hemlock decline using visible and near-infrared spectroscopy: indices comparison and algorithm development. Applied Spectroscopy 59, 836-843.
- Pontius, J., Martin, M., Plourde, L., Hallett, R. 2008. Ash decline assessment in emerald ash borer-infested regions: atest of tree-level, hyperspectral technologies. Remote Sensing of Environment 112, 2665-2676.
- Riggins, J.J., Defibaugh y Cha'vez, J. M., Tullis, J.A., Stephen, F.M., 2011. Spectral identification of previsual northern red oak (*Quercus rubra* L.) foliar symptoms related to oak decline and red oak borer (Coleoptera: Cerambycidae) attack. Southern Journal of Applied Forestry, 35 18-25.
- Rinnan, A., van den Berg, F., Engelsen, S.B., 2009. Review of the most common pre-processing techniques for near-infrared spectra. Trends in Analytical Chemistry 28, 1201-1222.
- Roberts, C.A., Workman, J., Reeves, J.B. III, (Eds.), 2004. Near-Infrared Spectroscopy in Agriculture. Agronomy, vol. 44, American Societies of Agronomy, Crop and Soil Science, Madison, WI.
- Sandak, A., Sandak, J., Negri, M., 2011. Relationship between near-infrared (NIR) spectra and the geographical provenance of timber. Wood Science and Technology 45, 35-48.
- Savitzky, A., Golay, M.J.E., 1964. Smoothing and differentiation of data by simplified least squares procedures. Analytical Chemistry 36, 1627-1639.

- Shenk, J.S., Workman, J.J., Westerhaus, M.O., 2008. Application of NIR spectroscopy to agricultural products. In: Handbook of Near-Infrared Analysis, 3rd edn. (eds Burns D.A., and Ciurczak, E.W.), pp. 347-386. Taylor and Francis Group, Florida.
- Schwanninger, M., Rodrigues, J.C., Fackler, K., 2011. A review of band assignments in near infrared spectra of wood and wood components. Journal of Near Infrared Spectroscopy 19, 287-308.
- Schimleck, L.R., Evans, R., Ilic, J., Matheson, A.C., 2002. Estimation of wood stiffness of increment cores by near-infrared spectroscopy. Canadian Journal of Forest Research 32, 129-135.
- Schimleck, L.R., Evans, R., 2004. Estimation of *Pinus radiata* D. Don tracheid morphological characteristics by near infrared spectroscopy. Holzforschung 58, 66-73.
- So, C., Via, B.K., Groom, L.H., Schimleck, L.R., Shupe, T.F., Kelley, S.S., Rials, T.G., 2004. Near infrared spectroscopy in the forest products industry. Forest Products Journal, 54, 6-16.
- So, C., Eberhardt, T.L., 2006. Rapid analysis of inner and outer bark composition of southern yellow pine bark from industrial sources. European Journal of Wood and Wood Products 64, 463-467.
- SYSTAT Software Incorporated, 2002. SYSTAT 10.2 Statistics 1, Richmond, CA.
- Taylor, A., Cooper, P. 2002. The effect of stem girdling on wood quality. Wood and Fiber Science 34, 212-220.
- Tsuchikawa, S., 2007. A review of recent near infrared research for wood and paper. Applied Spectroscopy Reviews 42, 43-71.
- Tsuchikawa, S., Schwanninger, M., 2013. A review of recent near-infrared research for wood and paper (part 2). Applied Spectroscopy Reviews 48, 560-587.
- Tsuchikawa, S., Yamato, K., Inoue, K., 2003. Discriminant analysis of wood-based materials using near-infrared spectroscopy. Journal of Wood Science 49, 275-280.
- Watanabe, K., Mansfield, S.D., Avramidis, S., 2012. Wet-pocket classification in *Abies lasiocarpa* using spectroscopy in the visible and near infrared range. European Journal of Wood Products 70, 61-67.
- Wu, Y., Zheng, Y., Li, Q., Iqbal, J., Zhang, L., Zhang, W., Du, Y., 2011. Study on difference between epidermis, phloem and xylem of Radix Ginseng with near-infrared and infrared spectroscopy coupled with principal component analysis. Vibrational Spectroscopy 55, 201-206.
- Zhang, K.W., Hu, B.X., Robinson, J., 2014. Early detection of emerald ash borer infestation using multisourced data: a case study in the town of Oakville, Ontario, Canada. Journal of Applied Remote Sensing 8, 083602. doi:10.1117/1.JRS.8.083602.

CHAPTER 4

CONCLUSIONS

In chapter two, a strong negative relationship between radial growth of white ash in Michigan and previous summer precipitation and climatic moisture index (CMI) was identified over a 21 year period using regression modelling. This response was seen in both the Upper and Lower Peninsulas, in natural and high impact recreational sites, in both symptomatic and non-symptomatic trees, and trees with varying levels of crown vigor due to EAB infestation. This study speculates that the negative response is possibly due to damaging winds associated with previous summer precipitation characteristic of Michigan. Compromised structural integrity and increased risk of branch damage of EAB infested ash may further pre-dispose trees to damage due to wind disturbance or heavy precipitation events. Land-use categories and region did not appear to influence radial growth relationships to climate. A negative response in the current year's growth due to CMI at the end of the growing season for trees with higher severity EAB infestation levels was also observed. Given the complexity of the study, multivariate analysis is required to identify relationships between radial growth, EAB infestation, land-use category, and latitudinal region. The results of this exploratory study were inconclusive on the feasibility of dendroclimatology for detection of emerald ash borer in Michigan.

The explanations provided for the dendroclimatic analysis are based on educated assumptions and future research is needed to further explore the relationships between white ash (and other ash species) in Michigan with climate and emerald ash borer infestation. Obtaining long-term wind data could help support or disprove the inferred explanation for the negative relationship to high precipitation in the previous summer. One possibility for the current dataset is to apply the climate regression modeling for individual tree chronologies in addition to the combined chronology groups from multiple trees used in this study. Future research is also needed in different regions of North America (ideally where EAB has not yet been detected) to assess the current responses of ash to regional climatic variables. Trees are highly sensitive to climate and it is possible that typical radial growth responses to climate may change

due to EAB infestation before visual symptoms appear. Additionally, a tree's response to climate can change over time and the short chronology lengths observed in this study prevented the ability to separate the analysis into two time periods. While the results of this study were inconclusive on the ability of dendrochronology for detection of EAB infestation in Michigan, the techniques used could be applied in conjunction with currently used detection methods for future research purposes. As girdled trap trees are still a commonly used and reliable method for detection of emerald ash borer, collecting cross sections at the time of sampling for dendrochronological analysis would be highly feasible. There is also value to collecting multiple cross sections from different stem heights in order to examine the downward progression dynamics of EAB feeding. Inspecting the stem for EAB presence would confirm infestation status and provide larval density information.

In chapter three, stepwise discriminant analysis for bark, phloem and xylem samples from white ash in Michigan was successfully able to differentiate between near-infrared diffuse reflectance spectra from visually healthy trees and trees with known EAB infestation. The samples were clearly from two separate populations, despite a minor amount of misclassification between EAB and control samples. This study was robust in that the calibration dataset was collected from trees grown in a wide geographical area and a variety of site conditions. Discrimination was highly accurate when comparing between bark, phloem and xylem spectra. The stepwise discriminant analysis with the highest accuracy comparing between spectra from EAB infested and control tissues was for the xylem, 1st derivative transformation over the full NIR wavelength range (implemented in this study: 1134-2190 nm) at 97% correct classification. There was a slight loss of classification accuracy in the lower wavelength range (1134-1696 nm), indicating that cheaper, lower range models (up to 1700 nm) still have potential for EAB detection. Overall, classification accuracies were slightly different for the multiple transformation methods, although the first and second derivatives were generally more reliable compared to applying the smoothing filter alone. Using different transformation methods changed the particular wavelengths that contributed the most towards group separation. However, it is commonly acknowledged that some form

of pre-treatment method is required to transform raw, diffuse reflectance spectra in near-infrared spectroscopy before multivariate analysis can be applied.

Future chemical analysis of the current dataset is needed to assign specific wavelength bands to plant defense chemicals of interest. This would also help for a better understanding of how the chemical properties of ash tissues change due to EAB infestation. Near-infrared spectroscopy could also be used for measuring additional ash tissues (i.e., branches and foliage) as well as soil substrates. Additional future research could include a greenhouse experiment with trees grown from the same seed stock and environmental conditions, where the infestation by EAB could be strictly controlled for each tree. A greenhouse experiment could help clarify whether the classification accuracy observed in the current study was due to EAB infestation or site specific differences. The clear separation between the two groups is promising, and further investigations into the application this technology for early detection of additional forest health concerns is recommended. As the application of widespread chemical analysis is not feasible for regional detection of EAB, calibration datasets developed with NIR reflectance spectra has potential for future rapid, non-destructive analysis of ash tissues. As handheld increment borers are a commonly used and inexpensive tool in forestry, this preliminary study shows that there is potential for NIR spectroscopy being developed for early detection of insect infestations by measuring NIR, diffuse reflectance spectra on increment cores.